Scaling of ecosystem phenology across satellite sensors and field-based observations: A case-study of contrasting vegetation types in a semi-arid savanna

by

Richard John Damant

(2414038)

Dissertation

Submitted in fulfilment of the requirements for the degree

Master of Science

in

Animal Plant and Environmental Science

in the Faculty of Science, University of the Witwatersrand, Johannesburg, South Africa

Supervisor: Dr Kaera Coetzer-Hanack

Co-supervisors: Dr Yolandi Ernst and Prof. Francesca Parrini

August 2022

DECLARATION

I declare that this dissertation is my own, unaided, original work. It is being submitted for the Master of Science degree at the University of the Witwatersrand, Johannesburg. It has not been submitted before for any degree or any other examination at any other university.

This project was carried out under the supervision of Dr Kaera Coetzer-Hanack (Global Change Institute) and the co-supervision of Dr Yolandi Ernst (Global Change Institute) and, Prof Francesca Parrini (School of Animal Plant and Environmental Science).

(Signature of candidate)

16/08/2022

ABSTRACT

Savannas are characteristically heterogenous and are driven by factors such as rainfall, herbivory, fire, and soil nutrients. All these factors interact differently at different spatial and temporal scales. Savanna phenology is highly unpredictable and is influenced predominantly by rainfall among other environmental factors. Climate change is therefore likely to alter phenological responses which emphasises the need for monitoring. However, the heterogeneous nature of savanna phenology makes it difficult to monitor as savanna tree-grass ratios are unpredictable and are not comparable across spatial scales. This similarly applies to the use of remotely sensed data sources used to estimate phenological events, which have different spatial and temporal properties, thus phenological observations are limited to the scales they were derived from. Many studies have made use of the Normalised Difference Vegetation Index (NDVI) to estimate both vegetation biomass and phenological metrics from a variety of different satellite products. However, no studies were found that explicitly investigated how spatial scale influences phenological metric and vegetation biomass estimates in a southern African savanna setting. Therefore, this study aimed to explore the influence of spatial scale on phenology and biomass estimates derived from remotely sensed products in a semi-arid savanna. A spatially nested data collection process was followed from which *in situ* biomass and remotely sensed NDVI products were collected. Results suggest that finer scale NDVI products are better predictors of herbaceous biomass and, on average, phenological metrics occurred later at coarser scale and earlier at finer spatial scales (~17 days). The conclusions from this study highlight the need for monitoring programs to carefully consider the use of coarse scale NDVI products as a proxy for biomass, particularly in heterogeneous landscapes, and the need to use a multi-scale approach when estimating phenological processes.

Keywords: Biomass, Multi-scale, NDVI, Phenology, Savanna, Spatio-temporal scales

ACKNOWLEDGEMENTS

Special acknowledgements must go to my supervisors, Dr Kaera Coetzer-Hanack, Dr Yolandi Ernst, and Professor Francesca Parrini. Thank you so much for all the guidance, support, and invaluable suggestions you have provided me with for the duration of this degree. The Covid-19 pandemic threw everyone a curveball in the form of lockdowns and social distancing; however, it did not hinder you all from being available despite the various challenges. Having to practice social distancing, I don't think I've ever looked forward to an online meeting so much. Your encouragement and belief in my ability throughout the last two years is truly appreciated.

I would like to thank Professor Wayne Twine for all your assistance at the Wits Rural Facility and for helping me identify plant samples. Thank you, Minah Nkuna, for processing all my bookings and ensuring that everything was in order at the facility. I would like to thank my field assistant Justice Mosum, my field data collection would not have been possible without your assistance and your incredible ability to memorise the exact locations of each sampling point (better than a GPS) made it a whole lot easier. I would also like to thank James at Swift Geospatial for your help processing PlanetScope data, and Melinda Boyers for showing me how to use the NDVI reader.

Thank you to all my family and friends for your interest and support, I always joked that my dissertation would help some of you with insomnia, but your genuine interest further motivated me and, made me realise what a privilege it is to be doing an MSc degree. Special thanks to Janais for your continued support, from proofreading my drafts to being there during my moments of 'lockdown blues'.

I would also like to thank the University of Witwatersrand for providing me with the opportunity to study at one of the best universities in South Africa, and for the provision of online learning tools and mobile data which made working from home much easier. Lastly, I would like to thank the National Research Foundation for funding this project, I am truly grateful for the opportunity this funding provided.

LIST OF ABBREVIATIONS

AVHRR	-	Advanced Very High Resolution Radiometer
DOY	-	Day of Year
DPM	-	Disc Pasture Meter
EOS	-	End of Season
GEE	-	Google Earth Engine
GPS	-	Global Positioning System
KNP	-	Kruger National Park
LOS	-	Length of Season
MODIS	-	Moderate Resolution Imaging Spectroradiometer
MVC	-	Maximum Value Composite
NDVI	-	Normalised Difference Vegetation Index
NIR	-	Near Infrared
POS	-	Peak of Season
R^2	-	Coefficient of Determination
RS	-	Remote Sensing
SD	-	Standard Deviation
SOS	-	Start of Season
SS2	-	SpectroSense 2
STL	-	Seasonal Trend decomposition by LOESS
TCR	-	Timbavati Communal Rangeland
VIs	-	Vegetation Indices
WRF	-	Wits Rural Facility

TABLE OF CONTENTS

LIST OF FIGURES

LIST OF TABLES

CHAPTER ONE: General introduction

1.1. Rationale

Savanna ecosystems cover close to 20% of terrestrial land globally (Kutsch *et al*., 2008) and up to 50% of Africa, making them highly valuable from an economic and ecological perspective (Osborne *et al*., 2018). Savanna ecosystems contribute to people's livelihoods as they provide food, grazing land, and materials such as firewood (Marchant, 2010). Savannas also provide many regulating ecosystem services such as carbon storage and regulation, as well as water and energy flows (Marchant, 2010).

Savannas consist of mainly woody plants and grasses, both of which vary in their composition and distribution across temporal and spatial scales (du Toit, 2003). The phenology of savanna vegetation functional types also varies. Grass green-up is closely linked to water availability (February *et al*., 2013), whereas some tree species can flush new leaves before the first seasonal rainfall (Whitecross *et al*., 2016) due to a response to photoperiod (Borchert and Rivera, 2001).

African savanna phenology has been described as highly unpredictable due to the inconsistency in seasonal rainfall that subsequently results in variable seasonal green-up events (Whitecross *et al*., 2016). The influence of climate change is also likely to shift phenological responses over the next 30 years (Hoegh-Guldberg *et al*., 2018), resulting in the 'mistiming' of seasonal activities between species that respond to phenological shifts at different rates (Visser *et al*. 2004). This food web disengagement between species will result in biodiversity loss (Visser *et al*. 2004). Changes in phenology could potentially lead to ecological divergence (Borcherding *et al*., 2010), which is the reproductive isolation of a population due to ecological changes that eliminate or reduce gene flow between populations (Coyne and Orr, 2004). For example, Sherry *et al*. (2007) demonstrated how warming temperatures resulted in reproductive divergence in plant phenology, which could bring about clashes in the reproductive periods of different species. This would lead to greater competition for pollinators and over time could result in species replacement, affecting higher trophic levels (Ackerly, 2003). According to Ibáñez *et al.* (2010), continuous shifts in phenology will influence the duration of the growing season which is of great ecological importance for biological communities. For instance, an increase in the growing season leads to higher accumulations of biomass due to the extended photosynthetically active period

(Moyo *et al*., 2015) which can increase the likelihood of fires (van Wilgen *et al.*, 2000), potentially influencing vegetation structure (Gandiwa and Kativu, 2009). For example, Higgins *et al*. (2007) found that the biomass and structure of savanna trees were influenced by fire, which could affect the carbon sequestration potential of African savannas

The reliance and subsequent impacts humans have on land has a major impact on the composition and diversity of vegetation (Tylianakis *et al*., 2008). Wolf *et al*. (2017) suggest that human induced changes to vegetation composition and diversity affect ecosystem function and diversity loss, which directly impinge on phenology. Land use change and climate change both alter phenology independently; however, the integration of these two drivers intensifies the effects on phenology. According to De Chazal and Rounsevell (2009), biodiversity studies should incorporate both climate change and land use change as drivers of influence to adequately assess impacts.

Given that human activities and climate change both influence phenology independently and interdependently (De Chazal and Rounsevell, 2009), monitoring programmes need to incorporate land use processes and monitor their impacts on vegetation structure and composition (Wessels *et al*., 2011). For example, communal rangelands have significantly less woody cover due to human utilisation for grazing and fuel wood collection, compared to the woody cover of conservation areas (Wessels *et al*., 2011). This highlights the importance of considering a land use gradient when evaluating factors that contribute to spatial and temporal shifts in phenological dynamics. Within an area of open canopy where land use processes are present (resource collection, grazing), tree-grass ratios are skewed to a more homogenous grass and herbaceous vegetation layer, however, this can also occur as a result of natural variation (Wessels *et al.*, 2011) This is an crucial aspect when it comes to monitoring savanna regions as these patches of homogenous vegetation can alter savanna variability at different spatial scales.

Many studies that investigate the human impacts on savanna landscapes are often localised to small areas and do not encompass the spatial heterogeneity representative of larger areas, especially in savanna landscapes (Asner *et al*., 2009). This is problematic for holistic understandings of system behaviour as the alterations of vegetation structure and composition influence ecosystem processes at various spatio-temporal scales, which are not transferable across different scales of observation (Levick and Rogers, 2011; McCleery *et al*., 2018). This suggests that changes at one scale would not necessarily translate to changes at a

different scale, essentially showing the non-linearity between scales (Chandola *et al*., 2010). In addition to human influences on vegetation structure and function, biophysical factors also play a pivotal role in determining ecosystem processes (Fisher *et al*., 2012). These two realms of influence make vegetation change trajectories non-linear, scale dependent, and thus difficult to predict at unmeasured scales (Chase *et al*., 2018).

The Normalised Difference Vegetation Index (NDVI) is one of the most used vegetation indices (VIs) for phenology based research as it can be derived from satellite sensors with a long temporal range, various spatial resolutions, and is easily accessible. The NDVI provides information regarding relative vegetation greenness, which can be used to infer green biomass (Santin-Janin *et al*., 2009) and vegetation productivity. Furthermore, Wessels *et al*. (2006) demonstrated that there is a strong correlation between total seasonal NDVI, biomass and rainfall. Given that the NDVI can be used as a means of measuring vegetation greenness or healthy vegetation productivity, it can be used to derive phenological metrics such as Start of Season (SOS), End of Season (EOS), Length of Season (LOS), and Peak of Season (POS) (Zeng *et al*., 2020). By monitoring temporal changes of these phenology metrics, it is possible to infer the impact of climate change and human activity on vegetation phenology. However, given the variety of data products available at differing spatial resolutions (Anderson, 2018), it is imperative to understand the effect of monitoring across different scales of observation.

Remotely sensed data are widely used as a tool for measuring and monitoring large scale vegetation structure and function as well as identifying trends. Data products with coarse spatial resolution are widely used as these often have a more consistent and continuous temporal range. Many studies have used coarse resolution imagery derived from the Moderate Resolution Imaging Spectroradiometer (MODIS) (250 m) and Advanced Very High Resolution Radiometer (AVHRR) (1 km) to measure phenological metrics, which is ideal for homogeneous landscapes where there is little variation over a large area (Zhang *et al*., 2003; Heumann *et al*., 2007; Gray *et al.*, 2014). However, in heterogeneous landscapes, the interpretation of phenological metrics becomes difficult as mixed canopies and species-specific phenological periods are not captured at coarse spatial scales (White *et al*., 2009). For savanna ecosystems, which show a larger degree of heterogeneity both spatially and temporally, the use of coarse scale NDVI data is limited in its ability to represent the true structure and function of a savanna landscape at the finer patch scale.

In this respect, finer scale sensors such as Landsat (30 m) and Sentinel (10 m) are particularly useful. They provide improved spatial resolutions which are better suited in describing heterogeneity associated with savanna landscapes as they are able to capture multi-scale patches such as fire burns, grazing lands, and various vegetation distributions (Liu *et al*., 2017). Furthermore, the subtle differences in the spectral response between vegetation are not accurately captured by coarse scale sensors, particularly in mixed vegetation ecosystems. For instance, the physiological, structural and phenological differences between C3 and C4 grasses (Duckworth *et al*., 2000; Slaton *et al*., 2001) result in subtle differences in their interactions with incoming radiation (Ustin and Gamon, 2010). These differing interactions of incoming radiation between C3 and C4 grasses influences the accuracy of remotely sensed vegetation dynamics, such as biomass estimation and phenology (Shoko *et al*., 2016). However, finer scale sensors like Sentinel-2 with wider spectral ranges can be used to disentangle the reflective differences between C3 and C4 grasses, allowing for more accurate estimates of biomass and phenological cycles (Shoko *et al*., 2016). Since savanna heterogeneity manifests itself at multiple spatial and temporal scales, comparing open and closed canopy cover areas may provide insights as to how NDVI signals differ between contrasting vegetation covers as tree-grass ratios differ between the two. Looking at both fine and coarse scaled NDVI measurements, I will investigate how spatial scale influences the relationship between NDVI and collected *in situ* biomass, and NDVI derived phenological metrics, in both Closed and Open canopy covers.

1.2. Aim and Objectives

The aim of this study was to investigate the influence of spatial scale on vegetation greenness estimates and phenology metrics derived from different remotely sensed products and *in situ* measurements on two structurally contrasting vegetation cover types (Open and Closed canopy cover) in a semi-arid savanna.

> *Objective 1*: To assess and compare satellite derived NDVI and *in situ* biomass estimates from field measurements, and how spatially aggregated NDVI data correlate from fine to coarse scale between sensors within Open and Closed canopy savanna vegetation.

Objective 2: To determine how phenological metrics and NDVI time series datasets from 2016-2021 compare at different spatial scales, and how precipitation and temperature influence phenological metrics at different spatial scales in Closed and Open canopy vegetation in a semi-arid savanna landscape.

1.3. Literature Review

Approximately 50% of Africa's terrestrial surface is occupied by the savanna biome (Scholes and Archer 1997). Savannas in the southern hemisphere are characterised by highly seasonal climates with hot summer periods with high precipitation, and warm and dry winters (Huntley and Walker, 2012). Savannas consist of a variable assortment of a discontinuous tree and continuous grass layers which are driven by wet and dry seasonal cycles (Scholes and Archer, 1997; Huntley and Walker, 2012). Other factors influencing savanna vegetation dynamics include the underlying geology, fire regimes, herbivory, and soil moisture (du Toit, 2003). For example, fire regimes influence savanna structure by altering the ratio between trees and grasses (Smit *et al*., 2010). This ratio between trees and grasses has a significant ecological role as it influences nutrient recycling, water infiltration and seedling establishment (Facelli and Brock, 2000). Savannas also provide essential resources for millions of people, such as fuelwood, and traditional medicines (Twine, 2005).

Plant phenology is the study of episodically recurring patterns of plant growth and development (Lieth, 1975). Several mechanisms influence phenology, such as temperature, rainfall, and photoperiod (Tang *et al*., 2016). These mechanisms differ in importance at different scales, based on biomes, species, and environmental constraints (Tang *et al*., 2016). During each growing season, plant phenology changes throughout the season which changes the composition, structure, and total biomass (Gibson *et al*., 2016). The changes in plant phenology are used as environmental cues for many animals' life cycle processes such as reproduction (Gibson *et al*., 2016).

Evidence regarding anthropogenic influences on phenology is mounting, and several studies (e.g., Root *et al*., 2003; Wolkovich *et al*., 2012; Buitenwerf *et al*., 2015; Gallinat *et al*., 2021) have suggested that human induced climate change has shifted phenology by several days in some areas, and by weeks in others. This temporal change of phenology

affects animals by creating a phenological mismatch, shifting key life-cycle indicators and resulting in disconnects between species (Miller-Rushing *et al*., 2010).

It may however be difficult to understand the spatio-temporal influence that climate change has on phenology in certain biomes, particularly savannas. Deciduous vegetation within African savannas displays highly unpredictable phenological patterns since their phenology is closely linked to water availability governed by highly variable rainfall (Whitecross *et al*., 2016). This non-linearity of phenological cycles within savanna landscapes demonstrates the need to monitor long-term phenology trends in savannas to separate the influence of climate change from the natural phenological variation.

Over the past 40 years, the advancement of Remote Sensing (RS) techniques has increased our ability to study surface vegetation at a regional and global scale (Piao *et al*., 2019; Gallinat *et al*., 2021). Through the advancement of RS techniques, interest in plant phenology has increased with peer-reviewed journal articles on the subject increasing 10-fold since the 1980s (Tang *et al*., 2016). Many plant phenology studies make use of data from the AVHRR and MODIS sensors due to their long availability period and frequent revisit periods (e.g., Gray *et al.*, 2014; Heumann *et al*., 2007; Zhang *et al*., 2003). These sensors, along with many others, can capture different wavelength ranges of the electromagnetic spectrum (Xue and Su, 2017). Typically, the multispectral bands used for surface vegetation research include Red (630-690 nm), Green (510-580 nm), Blue (450-510 nm), and Near Infrared (NIR, 770-895 nm). These bands are used to calculate vegetation indices (VIs).

One of the most widely used VIs is the NDVI, which looks at the difference between Red and NIR since healthy vegetation absorbs Red and reflects NIR (Tucker, 1979). The NDVI provides information regarding relative vegetation greenness, which can be used to infer green biomass and vegetation patterns (Santin-Janin *et al*., 2009). Using remotely sensed NDVI, phenological phases of vegetation can be tracked through a time series analysis. These phases (alternatively, 'phenology metrics') consist of key events that occur during a phenological cycle that include: Start of Season (SOS), Peak of Season (POS), End of Season (EOS), and Length of Season (LOS) (Zhang *et al*., 2003). This assists in regional and global scale phenology monitoring by analysing the inter-annual temporal changes of these metrics.

One of the main challenges with regards to remotely sensed phenology monitoring is scaling up from species level to landscape level, depending on the type of vegetation cover of

the area (Piao *et al*., 2019). It has been established that ecological events are scale dependent as events at one scale cannot be assumed to occur at another (Crawley *et al*., 2001). This is particularly relevant in savannas which exhibit high spatial heterogeneity, thus the influence of the scale of remotely sensed observations on phenological metrics is expected to be greater in savannas, compared to a more homogenous landscape such as a deciduous forest (Wang *et al*., 2005). While the MODIS and AVHRR sensors, with a spatial resolution of 250 m and 1 km respectively remain popular for phenology research, this coarse spatial resolution is not suitable in capturing the complex vegetation mosaic associated with savannas (Nijland *et al*., 2013). This has brought about the need for finer spatial resolution phenology studies to capture fine-scale heterogeneous dynamics within savannas (Walker *et al*., 2014). Over the past decade, new RS sensors with finer spatial resolutions have become active (Gallinat *et* al., 2021) such as Sentinel-2 (10 m), Landsat-8 (30 m) and PlanetScope (3 m). In this respect, these sensors are better suited to obtain fine scale NDVI measures, relative to the coarser scale measure one would derive from AVHRR and MODIS sensors. However, the choice of an appropriate sensor often also depends on the temporal scale of surface vegetation studies, as data products with finer temporal resolution often have courser spatial resolution and vice versa. For example, the daily acquisition rate of AVHRR allows for detailed incremental changes in vegetation to be observed, however, its coarse spatial scale generalises the changes of all vegetation within its spatial resolution and does not allow for species-specific changes to be observed. This makes decisions about 'acceptable' spatial versus temporal trade-offs fundamental in determining the most appropriate RS data product to use relative to the biome and/or phenomenon under investigation (e.g., Anderson *et al.*, 2018). Similarly, even though Sentinel-2 and Landsat-8 provide finer spatial resolution in comparison to other traditionally used sensors, there will often still be variation within these scales at the ground surface owing to vegetation distributions, which is why *in situ* data are needed in order to validate remotely sensed measurements (Anderson *et al*., 2018).

Several studies have used handheld NDVI sensors to monitor the changes of *in situ* vegetation health (Zhang *et al*., 2019) and to upscale VIs to larger areas (Tang *et al*., 2016). Handheld NDVI sensors are active sensors making them particularly useful in gathering field data as they are not affected by atmospheric conditions and the angle of incidence of solar radiation (Verhulst and Govaerts, 2010), however, these devices are developed mainly for crop monitoring.

It is difficult to directly correlate such field measurements with remotely sensed data. For instance, remotely sensed data does not account for below canopy cover, which is instead measured by handheld sensors. However, when taking field measurements, it is important to consider that savanna grasses cannot be treated uniformly due to the varying green-up and growth rates between 'below canopy' grasses and 'between canopy' grasses (Whitecross *et al*., 2017). It is also difficult to apply an area-averaged NDVI from fine to coarse scales as this causes an aggregation effect which makes ecological patterns appear more predictable than they actually are (Wiens, 1989).

Given the above limitations of upscaling *in situ* NDVI measures to larger areas, ground sampling techniques can provide useful insights regarding vegetation biomass at local scales (Ali *et al*., 2016). As a cost-effective method for correlating NDVI across scales, the disc pasture meter is a simple tool used to determine yield estimates of forage and is regularly used for biomass estimates (Ali *et al*., 2016). However, this method is time consuming and often requires calibration to account for the compressive strengths of vegetation sampled. Thus, a more efficient technique that can cover large areas is needed.

1.4. Study Area

The study area was located centrally within the Lowveld region that stretches across the Limpopo and Mpumalanga provinces in the north-eastern part of South Africa (31.10038, -24.56402, Figure 1.1). Situated within the Lowveld region on the western side of the Kruger National Park (KNP), the Wits Rural Facility (WRF) covers 315 ha of conserved semi-arid savanna. Directly south of WRF are 370 ha of communal rangelands, referred to as the Timbavati Communal Rangeland (TCR), utilised by the Tintswalo and OkkernootBoom-A communities within the Acornhoek ward (Estimated Population-33,530). These two sites have contrasting land uses and governance approaches, which represent different levels of savanna utilisation.

The WRF is a privately owned research facility that takes a conservation-management approach. The area is occupied by dense vegetation and has several herbivores such as greater kudu (*Tragelaphus strepsiceros*), impala (*Aepyceros melampus*), and giraffe (*Giraffa camelopardalis*). Controlled fires are conducted in the area every 5 to 10 years, depending on the fuel load (NeSmith *et al*., 2021). In contrast, TCR is managed under tribal authority with

communal use as its primary function. The area is sparsely vegetated and is heavily utilised for cattle grazing as well as firewood and building material collection (Twine, 2005). These two sites represent continuums of natural semi-arid savanna between a densely vegetated Closed canopy (WRF) and a sparsely vegetated Open canopy (TCR). Based on these differences in land use and vegetation composition between these two sites, WRF and TCR are hereon referred to as Closed canopy and Open canopy, respectively.

The study area has hot, wet summers and warm, dry winters with a mean annual rainfall of 651 ± 123 mm which occur primarily during summer months (October to May). Temperatures generally range between 20-31°C during summer and 8-26°C in winter (Shackleton and Scholes, 2011; Mograbi *et al*., 2019). Dominant tree species include *Combretum zeyheri*, *Terminalia sericea*, *Senegalia nigrescens* and *Dichrostachys cinerea* (Mucina and Rutherford, 2006), with the grass layer comprised of mostly C4 perennial grasses, predominantly, *Panicum maximum* and *Hyperthelia dissoluta*. The underlying geology consists mainly of granite with Timbavati gabbro intrusions (Mucina and Rutherford, 2006). Soils are deep and clayey with the presence of sodic soils being delineated by the occurrence of *Terminalia sericea* in seep zones (Mucina and Rutherford, 2006).

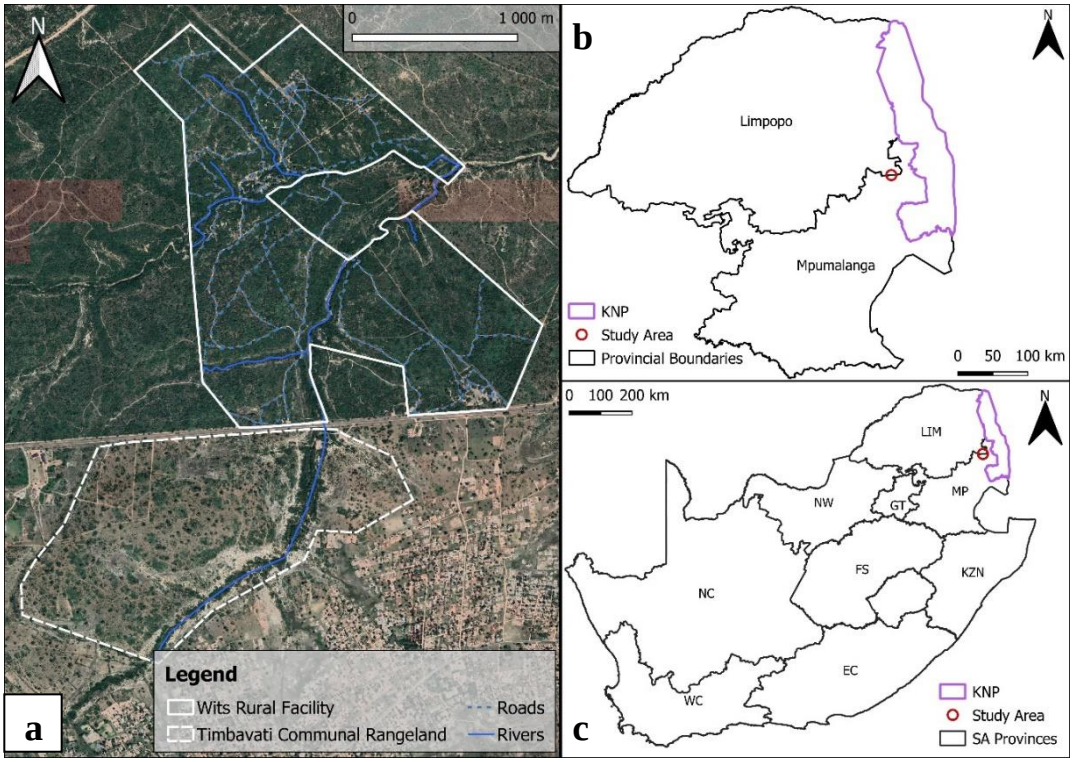

Figure 1.1: Map of the study area showing (a) the contrast between the Wits Rural Facility (north of the road) and the Timbavati Communal Rangelands (south of the road) located within the central lowveld between (b) Mpumalanga and Limpopo provinces to the (c) west of the Kruger National Park within South Africa.

1.5. Methods

1.5.1. Satellite Data Collection

The NDVI, from four different satellite sensors (MODIS v6, Landsat-8, Sentinel-2C, and PlanetScope) was used in this study for the period between January 2016 and April 2021 (Table 1A APPENDIX A). I acquired and pre-processed all data, apart from PlanetScope, using Google Earth Engine (GEE) which is a cloud-based geospatial analysis platform that allows users to access publicly available geospatial datasets from a variety of imaging systems (Gorelick *et al*., 2017). I clipped all datasets to the study area extent. Pre-processing included atmospheric corrections for all Sentinel-2C data using the 'Sen2Cor' which converts Top of Atmosphere products to Bottom of Atmosphere products, allowing for comparable surface reflectance products (Main-Knorn *et al*., 2017). I applied cloud and shadow masking based on the quality assessment band associated with each sensor and set 'Nodata' pixel values to 0 (GEE Code in Appendix B). Thereafter I created NDVI surfaces using the Red and NIR bands associated with each sensor (Equation 1).

$$NDVI = \frac{NIR-RED}{NIR+RED} \quad \text{(Equation 1)}$$

All datasets acquired were downloaded in GeoTIFF file format using the WGS 84 (EPSG:4326) projection. I acquired PlanetScope data for the period from September 2020 to June 2021, a period analogous to the field data collection dates. The cost of post-processing by a third party did not allow for the same temporal range as the other sensors. PlanetScope images were calibrated for surface reflectance analysis, converted to NDVI surfaces, and were also reprojected to WGS 84 (EPSG: 4326). The details of the individual sensors used are as follows:

MODIS

The MODIS-Terra MOD13Q1 (hereon referred to as MODIS), provided by the Land Processes Distributed Active Archive Centre (LP DAAC), is a 16-day composite dataset with

a spatial resolution of 250 m available from February 2000 to present. MODIS NDVI products are atmospherically corrected surface reflectances which have been masked for water, clouds, and cloud shadows (Huete et al., 2002). Each composite is created using a maximum value compositing (MVC) algorithm which selects MODIS tiles with the best quality pixel values within the 16-day period. The selection of these tiles is based on criteria such as low view angle, low cloud cover and maximum NDVI value (LP DAAC, 2020). A total of 23 composites are produced each year, providing two composites per month, barring October and November which alternate from two to one composite respectively every four years, due to leap years. This dataset has the coarsest resolution of all sensors used in this study and was therefore used as the 'sampling footprint' for the other sensors.

Landsat 8

Landsat 8 OLI Surface Reflectance Tier 1 (hereon referred to as Landsat), provided by the United States Geological Survey, has a spatial resolution of 30 m. Bands 4 and 5, which provide red and NIR respectively, were used to calculate NDVI. The Landsat satellite has a near-polar, sun-synchronous orbit, with data acquired in 185 km swaths, with a 16-day repeat cycle (Roy *et al.*, 2014). The Landsat product is therefore more susceptible to noise such as cloud cover and shadows due to its lower acquisition rate than the other sensors used in this study.

Sentinel-2C

Sentinel-2C (hereon referred to as Sentinel) provides global coverage of land surfaces (56°N - 84°S) with images comprising 13 spectral bands at spatial resolutions of 10, 20, and 60 m, depending on the spectral band of interest (Languille *et al.*, 2015). Band 4 and 8 provide Red and NIR respectively, at 10 m spatial resolution, thus allowing NDVI surfaces to be created at the finest, publicly available, spatial resolution for this study. Sentinel has a revisit period of five days which allows for a maximum of three Sentinel images to be acquired within the 16-day acquisition period of one MODIS and Landsat image.

PlanetScope

PlanetScope (launched March 2016) satellite data, provided by Planet Labs, consists of a constellation of more than 150 CubeSats which are small, low-cost satellites (Woellert *et al.,* 2011). This large constellation of CubeSats allows PlanetScope to image all of earth land surfaces every day (Ghuffar, 2018). PlanetScope imagery is captured in four bands which include Red, Blue, Green, and NIR, at a spatial resolution of 3 m (Kääb et al., 2017). Planet Labs provided access to the imagery (Planet Team, 2017) through a research/educational license (Subscription ID-502979) where imagery was downloaded using the Planet Explorer user interface for the period that matched that of the *in situ* data collection (September 2020 – April 2021).

1.5.2. Sampling Design

Several key aspects were considered when linking *in situ* and *ex situ* data. The date of field data and remotely sensed data were collected in similar time periods, samples were selected randomly, and Global Positioning System (GPS) coordinates were used to georeference field and remotely sensed data (Ali *et al*., 2016). Field data collection points were stratified according to the spatial location and extent of the MODIS 250 m^2 pixels. The selection of MODIS pixels was determined by their accessibility via roads and being completely within the boundaries of the Closed or Open canopy site (Figure 1.2). I accounted for spatial autocorrelation by omitting all MODIS pixels that were directly adjacent to each other. However, due to the spatial limitations, i.e., ensuring all pixels were contained within the study site boundaries and the need to sample the same number of MODIS pixels in each land cover type, several MODIS pixel vertices are adjacent to each other. This was necessary as it ensured that sampled pixels were accessible by roads and were not influenced by riparian zones. Sampled pixels were however at least 160 m apart, which is a distance threshold previously used in this particular landscape to avoid spatial autocorrelation (Mograbi *et al*., 2017; 2019). Based on these criteria, a total of 12 MODIS pixels were selected, six in the Closed canopy site and six in the Open canopy site. Thereafter, a spatially nested sampling design was undertaken.

Within each MODIS pixel, I randomly selected 20 Landsat pixels and within each Landsat pixel, I randomly selected one Sentinel pixel. For each Sentinel pixel, I extracted the

centre coordinates as the locations for the field data collection and the PlanetScope pixel locations (Figure 1.2). For each of the 12 MODIS pixels and their associated Landsat (n=240), Sentinel (n=240) and PlanetScope (n=240) pixels, I created polygons using the 'Raster pixels to polygon' tool in QGIS v3.10.2 (GQIS Development Team, 2020). To allow for accurate NDVI and seasonality extraction, I then assigned row and column identifications to these polygons based on the row-column extent of the downloaded NDVI rasters of the various satellites.

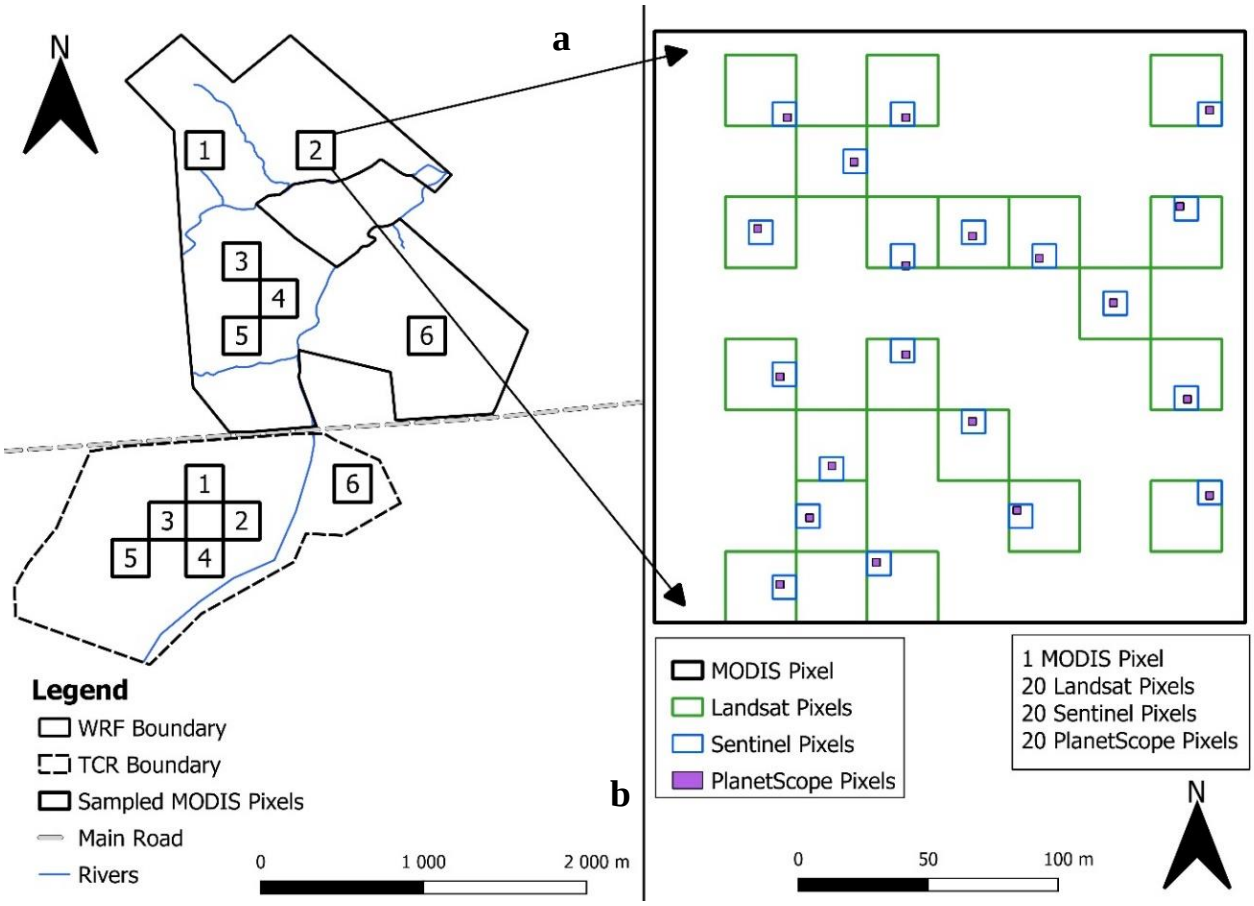

Figure 1.2: Illustration of the (a) location of sampled MODIS pixels within Closed and Open canopy and (b) the spatially nested data collection structure whereby *in situ* data were captured within the spatial extent of PlanetScope pixels that were located within Sentinel pixels, which occurred in Landsat pixels, all of which are present in one MODIS pixel. Field data were collected from fixed locations within the extent of the PlanetScope pixels.

The field data collection took place from 14th September 2020 to 16th April 2021. Field data collection was done on the 2nd and 4th week of each month to match every other 16-day composite period of the MODIS satellite. Field data from 3-4 MODIS pixel footprints were collected per day from Closed and Open canopy, alternating between morning and afternoon collection times to avoid temporal bias (Zhang *et al.*, 2015). The centre of each target Sentinel pixel within the selected MODIS tile was located using a Garmin ETrex 10 GPS and marked with a visual marker for re-location purposes. In instances where the centre of a target Sentinel pixel could not be marked (trees, thick bush) a permanent marker was placed as close as possible to the intended centre. The coordinates of these marked locations were recaptured every second week of the field data collection period to obtain standard errors on GPS readings, which were necessary to ensure that field measurements were recorded within sampling pixels (GPS error: WRF = 0.93 m; TCR = 0.40 m; see APPENDIX B for calculations).

1.6. Dissertation Structure

Chapter 1 comprises a general introduction with details regarding the rationale for this study and a literature review of previous works and some concepts related to vegetation phenology. Chapter 1 also details the study area, data collection and sampling design methods which are used in chapters 1 and 2. Chapters 2 and 3, the two data chapters, are compiled in a publication format, with their own introduction, methods, results, discussion, and references. For this reason, there are some instances of repetition which I have tried to keep to a minimum where possible. Tables and figures are shown at the end of each chapter, while supplementary details can be found in appendices A and B. Chapter 2 assesses the relationship between NDVI and *in situ* biomass (objective 1), while chapter 3 focuses on how phenological metrics differ between spatial scales (objective 2). These two chapters are synthesized in chapter four, where key conclusions are drawn, and recommendations are made.

1.7. References

Ackerly, D.D., 2003. Community assembly, niche conservatism, and adaptive evolution in changing environments. *International Journal of Plant Sciences*, 164(S3), S165-S184.

Ali, I., Cawkwell, F., Dwyer, E., Barrett, B. and Green, S., 2016. Satellite remote sensing of grasslands: from observation to management. *Journal of Plant Ecology*, 9(6), 649-671

Anderson, C.B., 2018. Biodiversity monitoring, earth observations and the ecology of scale. *Ecology Letters*, 21(10), 1572-1585.

Asner, G.P., Levick, S.R., Kennedy-Bowdoin, T., Knapp, D.E., Emerson, R., Jacobson, J., Colgan, M.S. and Martin, R.E., 2009. Large-scale impacts of herbivores on the structural diversity of African savannas. *Proceedings of the National Academy of Sciences*, 106(12), 4947-4952.

Borcherding, J., Beeck, P., DeAngelis, D.L. and Scharf, W.R., 2010. Match or mismatch: the influence of phenology on size-dependent life history and divergence in population structure. *Journal of Animal Ecology*, 79(5), 1101-1112.

Borchert, R. and Rivera, G., 2001. Photoperiodic control of seasonal development and dormancy in tropical stem-succulent trees. *Tree Physiology*, 21(4), 213-221.

Buitenwerf, R., Rose, L., and Higgins, S.I., 2015. Three decades of multi-dimensional change in global leaf phenology. *Nature Climate Change*, 5(4), 364-368.

Cerasoli, S., Campagnolo, M., Faria, J., Nogueira, C. and Caldeira, M.D.C., 2018. On estimating the gross primary productivity of Mediterranean grasslands under different fertilization regimes using vegetation indices and hyperspectral reflectance. *Biogeosciences*, 15(17), 5455-5471.

Chandola, V., Hui, D., Gu, L., Bhaduri, B. and Vatsavai, R.R., 2010, December. Using time series segmentation for deriving vegetation phenology indices from MODIS NDVI data. In *2010 IEEE International Conference on Data Mining Workshops*, 202-208.

Chase, J.M., McGill, B.J., McGlinn, D.J., May, F., Blowes, S.A., Xiao, X., Knight, T.M., Purschke, O. and Gotelli, N.J., 2018. Embracing scale-dependence to achieve a deeper understanding of biodiversity and its change across communities. *Ecology Letters*, 21(11), 1737-1751.

Coyne, J.A., and Orr, H.A., 2004. *Speciation* (Vol. 37). Sunderland, MA: Sinauer Associates.

Crawley, M.J. and Harral, J.E., 2001. Scale dependence in plant biodiversity. *Science*, 291(5505), 864-868.

De Chazal, J. and Rounsevell, M.D., 2009. Land-use and climate change within assessments of biodiversity change: a review. *Global Environmental Change*, 19(2), 306-315.

du Toit, J.T., 2003. Large herbivores and savanna heterogeneity. In: *du Toit, J.T., Rogers, K.H., Biggs, H.C. (Eds.), The Kruger Experience: Ecology and Management of Savanna Heterogeneity*. Island Press, Washington, 292–309.

Duckworth, J.C., Kent, M. and Ramsay, P.M., 2000. Plant functional types: an alternative to taxonomic plant community description in biogeography?. *Progress in Physical Geography*, 24(4), 515-542.

Facelli, J.M. and Brock, D.J., 2000. Patch dynamics in arid lands: localized effects of Acacia papyrocarpa on soils and vegetation of open woodlands of South Australia. *Ecography*, 23(4), 479-491.

February, E.C., Higgins, S.I., Bond, W.J. and Swemmer, L., 2013. Influence of competition and rainfall manipulation on the growth responses of savanna trees and grasses. *Ecology*, 94(5), 1155-1164.

Fisher, J.T., Witkowski, E.T.F., Erasmus, B.F.N., Van Aardt, J., Asner, G.P., Wessels, K.J. and Mathieu, R., 2012. Human-modified landscapes: patterns of fine-scale woody vegetation structure in communal savannah rangelands. *Environmental Conservation*, 39(1), 72-82.

Gallinat, A.S., Ellwood, E.R., Heberling, J.M., Miller-Rushing, A.J., Pearse, W.D. and Primack, R.B., 2021. Macrophenology: insights into the broad-scale patterns, drivers, and consequences of phenology. *American Journal of Botany*, 108(11), 2112-2126.

Gandiwa, E. and Kativu, S., 2009. Influence of fire frequency on Colophospermum mopane and Combretum apiculatum woodland structure and composition in northern Gonarezhou National Park, Zimbabwe. *Koedoe: African Protected Area Conservation and Science*, 51(1), 36-48.

Ghuffar, S., 2018. DEM generation from multi satellite PlanetScope imagery. *Remote Sensing*, 10(9), 1462.

Gibson, D., Blomberg, E.J. and Sedinger, J.S., 2016. Evaluating vegetation effects on animal demographics: the role of plant phenology and sampling bias. *Ecology and Evolution*, 6(11), 3621-3631.

Gorelick, N., Hancher, M., Dixon, M., Ilyushchenko, S., Thau, D. and Moore, R., 2017. Google Earth Engine: Planetary-scale geospatial analysis for everyone. *Remote Sensing of Environment*, 202, 18-27.

Gray, J., Friedl, M., Frolking, S., Ramankutty, N., Nelson, A., and Gumma, M.K., 2014. Mapping Asian cropping intensity with MODIS. *IEEE Journal of Selected Topics in Applied Earth Observations and Remote Sensing*, 7(8), 3373-3379.

Heumann, B.W., Seaquist, J.W., Eklundh, L. and Jönsson, P., 2007. AVHRR derived phenological change in the Sahel and Soudan, Africa, 1982–2005. *Remote Sensing of Environment*, 108(4), pp.385-392.

Higgins, S.I., Bond, W.J., February, E.C., Bronn, A., Euston-Brown, D.I., Enslin, B., Govender, N., Rademan, L., O'Regan, S., Potgieter, A.L. and Scheiter, S., 2007. Effects of four decades of fire manipulation on woody vegetation structure in savanna. *Ecology*, 88(5), 1119-1125.

Higgins, S.I., Delgado-Cartay, M.D., February, E.C. and Combrink, H.J., 2011. Is there a temporal niche separation in the leaf phenology of savanna trees and grasses? *Journal of Biogeography*, 38(11), 2165-2175.

Hoegh-Guldberg, O., Jacob, D., Taylor, M., Bindi, M., Brown, S., Camilloni, I., Diedhiou, A., Djalante, R., Ebi, K., Engelbrecht, F. and Guiot, J., 2018. Impacts of 1.5 C global warming on natural and human systems. *In Global warming of 1.5° C.: An IPCC Special Report* (175-311). IPCC Secretariat.

Huete, A., Didan, K., Miura, T., Rodriguez, E.P., Gao, X., and Ferreira, L.G., 2002. Overview of the radiometric and biophysical performance of the MODIS vegetation indices. *Remote sensing of environment*, 83(1-2), 195-213.

Huntley, B.J. and Walker, B.H. eds., 2012. *Ecology of Tropical Savannas* (Vol. 42). Springer Science & Business Media.

Ibáñez, I., Primack, R.B., Miller-Rushing, A.J., Ellwood, E., Higuchi, H., Lee, S.D., Kobori, H. and Silander, J.A., 2010. Forecasting phenology under global warming. *Philosophical Transactions of the Royal Society B: Biological Sciences*, 365(1555), 247-3260.

Kääb, A., Altena, B. and Mascaro, J., 2017. Coseismic displacements of the 14 November 2016 M w 7.8 Kaikoura, New Zealand, earthquake using the Planet optical cubesat constellation. *Natural Hazards and Earth System Sciences*, 17(5), 627-639.

Kutsch, W.L., Hanan, N., Scholes, B., McHugh, I., Kubheka, W., Eckhardt, H. and Williams, C., 2008. Response of carbon fluxes to water relations in a savanna ecosystem in South Africa. *Biogeosciences*, 5(6), 1797-1808.

Languille, F., Déchoz, C., Gaudel, A., Greslou, D., De Lussy, F., Trémas, T. and Poulain, V., 2015, October. Sentinel-2 geometric image quality commissioning: first results. *Image and Signal Processing for Remote Sensing XXI*, 9643, 964306. International Society for Optics and Photonics.

Leith, H., 1975. Phenology and seasonality modelling. *Soil Science*, 120(6), 461.
Levick, S.R. and Rogers, K.H., 2011. Context-dependent vegetation dynamics in an African savanna. *Landscape Ecology*, 26(4), 515-528.

Levick, S.R. and Rogers, K.H., 2011. Context-dependent vegetation dynamics in an African savanna. *Landscape Ecology*, 26(4), 515-528.

Levin, S.A., 1992. The problem of pattern and scale in ecology: the Robert H. MacArthur award lecture. *Ecology*, 73(6), 1943-1967.

Liu, Y., Hill, M.J., Zhang, X., Wang, Z., Richardson, A.D., Hufkens, K., Filippa, G., Baldocchi, D.D., Ma, S., Verfaillie, J. and Schaaf, C.B., 2017. Using data from Landsat, MODIS, VIIRS and PhenoCams to monitor the phenology of California oak/grass savanna and open grassland across spatial scales. *Agricultural and Forest Meteorology*, 237, 311-325.

Lpdaac.usgs.gov. 2020. *LP DAAC - MOD09A1*. [online] Available at: <https://lpdaac.usgs.gov/products/mod09a1v006/> [Accessed 19 April 2020].

Main-Knorn, M., Pflug, B., Louis, J., Debaecker, V., Müller-Wilm, U. and Gascon, F., 2017, October. Sen2Cor for sentinel-2. In *Image and Signal Processing for Remote Sensing XXIII* (Vol. 10427, p. 1042704). International Society for Optics and Photonics.

Marchant, R., 2010. Understanding complexity in savannas: climate, biodiversity, and people. *Current Opinion in Environmental Sustainability*, 2, 101-108.

McCleery, R., Monadjem, A., Baiser, B., Fletcher Jr, R., Vickers, K. and Kruger, L., 2018. Animal diversity declines with broad-scale homogenization of canopy cover in African savannas. *Biological Conservation*, 226, 54-62.

Miller-Rushing, A.J., Høye, T.T., Inouye, D.W. and Post, E., 2010. The effects of phenological mismatches on demography. *Philosophical Transactions of the Royal Society B: Biological Sciences*, 365(1555), 3177-3186.

Mograbi, P.J., Asner, G.P., Witkowski, E.T., Erasmus, B.F., Wessels, K.J., Mathieu, R., and Vaughn, N.R., 2017. Humans and elephants as treefall drivers in African savannas. *Ecography*, 40(11), 1274-1284.

Mograbi, P.J., Witkowski, E.T., Erasmus, B.F., Asner, G.P., Fisher, J.T., Mathieu, R. and Wessels, K.J., 2019. Fuelwood extraction intensity drives compensatory regrowth in African savanna communal lands. *Land Degradation & Development*, 30(2), 190-201.

Moyo, H., Scholes, M.C. and Twine, W., 2016. Effects of water and nutrient addition on the coppice growth response of cut Terminolio sericea. *Koedoe*, 58(1), 1-10.

Mucina, L. and Rutherford, M.C., 2006. *The vegetation of South Africa, Lesotho and Swaziland*. South African National Biodiversity Institute.

NeSmith, J.E., Twine, W. and Holdo, R.M., 2021. Interspecific variation in post-disturbance growth responses of a savanna tree community and its implications for escaping the fire trap. *Biotropica*, 53(3), 896-905.

Nijland, W., Coops, N.C., Coogan, S.C.P., Bater, C.W., Wulder, M.A., Nielsen, S.E.,McDermid, G., Stenhouse, G.B., 2013. Vegetation phenology can be captured with digital repeat photography and linked to variability of root nutrition in Hedysarum alpinum. *Applied Vegetation Science*. 16, 317–324.

Osborne, C.P., Charles-Dominique, T., Stevens, N., Bond, W.J., Midgley, G. and Lehmann, C.E., 2018. Human impacts in African savannas are mediated by plant functional traits. *New Phytologist*, 220(1), 10-24.

Piao, S., Liu, Q., Chen, A., Janssens, I.A., Fu, Y., Dai, J., Liu, L., Lian, X., Shen, M. and Zhu, X., 2019. Plant phenology and global climate change: Current progresses and challenges. *Global Change Biology*, 25(6), 1922-1940.

Planet Team (2017). Planet Application Program Interface*: In Space for Life on Earth*. San Francisco, CA.

QGIS Development Team 2020. QGIS Geographic Information System. Open Source Geospatial Foundation Project. http://qgis.osgeo.org

Root, T.L., Price, J.T., Hall, K.R., Schneider, S.H., Rosenzweig, C. and Pounds, J.A., 2003. Fingerprints of global warming on wild animals and plants. *Nature*, 421(6918), 57-60.

Roy, D.P., Wulder, M.A., Loveland, T.R., Woodcock, C.E., Allen, R.G., Anderson, M.C., Helder, D., Irons, J.R., Johnson, D.M., Kennedy, R. and Scambos, T.A., 2014. Landsat-8: Science and product vision for terrestrial global change research. *Remote Sensing of Environment*, 145, 154-172.

Santin-Janin, H., Garel, M., Chapuis, J.L. and Pontier, D., 2009. Assessing the performance of NDVI as a proxy for plant biomass using non-linear models: a case study on the Kerguelen archipelago. *Polar Biology*, 32(6), 861-871.

Scholes, R.J. and Archer, S.R., 1997. Tree-grass interactions in savannas. *Annual Review of Ecology and Systematics*, 28(1), 517-544.

Shackleton, C.M. and Scholes, R.J., 2011. Above ground woody community attributes, biomass, and carbon stocks along a rainfall gradient in the savannas of the central Lowveld, South Africa. *South African Journal of Botany*, 77(1), 184-192.

Sherry, R.A., Zhou, X., Gu, S., Arnone, J.A., Schimel, D.S., Verburg, P.S., Wallace, L.L. and Luo, Y., 2007. Divergence of reproductive phenology under climate warming. *Proceedings of the National Academy of Sciences*, 104(1), 198-202.

Shoko, C., Mutanga, O. and Dube, T., 2016. Progress in the remote sensing of C3 and C4 grass species aboveground biomass over time and space. *ISPRS Journal of Photogrammetry and Remote Sensing*, 120, 13-24.

Slaton, M.R., Raymond Hunt Jr, E. and Smith, W.K., 2001. Estimating near-infrared leaf reflectance from leaf structural characteristics. *American Journal of Botany*, 88(2), 278-284.

Smit, I.P., Asner, G.P., Govender, N., Kennedy-Bowdoin, T., Knapp, D.E. and Jacobson, J., 2010. Effects of fire on woody vegetation structure in African savanna. *Ecological Applications*, 20(7), 1865-1875.

Tang, J., Körner, C., Muraoka, H., Piao, S., Shen, M., Thackeray, S.J. and Yang, X., 2016. Emerging opportunities and challenges in phenology: a review. *Ecosphere*, 7(8), e01436.

Tucker, C.J., 1979. Red and photographic infrared linear combinations for monitoring vegetation. *Remote Sensing of Environment*, 8(2), 127-150.

Twine, W.C., 2005. Socio-economic transitions influence vegetation change in the communal rangelands of the South African Lowveld. *African Journal of Range and Forage Science*, 22(2), 93-99.

Tylianakis, J.M., Didham, R.K., Bascompte, J. and Wardle, D.A., 2008. Global change and species interactions in terrestrial ecosystems. *Ecology Letters*, 11(12), 1351-1363.

Ustin, S.L. and Gamon, J.A., 2010. Remote sensing of plant functional types. *New Phytologist*, 186(4), 795-816.

Van Wilgen, BW, Biggs, HC, O'Regan, SP, Mare, N., 2000. A fire history of the savanna ecosystems in the Kruger National Park, South Africa, between 1941 and 1996. *South African Journal of Science*, 96(4), 167-178.

Verhulst, N. and Govaerts, B., 2010. The normalized difference vegetation index (NDVI) GreenSeekerTM handheld sensor. *Toward the integrated evaluation of crop management. Part A: Concepts and case studies*.

Visser, M.E., Both, C. and Lambrechts, M.M., 2004. Global climate change leads to mistimed avian reproduction. *Advances in Ecological Research*, 35, 89-110.

Walker, J.J., De Beurs, K.M. and Wynne, R.H., 2014. Dryland vegetation phenology across an elevation gradient in Arizona, USA, investigated with fused MODIS and Landsat data. *Remote Sensing of Environment*, 144, 85-97.

Wang, Q., Adiku, S., Tenhunen, J. and Granier, A., 2005. On the relationship of NDVI with leaf area index in a deciduous forest site. *Remote Sensing of Environment*, 94(2), 244-255.

Wessels, K.J., Mathieu, R., Erasmus, B.F.N., Asner, G.P., Smit, I.P.J., Van Aardt, J.A.N., Main, R., Fisher, J., Marais, W., Kennedy-Bowdoin, T., and Knapp, D.E., 2011. Impact of

communal land use and conservation on woody vegetation structure in the Lowveld savannas of South Africa. *Forest Ecology and Management*, 261(1), 19-29.

Wessels, K.J., Prince, S.D., Zambatis, N., MacFadyen, S., Frost, P.E. and Van Zyl, D., 2006. Relationship between herbaceous biomass and 1-km2 Advanced Very High Resolution Radiometer (AVHRR) NDVI in Kruger National Park, South Africa. *International Journal of Remote Sensing*, 27(5), 951-973.

White, M.A., de Beurs, K.M., Didan, K., Inouye, D.W., Richardson, A.D., Jensen, O.P., O'keefe, J., Zhang, G., Nemani, R.R., van Leeuwen, W.J. and Brown, J.F., 2009. Intercomparison, interpretation, and assessment of spring phenology in North America estimated from remote sensing for 1982–2006. *Global Change Biology*, 15(10), 2335-2359.

Whitecross, M.A., Witkowski, E.T.F. and Archibald, S., 2016. No two are the same: Assessing variability in broad-leaved savanna tree phenology, with watering, from 2012 to 2014 at Nylsvley, South Africa. *South African Journal of Botany*, 105, 123-132.

Wiens, J.A., 1989. Spatial scaling in ecology. *Functional Ecology*, 3(4), 385-397.

Woellert, K., Ehrenfreund, P., Ricco, A.J. and Hertzfeld, H., 2011. Cubesats: Cost-effective science and technology platforms for emerging and developing nations. *Advances in Space Research*, 47(4), 663-684.

Wolf, A.A., Zavaleta, E.S. and Selmants, P.C., 2017. Flowering phenology shifts in response to biodiversity loss. *Proceedings of the National Academy of Sciences*, 114(13), 3463-3468.

Wolkovich, E.M., Cook, B.I., Allen, J.M., Crimmins, T.M., Betancourt, J.L., Travers, S.E., Pau, S., Regetz, J., Davies, T.J., Kraft, N.J., and Ault, T.R., 2012. Warming experiments underpredict plant phenological responses to climate change. *Nature*, 485(7399), 494-497.

Xue, J. and Su, B., 2017. Significant remote sensing vegetation indices: A review of developments and applications. *Journal of Sensors*, *2017*.

Zeng, L., Wardlow, B.D., Xiang, D., Hu, S. and Li, D., 2020. A review of vegetation phenological metrics extraction using time-series, multispectral satellite data. *Remote Sensing of Environment*, 237, 111511.

Zhang, J., Liu, X., Liang, Y., Cao, Q., Tian, Y., Zhu, Y., Cao, W. and Liu, X., 2019. Using a portable active sensor to monitor growth parameters and predict grain yield of winter wheat. *Sensors*, 19(5), 1108.

Zhang, X., Friedl, M.A., Schaaf, C.B., Strahler, A.H., Hodges, J.C., Gao, F., Reed, B.C. and Huete, A., 2003. Monitoring vegetation phenology using MODIS. *Remote Sensing of Environment*, 84(3), 471-475.

Zhang, Z., Lan, Y., Wu, P. and Han, W., 2015. Optimum Monitoring Time for the Normalized Difference Vegetation Index of Crops. *Transactions of the ASABE*, 58(3), 641-647.

CHAPTER TWO: The relationship between herbaceous biomass and NDVI across a range of spatial scales in contrasting savanna landscapes, South Africa

2.1. Abstract

Monitoring vegetation biomass through the use of satellite remote sensing is critical to our understanding of large scale ecosystem dynamics. Many studies have used coarse scale NDVI products such as AVHRR (1 km) and MODIS (250 m) to monitor vegetation biomass with constructive results. However, in heterogeneous environments such as savannas, the spatial scale of NDVI products can influence the accuracy of biomass estimates. Here, I compared the relationships between NDVI at various spatial scales, and *in situ* biomass estimates from both Closed and Open canopy cover areas in a semi-arid savanna. A spatially nested data collection process was followed, allowing for NDVI-Biomass relationships to be established across spatial scales using regression models. The NDVI variability across spatial scales was calculated to compare the degree of variability different spatial scales capture. The results indicated that Sentinel (10 m) was the best predictor of herbaceous biomass in both Closed (R^2 = 0.53) and Open canopy (R^2 = 0.63). The relationship between MODIS (250 m) NDVI and biomass showed a weak relationship (R^2 = 0.4) and did not differ between Closed and Open canopy cover. I concluded that both NDVI-Biomass relationships, and NDVI variability are influenced by spatial scale in both Closed and Open canopy vegetation, which should prompt monitoring programmes to carefully consider the use of coarse scale remote sensing products.

Keywords: Biomass, Canopy cover, Heterogeneity, Land use, Monitoring, NDVI, Spatial scale

2.2. Introduction

Savanna ecosystems are characterised by the coexistence of trees and grasses with strong relations between these two plant guilds (Scholes and Archer, 1997; Sankaran *et al*., 2005). These ecosystems cover up to one-fifth of the earths' terrestrial surface and support large herds of ungulate herbivores, whilst sustaining the livelihoods of human populations in these areas (Scholes and Archer, 1997). The socio-economic and ecological significance of savanna ecosystems highlights the importance of monitoring the impacts of climate change and anthropogenic influences. However, savanna systems are particularly difficult to monitor as they are naturally heterogeneous, both spatially and temporally, with savanna structure being generally influenced by precipitation, herbivory, fire, and nutrient availability (Frost *et al*., 1986). Climate change and anthropogenic influences further complicate our ability to forecast changes and patterns in savanna landscapes (Staver, 2018). The complexity and interactions between determinants of savanna structure and composition operate differently at different spatio-temporal scales (Levick and Rogers, 2011), advocating for multi-scale approaches to savanna monitoring.

Before the advent of satellite remote sensing techniques, vegetation monitoring methods mainly involved *in situ* sampling methods such as visual observations (Catchpole and Wheeler, 1992), cuttings (Nordh and Verwijst, 2004), and compressed vegetation heights (Hakl *et al*., 2012). However, these methods are labour intensive and expensive, especially for large landscape scale analyses (Ali *et al*., 2016). Remote sensing technologies provide global vegetation coverage via Vegetation Indices (VIs). There are about 118 different VIs used as expressions of vegetation greenness (Xue and Su, 2017). One of the most commonly used VI is the Normalised Difference Vegetation Index (NDVI) which captures the absorptance of red light, and the reflectance of Near Infrared (NIR) light, characteristic of photosynthetically active vegetation (Tucker, 1979). Frequently used satellite sensor data sources for vegetation analysis include the Advanced Very High Resolution Radiometer (AVHRR), Moderate Resolution Imaging Spectroradiometer (MODIS), Landsat, Sentinel-2, and PlanetScope (Matongera *et al*., 2021). The spatial and temporal resolutions ('scales') of these data sources differ between satellite sensors, with spatial resolutions ranging from 1 km to 3 m, and temporal resolutions ranging from 16 days to daily acquisition rates. The availability (time series) of these satellite sensors ranges from 1972-present (Landsat) and more recently 2016-present (PlanetScope). The selection and use of satellite sensor data

products often involve trade-offs between the spatial and temporal resolutions and the time period for which data from a particular sensor are available. For example, sensors such as AVHRR and MODIS can detect detailed temporal changes and trends in vegetation productivity due to their frequent revisit period and extended availability going back in time. The low spatial resolution of these sensors, however, cannot detect finer spatial differences in vegetation (Shen *et al*., 2015).

The NDVI has often been used in ecological studies as a proxy for vegetation productivity (Pettorelli *et al*., 2005; Tian *et al*., 2016), with studies using this proxy to relate NDVI to vegetation biomass (Hobbs, 1995; Tucker *et al*., 1986), vegetation patterns (Lobo *et al*., 1998) and vegetation pattern responses to climate change (Guo *et al*., 2008). Understanding the link between NDVI and vegetation biomass can assist in improved monitoring efforts which in turn can inform conservation management decisions, such as fire management (Wessels *et al*., 2006) landscape carrying capacity (Long *et al*., 2010), and land degradation monitoring (Pollard *et al*., 2003; Wessels *et al*., 2004). In southern Africa, several studies have established significant relationships between NDVI and biomass (Du Plessis 1999; Wessels *et al*., 2006), however, these studies used coarse spatial resolution products which were insufficient in capturing landscape heterogeneity (Levin, 1992). Mutanga *et al*. (2012) used high spatial resolution WorldView-2 NDVI data (2 m spatial resolution) to estimate biomass in a homogenous forest landscape in northern Kwa-Zulu-Natal and were able to capture local spatial heterogeneity. No studies in southern Africa have used high spatial resolution data to relate NDVI to biomass in heterogenous landscapes such as savannas or compared NDVI-Biomass relationships across spatial scales to better understand the scale effect.

In heterogenous landscapes, coarse spatial resolution VIs are a source of uncertainty and bias, given that they record VI values that come from mixed composition vegetation (i.e., a mix of trees and grasses) within their spatial footprint (Zhang *et al*., 2017; Park *et al*., 2021). This calls for the use of finer spatial resolution satellite products in spatially heterogenous landscapes which are more likely to capture fine scale vegetation variability (Zeng *et al*., 2020), thus being more representative of vegetation composition and structure.

Another consideration in establishing a relationship between VIs and biomass is the use of an appropriate regression approach for biomass estimation (Eisfelder *et al*., 2012). The coefficient of determination (R^2) between coarse spatial resolution VIs and biomass in semi-

arid areas have been shown to range between 0.32-0.95 (Eisfelder *et al*., 2012). One of the reasons for this variation is that different studies have used different regression approaches. In addition, the performance of the different regression models is site-specific. It has therefore been suggested that a multi-scale approach (Wu, 2004) to estimating biomass may provide more accurate results (Eisfelder *et al*., 2012).

Establishing a relationship between biomass and NDVI in a savanna environment is challenging for several reasons. Besides the heterogeneous nature of savanna ecosystems (Scanlon *et al*., 2005), other factors that play a role are soil reflectance (Montandon and Small, 2008), limited availability of field data (Zeng *et al*., 2020), and temporal limitations of satellite derived vegetation products (Pettorelli *et al*., 2005). In savanna ecosystems, canopy cover also plays an important role in NDVI-Biomass relationship. Open canopy areas are comprised of mainly herbaceous biomass and bare ground, which are more predictive and homogenous (Sala *et al*., 2012), relative to Closed canopy areas that represent the tree layer, which is highly unpredictable and structurally heterogenous (Staver *et al*., 2017).

While it was outside the scope of this study to evaluate the effect of all these variables, the aim was to compare the NDVI-Biomass relationship, as well as NDVI variability, across a range of different spatial scales. Specifically, I set out to (1) investigate the relationship between herbaceous biomass and NDVI at different spatial scales within Closed and Open canopy vegetation, (2) establish the relationship between NDVI estimates across a range of different spatial scales, (3) understand how NDVI variability differs across spatial scales. I expected the strength of the relationship between biomass and NDVI to increase at finer scales as they are less likely to capture mixed vegetation composition signals (trees, grasses, and bare ground). I also anticipated the relationship between NDVI from different sensors to be stronger in the more homogenous Open canopy site than in the more heterogeneous Closed canopy site. Lastly, I expected NDVI spatial variability to be greater at finer scales, with variability being noticeably higher in the more heterogenous Closed canopy site than in the Open canopy site.

2.3. Methods

2.3.1. Data Collection

Extracting NDVI from sensors

I identified 14 MODIS NDVI scenes that were available for my study period which corresponded with the field data collection dates (14 September 2020-16 April 2021). Both Sentinel and PlanetScope NDVI scenes closely coincided with MODIS dates, however, for Landsat, there were only 8 usable scenes in the Closed canopy site and 9 scenes in the Open canopy site that corresponded with MODIS dates. Sentinel provides a maximum of three images within the period that one MODIS composite is acquired. From these three Sentinel images, I used the highest quality image i.e., the image with the least amount of cloud cover. In instances where there was full cloud cover in all three images, I would then use the closest image to that 16-day period (4 of these instances occurred). Due to the download quota of PlanetScope data and processing costs, I only acquired PlanetScope data at the spatial extent of Sentinel pixels (10 m). Between 9 and 12 PlanetScope pixels fit within the spatial extent of one Sentinel pixel. This was done to make sure that the correct PlanetScope pixels were selected in instances where GPS coordinates did not accurately capture the true position of field data collection points.

In situ NDVI measurements

To evaluate *in situ* NDVI measurements, I used the SpectroSense2+ (hereon referred to as SS2) 4 Channel sensors (Skye Instruments LTD, Powys, UK). The sensors were calibrated to match the MODIS sensors with each channel being calibrated as follows; Channel 1-459-479 nm, Channel 2-545-565 nm, Channel 3-620-670 nm, and Channel 4-841-876 nm. Channels 3 and 4 were used to calculate NDVI as they acquire Red and NIR wavelengths, respectively. The sensors are attached to an extension pole which allows for the height of the sensors to be adjusted, and subsequently determines the instantaneous field of view. I set the height of the extension pole to 1.8 m (maximum height) which provided an area of measurement of 0.50 m^2. At each field data collection point (Figure 1.2, Chapter 1) I recorded one NDVI reading directly on marked locations with a further three readings within 2 m of the marked area to account for NDVI variation within the sampled area. In areas with

dense canopy cover, NDVI readings were captured where incident light was sufficient for the sensor to capture a stable reading (no more than 5 m from marked locations), as canopy cover affects the sensors' ratio of incoming reflected and incident light when calculating vegetation indices. I captured all data between 8:30 and 13:00 to reduce the effects of morning humidity and shadows (Zhang et al., 2015). Unfortunately, due to the impacts of Covid-19 lockdown and slow customs processing on equipment imports, the SS2 and extension pole were only received in time to capture the last five weeks of the field data collection period. This setback did not allow for *in situ* NDVI trends to be analysed, but the scaling of NDVI and NDVI/Biomass correlations could be explored.

Biomass sampling

I used a Disc-Pasture Meter (DPM) to take biomass measurements at each marked field collection point (Figure 1.2, Chapter 1). The DPM comprises a pole and sliding disk attached. The pole is placed on the ground and the sliding disk is dropped from the top of the pole. The height at which the sliding disk lands is recorded in length measurements (cm) located on the pole. I collected a total of 3360 DPM readings over the 14 week data collection period (240 per week). I then converted these measurements to biomass (kg/ha^{-1}) using an allometric equation developed for the neighbouring Kruger National Park (Equation 2; Zambatis et al., 2006).

$$\text{Kg ha}^{-1} = \left[31.7176\left(0.3218\ {}^{1}/_{x}\right) \times^{0.2834}\right]^{2} \qquad \text{(Equation 2)}$$

I used the measurements of biomass, derived from the DPM to establish the relationship between NDVI measurements from all sensors and ground biomass, and if these relationships differed between Closed and Open canopy.

Photographs and canopy cover estimates

At each field data collection point, I took five RGB format digital photographs (Canon PowerShot SX60 HS camera) with a pixel resolution of the 4608 x 3456, one directly above the sampled area, and four in the north, east, south, and west directions. The top of the

photograph frame was roughly aligned to match the borders of Sentinel pixels ~5 m to capture the representative vegetation within the sampled Sentinel pixel. Field data was captured in the middle of each Sentinel pixel, thus 5 m in all directions would represent the spatial borders of one Sentinel pixel. I recorded the canopy cover percentage at each sample site based on visual estimates, at 0%, 25%, 50%, 75% and 100% intervals. The photographs were used in this study to improve the accuracy of canopy cover estimates and assisted with the interpretation of results, particularly the timing of green-up and senescence of vegetation. A total of 16800 photographs were captured during the data collection period which will be archived for future studies in this area. An example demonstrating the contrast in vegetation composition between the Closed and Open canopy sites is provided in Figure 2.1.

2.3.2. Data Analysis

Biomass and NDVI comparisons

I calculated the mean and standard deviation (SD) of NDVI for each satellite pixel (MODIS 250 m, Landsat 30 m, Sentinel 10 m, and Planet 3 m) and the weekly biomass measurements over the 14 week period. I then calculated the average weekly mean value for Closed and Open canopy, respectively (Figure 2.2). To determine if there were differences between mean pixel biomass in Closed canopy, I used a non-parametric Kruskal-Wallis test as the data were significantly different from a normal distribution even after logarithmic transformation. Thereafter, I used the Games-Howell test to determine which pixels were significantly different. To test for differences in mean biomass between pixels in Open canopy, a parametric ANOVA followed by Tukey's 'Honest Significant Difference' test, was used as data showed a normal distribution with no evidence of unequal variance. I used the Pettitt test, which is a nonparametric test that can identify the probable point at which there is a significant shift in the central tendency of a time series (Pettitt, 1979), to identify statistically significant breakpoints in the distributions of mean biomass, biomass SDs, and the mean NDVI from each sensor. To determine if there were differences in the NDVI ranges between sensors in each canopy cover type, I used the Kruskal-Wallis test as the NDVI data from all sensors in both canopy cover types were significantly different from a normal distribution and contained outliers. I then followed up with a Dunn's test to determine which sensors' NDVI were significantly different from each other. I used the Kruskal-Wallis test to

determine if there were differences in weekly NDVI between all sensors and a pairwise rank sum test to identify which sensors' NDVI was significantly different for each week.

Relationship between biomass and NDVI at different scales

I tested the relationship between biomass and NDVI from MODIS, Landsat, Sentinel and PlanetScope using exponential regression models as they are better suited to biomass and NDVI relationships, compared to linear models (Fan *et al*., 2009; Umarhadi and Syarif, 2017). Coefficients of determination (R^2) derived from regression models tell us how much variation in the data is accounted for by the regression model (Bewick *et al*., 2003). For example, an R^2 of 0.5 suggests that 50% of the total variation in *y* is accounted for by the model, and the remaining 50% variation is caused by an unknown variable. For the SS2 (Handheld NDVI reader) I tested the relationship between SS2 NDVI and biomass using an exponential regression. Linear regressions were used to determine the relationship between SS2 NDVI and the mean weekly NDVI of MODIS, Landsat, Sentinel, and PlanetScope. Only data that corresponded with the availability of SS2 data (5 weeks) were used.

Relationship between MODIS NDVI and aggregated Landsat and Sentinel NDVI

To determine how NDVI from Landsat and Sentinel relate to MODIS NDVI, all the pixels of Landsat and Sentinel that occurred within the spatial extent of each MODIS pixel were aggregated to the MODIS extent (i.e., an average of all pixels within one MODIS pixel). These aggregated NDVI values of Landsat and Sentinel were then used in linear regression models to determine the relationships to the MODIS pixel values.

Comparing NDVI variation between different sensors

To determine how NDVI varies between sensors, I calculated the weekly mean SD of Closed and Open canopy for each sensor. The SD details how vegetation varies in the landscape and captures savanna heterogeneity, which changes at different spatial scales. To calculate the mean NDVI SD for MODIS, I averaged the NDVI SD of the 6 pixels for each week in both Closed and Open canopy. For the remaining sensors, the mean SD of the 20 sampled pixels within a MODIS pixel were then averaged to create a weekly mean SD for

both Closed and Open canopy. I used a one-way ANOVA to determine if there is a significant difference between the mean SD of all sensors, followed by a Tukey's 'Honest Significant Difference' test to determine which sensor' mean SD was significantly different. To identify significant breakpoints in the mean SD of each sensor, I used the Pettitt test. All data analyses were conducted in R version 1.4.1106 (R Core Team, 2020, APPENDIX B).

2.4. Results

Biomass comparison and distribution

Biomass varied significantly between Closed and Open canopy ($t_{(18)} = 9.04$, $p = <0.001$). Mean biomass in Closed canopy ranged between 954.8 to 1900.8 kg/ha with the highest biomass occurring in week 10 (1900.8kg/ha) and the lowest in week 3 (954.8 kg/ha). Mean biomass in Closed canopy showed statistically significant differences between sampled pixels ($H_{(5)} = 35.3$, $p = 0.001$), however only pixel 2 had significantly lower biomass than all the other pixels (Figure 2.4 a). Mean biomass in Open canopy ranged between 265.2 kg/ha to 745.7 kg/ha with the highest mean biomass occurring in week 11 (745.7 kg/ha) and the lowest in week 3 (265.2 kg/ha^{-1}). Mean biomass per pixel in Open canopy was consistently low and significantly different between pixels ($F_{(5, 78)} = 9.8$, $p = 0.001$), with the mean biomass of pixel 6 being significantly lower than all other pixels, and pixels 1 and 5 significantly higher than pixel 3 (Figure 2.3 b). Visual canopy cover estimates ranged between 38% - 59% in Closed canopy and between 8% - 17% in Open canopy.

Mean biomass was 1438 kg/ha in Closed canopy and 500 kg/ha in Open canopy, showing a mean difference of 938 kg/ha between the two canopy cover types (Figure 2.4 a - b). There was a significant change point in mean biomass at week 7 in both Closed and Open canopy (p=0.014). Mean biomass SD in Closed canopy was 348 kg/ha and 136 kg/ha in Open canopy, showing higher biomass variation in the Closed canopy site (Figure 2.4 c - d). There were significant change points in mean biomass SD at week 7 (p=0.014) in Closed canopy and at week 6 (p=0.026) in Open canopy.

Sensor NDVI distribution and changes through time

The distribution of NDVI samples recorded over the 14 week collection period of each sensor in Closed and Open canopy cover shows how sensor specific NDVI ranges across spatial scales (Figure 2.5). The Kruskal Wallis test showed there were significant differences in mean NDVI in both Closed canopy ($H_{(3)} = 7.4$, $p = 0.05$), and Open canopy ($H_{(3)} = 7.3$, $p = 0.05$), with the Dunn test indicating that in both canopy cover types, Sentinel NDVI was significantly lower than for MODIS and PlanetScope, but not different to Landsat NDVI values. The NDVI SD was higher in Closed canopy (MODIS = 0.146; Landsat = 0.174; Sentinel = 0.165; PlanetScope = 0.172) for all sensors compared to Open canopy (MODIS = 0.112; Landsat = 0.133; Sentinel = 0.122; PlanetScope = 0.133). In both canopy cover types, Landsat had the largest NDVI range when outliers were removed, with an NDVI range of 0.52 in Closed canopy and 0.35 in Open canopy.

The range of weekly sampled NDVI values between sensors in both canopy cover types shows how NDVI values rapidly increased in the first 5 weeks and how NDVI variation increased between week 6 to week 8 (Figure 2.6 a-b). There were significant differences in sensor specific NDVI for all weeks in Closed canopy. In Open canopy, only weeks 10 ($H_{(3)} = 1.4$, $p = 0.067$) and 11 ($H_{(3)} = 1.6$, $p = 0.16$) showed no significant difference in NDVI between sensors. The pairwise rank sum comparisons (Table 2A, APPENDIX A) showed that in Closed canopy there were significant differences between all sensors from week 1 to 5, thereafter only Sentinel was significantly lower than other sensors in most weeks. This pattern was similar for the weekly NDVI in Open canopy, however, the NDVI variation was higher for all sensors in Open canopy between weeks 8 to week 14 compared to those in Closed canopy.

The average weekly NDVI values of each sensor as well as the rate at which NDVI increases showed clear differences between the Open and Closed canopy types (Figure 2.7). MODIS had the highest average NDVI in both canopy covers at 0.66 in the Closed canopy and 0.53 in the Open canopy. Sentinel had the lowest average NDVI in both canopy covers with 0.56 and 0.44 for Closed and Open canopy, respectively. PlanetScope and Landsat NDVI values were intermediate with respect to the MODIS and Sentinel NDVI values. The change points in the 14 week time series differed between sensors in both canopy covers. In Closed canopy, both MODIS and Landsat ($p = 0.014$) had probable change points at week 7 ($p = 0.16$), while Sentinel ($p = 0.032$) and PlanetScope ($p = 0.026$) had earlier change points

at week 5 and 6 respectively. In Open canopy, MODIS had the earliest change-point at week 6 ($p = 0.018$), with both Landsat and Sentinel having change points at week 8 ($p = 0.018$) and PlanetScope at week 7 ($p = 0.014$).

Relationship between satellite sensor NDVI and biomass

Exponential regressions with MODIS as the predictor variable in Closed and Open canopy was statistically significant, with a moderately positive relationship in both canopies (Closed canopy: $F_{(1, 12)} = 8.03$, $R^2 = 0.4$, $p = 0.015$; Open canopy: $F_{(1, 12)} = 9.49$, $R^2 = 0.44$, $p = 0.0095$, Figure 2.8 a-b), showing only a 4% difference in the coefficient of determination between canopy covers. The relationship between Landsat and biomass was statistically significant, with a moderate positive relationship in both canopies (Closed canopy: $F_{(1, 5)} = 10.07$, $R^2 = 0.67$, $p = 0.024$; Open canopy: $F_{(1, 7)} = 11.65$, $R^2 = 0.62$, $p = 0.011$, Figure 2.8 c-d), showing a 5% difference in the coefficient of determination between canopy covers. The NDVI-Biomass relationship for Sentinel was statistically significant, with a moderate relationship in both canopies. (Closed canopy: $F_{(1, 12)} = 13.76$, $R^2 = 0.53$, $p = 0.003$; Open canopy: $F_{(1, 12)} = 20.24$, $R^2 = 0.63$, $p = 0.0007$, Figure 2.8 e-f), showing a 10% difference in the coefficient of determination between canopy covers. Lastly, the PlanetScope NDVI-Biomass relationship was statistically significant, with a moderate positive relationship in both canopies (Closed canopy - $F_{(1, 12)} = 14.12$, $R^2 = 0.54$, $p = 0.002$, Open canopy-$F_{(1, 12)} = 18.32$, $R^2 = 6$, $p = 0.001$, Figure 2.8 g-h), with a 6% difference in the coefficient of determination between canopy covers.

Relationship between in situ NDVI (SS2), biomass and satellite sensors

The relationship between *in situ* NDVI and mean biomass in Closed canopy was significant ($F_{(1, 3)} = 41.89$, $R^2 = 0.92$, $p = 0.007$), whereas this relationship was not significant in Open canopy with a lower coefficient of determination of 0.54 (Figure 2.9 a-b). The comparison between *in situ* NDVI and satellite sensor NDVI showed that in Closed canopy, the NDVI values for all sensors, except for Sentinel ($t_{(8)} = -0.4$, $p = 0.7$), were significantly higher than *in situ* NDVI. In Open canopy, only MODIS ($t_{(6.7)} = -2.5$, $p = 0.04$) and PlanetScope ($t_{(7.1)} = -3.0$, $p = 0.01$) were significantly higher than *in situ* NDVI. The relationships between *in situ* NDVI and the various satellite sensor's NDVI (Figure 2.10 a-h)

showed that there were significant relationships between MODIS ($F_{(1, 3)} = 22.09$, $R^2 = 0.88$, $p = 0.01$, Figure 2.10 a) and Landsat ($F_{(1, 3)} = 22.04$, $R^2 = 0.88$, $p = 0.01$, Figure 2.10 b) in Closed canopy. The relationship between finer scale NDVI (Sentinel and PlanetScope) and MODIS NDVI in Closed canopy was not significant for both Sentinel ($R^2 = 0.13$) and PlanetScope ($R^2 = 0.06$). Similarly, there was a significant relationship between *in situ* NDVI and MODIS ($F_{(1, 3)} = 16.4$, $R^2 = 0.85$, $p = 0.02$, Figure 2.10 e) and Landsat ($F_{(1, 3)} = 18.17$, $p = 0.02$, Figure 2.10 f) in Open canopy, with this relationship deteriorating for Sentinel ($R^2 = 0.35$) and PlanetScope ($R^2 = <0.01$). The difference in coefficient of determination between *in situ* NDVI and Sentinel NDVI in Closed and Open canopy indicated that this relationship was substantially higher (~0.20) in Open canopy, whereas there was no relationship at all between *in situ* NDVI and PlanetScope NDVI.

Relationship between MODIS NDVI and aggregated Landsat and Sentinel NDVI at MODIS scale

The linear regression with aggregated Landsat as the predictor variable in Closed and Open canopy was statistically significant, with a moderate positive relationship in Closed canopy, and a strong positive relationship in Open canopy (Closed canopy: $F_{(1, 6)} = 11.54$, $R^2 = 0.66$, $p = 0.014$, Figure 2.11 a; Open canopy: $F_{(1, 7)} = 19.31$, $R^2 = 0.73$, $p = 0.003$, Figure 2.11 b). The linear regression with aggregated Sentinel NDVI as the predictor variable in Closed and Open canopy was statistically significant, with a very strong relationship in both canopies (Closed canopy: $F_{(1, 12)} = 108.2$, $R^2 = 0.9$, $p = 0.001$, Figure 2.11 c; Open canopy: $F_{(1, 12)} = 79.6$, $R^2 = 0.87$, $p = 0.001$, Figure 2.11 d).

Comparison of NDVI variability between different satellite sensors

In both canopy types, MODIS had the lowest mean SD of 0.020 in Closed canopy and 0.028 in Open canopy (Figure 2.12). The SD of NDVI between Landsat, Sentinel, and PlanetScope ranged between 0.040-0.053 in Closed canopy, with a range of 0.050-0.056 in Open canopy, indicating similar variations in both sites. There was a significant difference in the NDVI SD between sensors in both Closed canopy ($F_{(3, 52)} = 15.4$, $p<0.001$) and Open canopy ($F_{(3, 52)} = 7.86$, $p<0.001$). Post hoc comparisons indicated that the NDVI SD of MODIS in both Closed and Open canopy sites was significantly lower ($p < 0.01$) than the

NDVI from the other sensors. In Closed canopy only the SD of Landsat had a significant change point at week 5 ($p = 0.03$), whereas the insignificant but probable change points of MODIS, Sentinel, and PlanetScope occurred at week 2, week 3, and week 3 respectively. The change points of NDVI SD in Open canopy were noticeably later than for Closed canopy, with significant change points for MODIS and Landsat occurring at week 6 ($p = 0.02$) and week 8 ($p = 0.01$) respectively. Insignificant but probable change points for Sentinel and PlanetScope NDVI SD in Open canopy occurred at week 4 ($p = 0.1$) and week 3 ($p = 0.2$) respectively.

2.5. Discussion

This study aimed to determine the scaling relationship between *in situ* biomass and NDVI in Closed and Open canopy savanna vegetation, and the scaling relationship between the NDVI and NDVI SD of the different sensors, respectively. I found that herbaceous biomass was, as expected, significantly higher in Closed canopy owing to reduced grazing pressure and longer fire revisit period, but herbaceous biomass variability was similar in both canopy cover types. The average NDVI value range was low at the MODIS scale and as expected, increased toward finer scales, with all NDVI ranges being higher in Closed canopy. MODIS NDVI had the weakest relationship with herbaceous biomass with only a slight difference between canopy cover types, while Landsat NDVI had the strongest relationship with herbaceous biomass in both canopy cover types. There was a strong relationship between *in situ* NDVI and coarse resolution MODIS and Landsat NDVI. The relationship between MODIS and aggregated Landsat and Sentinel NDVI was overall stronger for Sentinel, with both sensors having stronger relationships in Open canopy. NDVI variability was significantly lower at MODIS spatial scale compared to all other sensors, with overall variability being slightly higher in Open canopy.

Herbaceous biomass differed significantly between Closed and Open canopy vegetation and between several sampled MODIS pixels. Mean pixel herbaceous biomass was significantly higher in Closed canopy vegetation (1438 ± 348 kg/ha) compared to that of Open canopy (500 ± 136 kg/ha) indicating a 187% difference in mean herbaceous biomass between the two canopy cover types. This large difference could be attributed to several

factors, including 1) tree-grass ratios between sites (Dantas *et al*., 2015), 2) grazing intensity, and 3) land use type (Higgins *et al*., 1999).

Tree-grass ratios differed between these two sites with peak season canopy cover being 59% in Closed canopy and 17% in the Open canopy site. These differences in canopy cover (tree cover) can influence herbaceous biomass either negatively or positively. For instance, positive influences such as increased soil nutrient levels below tree canopies (Belsky *et al*., 1994), reduced evapotranspiration (Ludwig *et al*., 2004), and deterring grazing via low hanging thorny canopies (Riginos *et al*., 2009) all facilitate increased below-canopy biomass productivity. However, high canopy cover densities can also negatively impact below-canopy biomass by limiting light access to below-canopy herbaceous (Belsky, 1994), and increasing competition for water and nutrients (Scholes and Archer, 1997). Depending on the interaction between these limiting or enabling factors associated with canopy cover, biomass can either increase (Riginos *et al*. 2009) or decrease (Whitecross *et al*, 2016) below-canopy cover.

Disturbances such as fires, human utilisation and feeding by herbivores also influence tree-grass ratios (Scholes and Archer, 1997). In the Closed canopy site, these disturbances are limited to mainly browsing by the few free-ranging herbivores found here. In contrast to this, lower herbaceous biomass in the Open canopy site is a result of disturbances linked to utilisation, such as grazing and fuel wood collection which impact not only the tree-grass relationships (Scholes and Archer, 1997) but also the abundance of unpalatable vegetation present through woody plant encroachment (Roques *et al*., 2001). The low number of ungulates present in the Closed canopy site (WRF) relative to the large quantity of livestock in the Open canopy site (TCR), where average cattle and goat herd sizes in this area are 19.8 and 5.6 per livestock owning household respectively (Dovie *et al.*, 2006), which further explains the large difference in herbaceous biomass between the two sites.

The overall mean herbaceous biomass in Closed and Open canopy showed a continuous increase in herbaceous biomass starting at week 3 (early October 2020). Vegetation in semi-arid savanna environments is closely linked to the availability of water with the onset of vegetation green-up usually occurring after more than 15 mm of rainfall has fallen (Archibald and Scholes, 2007; Hachigonta *et al*., 2008). The biomass increase (green-up) occurrence in this study is comparable with findings by Whitecross *et al.* (2017), where the mean green-up date between 2003 - 2014 for savanna landscapes in South Africa

occurred between days 100-110 (day 100 = 9 Oct). Rainfall data from the WRF weather station shows a total of 123.2 mm during October 2020 with 60.4 mm (49%) of the total occurring within the first 5 days of October. This is well above the average October rainfall compared to total rainfall occurring during October in previous years (2019-10 mm, 2018-7.6 mm, 2017-12 mm, 2016-31.6 mm) (Table 7A, APPENDIX A). This large amount of October rainfall does not necessarily influence the green-up date but rather the end of the season is likely to be extended. This will be discussed in chapter 3 where phenological metrics are analysed. Notably, the change points in mean biomass occurred in week 7 (Early December) for both Closed and Open canopy sites, suggesting that the timing of herbaceous biomass increases were similar in both sites.

Drought events in the region are associated with climate variability (Malherbe *et al*., 2016) with the last major drought occurring in 2015/2016 due to the El Niño–Southern Oscillation. Savannas are resilient environments and can recover from moderate periods of drought with herbaceous and woody plants recovering within one to two years (Swemmer *et al*., 2018). Short-term droughts do not have a significant impact on trees but do impact grasses in the Lowveld region (Swemmer, 2020). This may explain some of the variation in mean biomass between canopy cover types but should not be considered a major factor as the last intense drought occurred in the 2015/2016 season. Although the study area received below average rainfall during the 2017/2018 season this can be viewed as part of the natural rainfall variability associated with savanna environments (Knapp and Smith, 2001). Peak biomass was reached at week 10 (January 2021) in Closed canopy and later, week 11, in Open canopy (February 2021). This delay in peak biomass in the Open canopy site may be due to anthropological influences such as biomass extraction via grazing and fuelwood collection (Higgins *et al*., 1999), which continuously slows grass recovery and subsequently extends the period at which peak biomass occurs. However, this assumption needs to consider the long-term variability of phenological phases associated with savanna landscapes. Herbaceous biomass variability was slightly higher in Closed canopy compared to Open canopy. The average SD was 24% and 27% of the mean herbaceous biomass in Closed and Open canopy, respectively. Variability also increased as mean herbaceous biomass increased in both Closed and Open canopy. In a similar study, Wessels *et al.* (2006) measured a SD of 50% of the mean biomass across the full extent of KNP. This large variation was suggested to be due to differences in herbivory intensity at sampling sites. This could explain why biomass variability in the Open canopy site is slightly higher than Closed canopy biomass variability,

as grazing intensity is more extensive in the Open canopy site compared to the Closed canopy site. In the Open canopy site, some sampled areas did not allow access to grazers due to fences and impenetrable bush encroachment which would also influence herbaceous biomass differences.

The NDVI value range of each sensors' time series increased at finer spatial scales in both canopy cover types, except for Landsat which has the highest range of all sensors in both canopy cover types, probably due to the lower sample size. This demonstrates the unpredictability of savannas between spatial scales, as vegetation structure (specifically trees layers) is unpredictable at the local scale, but predictability increases towards larger scales (Staver, 2018) due to spatial aggregation (Wiens, 1989). The NDVI range of all sensors was on average 27% higher in Closed canopy, reaffirming the more heterogeneous nature and higher biomass of the Closed canopy site. Sensor specific weekly NDVI ranges show that between week 1 and week 5 (September-November) MODIS NDVI is higher than all other sensors in both canopy cover types, however, the rate of NDVI increases between week 1-5 differs between sensors and canopy cover types. These differences in the rate of NDVI increase, from a canopy type perspective, could be due to 'early-greener' tree species which are able to flush new leaves before the arrival of seasonal rainfall (Archibald and Scholes, 2007), compared to herbaceous vegetation (predominantly in the Open canopy site) where green-up is strongly linked to water availability (February *et al*., 2013). This 'head-start' in terms of green-up between Closed and Open canopy would explain why the NDVI increase between weeks 1 and 5 is far greater in Closed canopy. In Closed canopy the finer resolutions of Sentinel and PlanetScope showed the greatest increases in NDVI between weeks 1-5, displaying their ability to obtain finer scale variation associated with the heterogeneous nature of the Closed canopy site. Contrastingly, in Open canopy, coarse resolution MODIS showed a similar percentage increase (76%) in NDVI between week 1-5, to PlanetScope (71%), showing that the 'scale effect' is less influential in homogenous landscapes.

The coefficients of determination (R^2) for all sensors at both sites ranged between 0.38 to 0.67, with higher values occurring in Open canopy. Wessels *et al.* (2006) investigated the NDVI-Biomass relationship using AVHRR NDVI at 1-km^2 resolution in KNP and found an average R^2 of 0.36. This is similar to the herbaceous biomass - MODIS relationship in the Closed canopy site (R^2=0.40). Interestingly, the study by Wessels *et al.* (2006), found that tree cover did not have a major influence on NDVI-Biomass relationship. This may be due to the larger 1 km spatial resolution of AVHRR which would aggregate the variations between

Closed and Open canopy within its measured NDVI. Open canopy herbaceous biomass - MODIS relationship (R^2=0.44) was very similar to the relationship in Closed canopy (R^2=0.40), which is the lowest difference between Closed and Open canopy cover of all sensors, suggesting that tree canopy cover does not influence the biomass-NDVI relationship at MODIS scale (250 m), within these two sites. However, given that these data are from only 2 case study sites, further research is needed to determine if these results can be applied in larger areas and/or other contexts. Landsat NDVI showed the strongest herbaceous NDVI-Biomass relationship with R^2 of 0.64 in Closed canopy and 0.60 in Open canopy, showing a similar outcome to MODIS in terms of a small difference in the relationship between Closed and Open canopy cover. However, due to the low sample size (owing to limited Landsat scene availability), these results may be subject to Type II errors. Chapungu *et al*. (2020) used Landsat Thematic Mapper NDVI, which has a spatial resolution of 30 m, to estimate biomass in northern Zimbabwe, and found a predictability value of R^2 = 0.46 based on 20 samples. This is significantly lower than the Landsat R^2 that I found, further suggesting that the small sample size in this study may have influenced the outcome. At Sentinel and PlanetScope scale there was a larger difference in R^2 between Closed canopy (Sentinel = 0.53; PlanetScope = 0.54) and Open canopy (Sentinel = 0.63; PlanetScope 0.60). This could be due to finer scale observations capturing local variations. The NDVI-Biomass relationship would be stronger in Open canopy as it is a direct measurement, whereas in Closed canopy the NDVI is capturing measurements from the top of canopy in most instances. Given that Landsat yielded fewer cloud free samples compared to all other sensors in this study, both Sentinel and PlanetScope seem to be more accurate predictors of herbaceous biomass in this study, with both having higher R^2 values in Open canopy.

The choice of spatial resolution depends on the type of management need, where coarse resolution could be used for large regions undergoing rapid environmental change and fine resolution could be used in localised areas where heterogeneity is high (Tsalyuk *et al*., 2017). This speaks well to the herbaceous biomass-NDVI relationship between Sentinel and Planet in Closed canopy (Sentinel Closed canopy, R^2 = 0.50, Planet Closed canopy, R^2 = 0.51) and Open canopy (Sentinel Open canopy, R^2 = 0.59, Planet Open canopy, R^2 = 0.58) as these finer scales show improved predictability of herbaceous biomass. This slight increase in herbaceous biomass predictability indicates that canopy cover may influence the reliability of NDVI in measuring biomass at finer scales, whereas coarse resolution products such as MODIS and AVHRR do not seem to be influenced by canopy cover in a savanna setting.

This can also be linked to the heterogeneous nature of savanna landscapes, as coarse resolution products are likely to capture more-or-less the same ratio of grass and trees which can result in an 'averaging-effect' (Wiens, 1989).

Very fine scale NDVI measurements derived from the SS2 device showed contrasting results in the *in situ* NDVI-Biomass relationship between Closed and Open canopy. There was a very strong relationship between *in situ* NDVI and biomass in Closed canopy (R^2 = 0.92), and a moderate relationship in Open canopy (R^2 = 0.54). This strong relationship in Closed canopy may be a consequence of the effect of shadows cast by tree canopies as the reduction of incoming solar radiation can cause an increase in NDVI values (Allen *et al*., 2009; de Souza *et al*., 2021). This would inaccurately correlate with the high herbaceous biomass measurements in the Closed canopy site. Marín *et al*. (2020) found a moderate relationship (R^2 = 0.48) between fine scale NDVI (using GreenSeeker handheld crop sensor) and turfgrasses. Their results reflect a similar relationship to the NDVI-Biomass relationship in the Open canopy site of this study (R^2 = 0.54), which was not influenced by the shadow effect. For this reason, caution must be taken in the interpretation of *in situ* NDVI results derived from Closed canopy.

The relationship between *in situ* NDVI and satellite derived NDVI showed a strong relationship at coarse scales in both canopy covers (MODIS and Landsat-R^2 >0.8). However, at finer scaled Sentinel and PlanetScope, but especially particularly for PlanetScope (R^2<0.05), this relationship collapses. Although the SS2 device was calibrated to match the Red and NIR bands of MODIS, this should not significantly influence these relationships as the NDVI ranges (Figure 2.5) showed that only Sentinel was significantly different. The strong relationship between *in situ* NDVI and MODIS and Landsat may be due to the aggregation effect whereby fine scale variance is averaged out at coarser scales (Wiens, 1989), making it appear as though there is a strong relationship. Lastly, it must be noted that only 5 weekly averaged *in situ* NDVI samples (due to equipment delay) for each canopy cover type were available, thus this small sample size may result in Type II errors.

Variability changes when the scale of measurement changes, thus averaging values from finer scale to coarser scale should increase the strength of the relationship (Tarnavsky *et al*., 2008). The strength of this relationship can provide insight into the nature of heterogeneity within a region of interest (Levin, 1992). Aggregating NDVI data from Landsat and Sentinel to the spatial scale of MODIS in Closed and Open canopy, provides insights as

to how savanna vegetation predictability differs between tree and grass layers. It is expected that aggregated Landsat and Sentinel NDVI in Open canopy (predominant grass layer) will correlate with MODIS NDVI better as grass biomass has less variation between scales (Staver, 2018), compared to the tree layer in the Closed canopy site which is more variable between spatial scales. The MODIS-aggregated Landsat NDVI relationship in Closed (R^2 = 0.66) and Open (R^2 = 0.73) canopy demonstrates how MODIS NDVI relates relatively well with aggregated Landsat NDVI, but more so in the more homogenous Open canopy. The MODIS-aggregated Sentinel relationship in Closed (R^2 = 0.90) and Open (R^2 = 0.87) is significantly higher in both canopy types compared to that of aggregated Landsat. Based on these spatially aggregated results, it is apparent that; 1) the relationship between coarse scale observations (MODIS) and spatially aggregated observations improves when aggregated observations are derived at fine scale and 2) the strength of this relationship can inform us about the level of heterogeneity (e.g., the MODIS-aggregated Landsat/Sentinel is stronger in Open canopy due to the homogenous nature of that area, and vice versa for Closed canopy). Given that the level of heterogeneity can be inferred by establishing a relationship between coarse scale observation and aggregated fine scale observations (High R^2 = low heterogeneity, Low R^2 = High heterogeneity) it may be possible to monitor savanna landscapes at coarser scales whilst still accounting for fine scale variability.

The NDVI variability between sensors within Closed and Open canopy showed that variability at coarse scale (MODIS) was significantly lower than variability at smaller scales in both canopy cover types, as local scale effects are averaged out at MODIS scale. Both Closed and Open canopy had relatively low NDVI variability at MODIS scale, with both having an average NDVI variation of 0.02, which further emphasises the ‘averaging out’ effect. However, only 6 MODIS pixels were sampled in each site which may have contributed to the low average NDVI variation. Thereafter, variability increases along a decreasing spatial gradient in both Closed canopy (Landsat = 0.04, Sentinel = 0.05, PlanetScope =0.05) and Open canopy (Landsat = 0.049, Sentinel = 0.056, PlanetScope = 0.056), but are very similar in terms of variability between spatial scales. Interestingly, although very similar, the average variability in Open canopy was slightly higher compared to Closed canopy, as it is assumed that the homogenous nature of the Open canopy site would have lower variability. This slight difference could be attributed to the previously mentioned impacts of extensive grazing and resource collection in the Open canopy site as anthropogenically induced grass/tree ‘patchiness’ fluctuates through space and time (Mograbi

et al., 2019). This highlights the importance of considering land use function as a determinant of savanna variability. Looking at NDVI variability at finer scales (Sentinel and Planet) these sensors showed an increase in variability up until week 6 after which variability gradually reduced. This rapid increase in variability could be due to the difference in species-specific green-up times, and the finer scaled sensors being able to capture this. Species such as *Termilia sericea* and *Combretum collinum* flushed new leaves between weeks 1 and 3 (Sep 16-Oct 17), whilst other species were yet to flush new leaves (Field observation). Interestingly, variability at fine scales in Closed canopy and Open canopy gradually decreased after week 6, however in the Open canopy site variability started to increase from week 10 until week 14 (end of data collection period). This may also be due to the difference in senescence timing between species (Masia *et al*., 2018). Photographs and *in situ* visual observations showed that in both sites, *Termilia sericea, Combetrum collinum, Croton megelobotrys* and *Vachelia exuvialis* began senescence by week 12 (late March 2021). Although these species-specific green-up and senescence events occurred in both Closed and Open canopy sites, canopy cover may have influenced observed NDVI variation in the Closed canopy site by obscuring the senescence of herbaceous biomass to the sensor.

In conclusion, I found that the relationship between NDVI and biomass was scale dependent in these heterogenous landscapes. This relationship at MODIS scale was moderate ($R^2 = 0.4$) and showed no clear difference in R^2 values between Closed and Open canopy vegetation suggesting that NDVI-Biomass regressions at MODIS scale in heterogenous landscapes are inaccurate as the Closed canopy site had a significantly higher average biomass. Finer scale Sentinel and PlanetScope were better predictors of biomass and showed an increase in R^2 in Open canopy. Surprisingly *in situ* NDVI related poorly with biomass in the Open canopy site, however, more research is needed as only a few samples of *in situ* NDVI were recorded in this study. The aggregation of fine scale NDVI to coarse scale increased the relationship between MODIS NDVI and finer scaled Landsat and Sentinel NDVI, as expected (Wiens, 1989), interestingly, the aggregation of Sentinel NDVI has enhanced capacity in capturing savanna heterogeneity as there was only a slight difference in the relationship between Closed and Open canopy. Lastly, as expected, NDVI variability increased at finer scale observations in both canopy covers. Unexpectedly though, NDVI variability was slightly higher for all sensors in Open canopy. This was likely due to land use functions such as extensive grazing and resource collection in this area, highlighting the influence of land use functions on landscape stability.

2.6. References

Ali, I., Cawkwell, F., Dwyer, E., Barrett, B. and Green, S., 2016. Satellite remote sensing of grasslands: from observation to management. *Journal of Plant Ecology*, 9(6), 649-671

Allen, P.B., Wilkerson, J.B., Ramirez, M.B. and Boyd, S., 2009, January. Evaluating temporal variation in active-light plant sensors. In *Proc 2009 Beltwide Cotton Conferences., San Antonio TX* Memphis, 5-8

Archibald, S. and Scholes, R.J., 2007. Leaf green-up in a semi-arid African savanna-separating tree and grass responses to environmental cues. *Journal of Vegetation Science*, 18(4), 583-594.

Belsky, A.J., 1994. Influences of trees on savanna productivity: tests of shade, nutrients, and tree-grass competition. *Ecology*, 75(4), 922-932.

Bewick, V., Cheek, L. and Ball, J., 2003. Statistics review 7: Correlation and regression. *Critical Care*, 7(6), 1-9.

Catchpole, W.R., and Wheeler, C.J., 1992. Estimating plant biomass: a review of techniques. *Australian Journal of Ecology*, 17(2), 121-131.

Chapungu, L., Nhamo, L., Gatti, R.C. and Chitakira, M., 2020. Quantifying changes in plant species diversity in a savanna ecosystem through observed and remotely sensed data. *Sustainability*, 12(6), 2345.

Dantas, V.D.L., Hirota, M., Oliveira, R.S. and Pausas, J.G., 2016. Disturbance maintains alternative biome states. *Ecology Letters*, 19(1), 12-19.

de Souza, R., Buchhart, C., Heil, K., Plass, J., Padilla, F.M. and Schmidhalter, U., 2021. Effect of Time of Day and Sky Conditions on Different Vegetation Indices Calculated from Active and Passive Sensors and Images Taken from UAV. *Remote Sensing*, 13(9), 1691.

Dovie, D.B., Shackleton, C.M. and Witkowski, E.T., 2006. Valuation of communal area livestock benefits, rural livelihoods, and related policy issues. *Land Use Policy*, 23(3), 260-271.

Du Plessis, W.P., 1999. Linear regression relationships between NDVI, vegetation and rainfall in Etosha National Park, Namibia. *Journal of Arid Environments*, 42(4), 235-260.

Eisfelder, C., Kuenzer, C. and Dech, S., 2012. Derivation of biomass information for semi-arid areas using remote-sensing data. *International Journal of Remote Sensing*, 33(9), 2937-2984.

Fan, L.Y., Gao, Y.Z., Brück, H.E.B.C. and Bernhofer, C., 2009. Investigating the relationship between NDVI and LAI in semi-arid grassland in Inner Mongolia using in-situ measurements. *Theoretical and Applied Climatology*, 95(1), 151-156.

February, E.C., Higgins, S.I., Bond, W.J. and Swemmer, L., 2013. Influence of competition and rainfall manipulation on the growth responses of savanna trees and grasses. *Ecology*, 94(5), 1155-1164.

Frost, P.G.H., Medina, E., Menaut, J.C., Solbrig, O., Swift, M. and Walker, B.H., 1986. Responses of Savannas to Stress and Disturbance. Biology International, Special Issue 10. *International Union of Biological Sciences, Paris*.

Guo, W.Q., Yang, T.B., Dai, J.G., Shi, L., and Lu, Z.Y., 2008. Vegetation cover changes and their relationship to climate variation in the source region of the Yellow River, China, 1990–2000. *International Journal of Remote Sensing*, 29(7), 2085-2103.

Hachigonta, S., Reason, C.J.C. and Tadross, M., 2008. An analysis of onset date and rainy season duration over Zambia. *Theoretical and Applied Climatology*, 91(1), 229-243.

Hakl, J., Hrevušová, Z., Hejcman, M. and Fuksa, P., 2012. The use of a rising plate meter to evaluate lucerne (Medicago sativa L.) height as an important agronomic trait enabling yield estimation. *Grass and Forage Science*, 67(4), 589-596.

Higgins, S.I., Shackleton, C.M. and Robinson, E.R., 1999. Changes in woody community structure and composition under contrasting landuse systems in a semi-arid savanna, South Africa. *Journal of Biogeography*, 26(3), 619-627.

Hobbs, T.J., 1995. The use of NOAA-AVHRR NDVI data to assess herbage production in the arid rangelands of Central Australia. *International Journal of Remote Sensing*, 16(7), 1289-1302.

Knapp, A.K. and Smith, M.D., 2001. Variation among biomes in temporal dynamics of aboveground primary production. *Science*, 291(5503), 481-484.

Levick, S.R. and Rogers, K.H., 2011. Context-dependent vegetation dynamics in an African savanna. *Landscape Ecology*, 26(4), 515-528.

Levin, S.A., 1992. The problem of pattern and scale in ecology: the Robert H. MacArthur award lecture. *Ecology*, 73(6), 1943-1967.

Long, Y.U., Li, Z., Wei, L. and Hua-Kun, Z., 2010. Using remote sensing and GIS technologies to estimate grass yield and livestock carrying capacity of alpine grasslands in Golog Prefecture, China. *Pedosphere*, 20(3), 342-351.

Ludwig, F., De Kroon, H., Berendse, F. and Prins, H.H., 2004. The influence of savanna trees on nutrient, water and light availability and the understorey vegetation. *Plant Ecology*, 170(1), 93-105.

Malherbe, J., Dieppois, B., Maluleke, P., Van Staden, M. and Pillay, D.L., 2016. South African droughts and decadal variability. *Natural Hazards*, 80(1), 657-681.

Marín, J., Yousfi, S., Mauri, P.V., Parra, L., Lloret, J. and Masaguer, A., 2020. RGB vegetation indices, NDVI, and biomass as indicators to evaluate C3 and C4 turfgrass under different water conditions. *Sustainability*, 12(6), 2160.

Masia, N.D., Stevens, N. and Archibald, S., 2018. Identifying phenological functional types in savanna trees. *African Journal of Range & Forage Science*, 35(2), 81-88.

Matongera, T.N., Mutanga, O., Sibanda, M. and Odindi, J., 2021. Estimating and Monitoring Land Surface Phenology in Rangelands: A Review of Progress and Challenges. *Remote Sensing*, 13(11), 2060.

Mograbi, P.J., Witkowski, E.T., Erasmus, B.F., Asner, G.P., Fisher, J.T., Mathieu, R. and Wessels, K.J., 2019. Fuelwood extraction intensity drives compensatory regrowth in African savanna communal lands. *Land Degradation & Development*, 30(2), 190-201.

Montandon, L.M. and Small, E.E., 2008. The impact of soil reflectance on the quantification of the green vegetation fraction from NDVI. *Remote Sensing of Environment*, 112(4), 1835-1845.

Mutanga, O., Adam, E. and Cho, M.A., 2012. High density biomass estimation for wetland vegetation using WorldView-2 imagery and random forest regression algorithm. *International Journal of Applied Earth Observation and Geoinformation*, 18, 399-406.

Nordh, N.E. and Verwijst, T., 2004. Above-ground biomass assessments and first cutting cycle production in willow (Salix sp.) coppice—a comparison between destructive and non-destructive methods. *Biomass and Bioenergy*, 27(1), 1-8.

Park, D.S., Newman, E.A. and Breckheimer, I.K., 2021. Scale gaps in landscape phenology: challenges and opportunities. *Trends in Ecology & Evolution*, 36(8), 709-721.

Pettitt, A.N., 1979. A non-parametric approach to the change-point problem. *Journal of the Royal Statistical Society: Series C (Applied Statistics)*, 28(2), 126-135.

Pettorelli, N., Vik, J.O., Mysterud, A., Gaillard, J.M., Tucker, C.J. and Stenseth, N.C., 2005. Using the satellite-derived NDVI to assess ecological responses to environmental change. *Trends in Ecology and Evolution*, 20(9), 503-510.

Pollard, S., Shackleton, C. and Carruthers, J., 2003. Beyond the fence: people and the lowveld landscape. *The Kruger experience: Ecology and Management of Savanna Heterogeneity*, 422(7).

R Core Team 2020. R: A language and environment for statistical computing. R Foundation for Statistical Computing, Vienna, Austria. UR https://www.R-project.org/.

Riginos, C., Grace, J.B., Augustine, D.J. and Young, T.P., 2009. Local versus landscape-scale effects of savanna trees on grasses. *Journal of Ecology*, 97(6), 1337-1345.

Roques, K.G., O'connor, T.G. and Watkinson, A.R., 2001. Dynamics of shrub encroachment in an African savanna: relative influences of fire, herbivory, rainfall, and density dependence. *Journal of Applied Ecology*, 38(2), 268-280.

Sala, O.E., Gherardi, L.A., Reichmann, L., Jobbagy, E. and Peters, D., 2012. Legacies of precipitation fluctuations on primary production: theory and data synthesis. *Philosophical Transactions of the Royal Society B: Biological Sciences*, 367(1606), 3135-3144.

Sankaran, M., Hanan, N.P., Scholes, R.J., Ratnam, J., Augustine, D.J., Cade, B.S., Gignoux, J., Higgins, S.I., Le Roux, X., Ludwig, F. and Ardo, J., 2005. Determinants of woody cover in African savannas. *Nature*, 438(7069), 846-849.

Scanlon, T.M., Caylor, K.K., Manfreda, S., Levin, S.A. and Rodriguez-Iturbe, I., 2005. Dynamic response of grass cover to rainfall variability: implications for the function and persistence of savanna ecosystems. *Advances in Water Resources*, 28(3), 291-302.

Scholes, R.J. and Archer, S.R., 1997. Tree-grass interactions in savannas. *Annual review of Ecology and Systematics*, 28(1), 517-544.

Shen, M., Piao, S., Dorji, T., Liu, Q., Cong, N., Chen, X., An, S., Wang, S., Wang, T. and Zhang, G., 2015. Plant phenological responses to climate change on the Tibetan Plateau: research status and challenges. *National Science Review*, 2(4), 454-467.

Staver, A.C., 2018. Prediction and scale in savanna ecosystems. *New Phytologist*, 219(1), 52-57.

Staver, A.C., Botha, J. and Hedin, L., 2017. Soils and fire jointly determine vegetation structure in an African savanna. *New Phytologist*, 216(4), 1151-1160.

Swemmer, A.M., 2020. Locally high, but regionally low: the impact of the 2014–2016 drought on the trees of semi-arid savannas, South Africa. *African Journal of Range & Forage Science*, 37(1), 31-42.

Swemmer, A.M., Bond, W.J., Donaldson, J., Hempson, G.P., Malherbe, J., and Smit, I.P., 2018. The ecology of drought-a workshop report. *South African Journal of Science*, 114(9-10), 1-3.

Tarnavsky, E., Garrigues, S. and Brown, M.E., 2008. Multiscale geostatistical analysis of AVHRR, SPOT-VGT, and MODIS global NDVI products. *Remote Sensing of Environment*, 112(2), 535-549.

Tian, F., Brandt, M., Liu, Y.Y., Verger, A., Tagesson, T., Diouf, A.A., Rasmussen, K., Mbow, C., Wang, Y. and Fensholt, R., 2016. Remote sensing of vegetation dynamics in drylands: Evaluating vegetation optical depth (VOD) using AVHRR NDVI and in situ green biomass data over West African Sahel. *Remote Sensing of Environment*, 177, 265-276.

Tsalyuk, M., Kelly, M., and Getz, W.M., 2017. Improving the prediction of African savanna vegetation variables using time series of MODIS products. *ISPRS Journal of Photogrammetry and Remote Sensing*, 131, 77-91.

Tucker, C.J., 1979. Red and photographic infrared linear combinations for monitoring vegetation. *Remote sensing of Environment*, 8(2), 127-150.

Tucker, C.J., Justice, C.O. and Prince, S.D., 1986. Monitoring the grasslands of the Sahel 1984-1985. *International Journal of Remote Sensing*, 7(11), 1571-1581.

Umarhadi, D. and Syarif, A., 2017. Regression model accuracy comparison on mangrove canopy density mapping. *International Conference on Science and Technology*, 2(7), 1-10.

Wessels, K.J., Prince, S.D., Frost, P.E. and Van Zyl, D., 2004. Assessing the effects of human-induced land degradation in the former homelands of northern South Africa with a 1 km AVHRR NDVI time-series. *Remote Sensing of Environment*, 91(1), 47-67.

Wessels, K.J., Prince, S.D., Zambatis, N., MacFadyen, S., Frost, P.E. and Van Zyl, D., 2006. Relationship between herbaceous biomass and 1-km2 Advanced Very High Resolution Radiometer (AVHRR) NDVI in Kruger National Park, South Africa. *International Journal of Remote Sensing*, 27(5), 951-973.

Whitecross, M.A., Witkowski, E.T. and Archibald, S., 2017. Assessing the frequency and drivers of early-greening in broad-leaved woodlands along a latitudinal gradient in southern Africa. *Austral Ecology*, 42(3), 341-353.

Whitecross, M.A., Witkowski, E.T.F. and Archibald, S., 2016. No two are the same: Assessing variability in broad-leaved savanna tree phenology, with watering, from 2012 to 2014 at Nylsvley, South Africa. *South African Journal of Botany*, 105, 123-132.

Wiens, J.A., 1989. Spatial scaling in ecology. *Functional Ecology*, 3(4), 385-397.

Wu, J., 2004. Effects of changing scale on landscape pattern analysis: scaling relations. *Landscape Ecology*, 19(2), 125-138.

Xue, J. and Su, B., 2017. Significant remote sensing vegetation indices: A review of developments and applications. *Journal of Sensors*, *2017*.

Zambatis, N., Zacharias, P.J.K., Morris, C.D. and Derry, J.F., 2006. Re-evaluation of the disc pasture meter calibration for the Kruger National Park, South Africa. *African Journal of Range and Forage Science*, 23(2), 85-97.

Zeng, L., Wardlow, B.D., Xiang, D., Hu, S. and Li, D., 2020. A review of vegetation phenological metrics extraction using time-series, multispectral satellite data. *Remote Sensing of Environment*, 237, 111511.

Zhang, X., Wang, J., Gao, F., Liu, Y., Schaaf, C., Friedl, M., Yu, Y., Jayavelu, S., Gray, J., Liu, L. and Yan, D., 2017. Exploration of scaling effects on coarse resolution land surface phenology. *Remote Sensing of Environment*, 190, 318-330.

Zhang, Z., Lan, Y., Wu, P. and Han, W., 2015. Optimum Monitoring Time for the Normalized Difference Vegetation Index of Crops. *Transactions of the ASABE*, 58(3), 641-647.

2.7. Tables and Figures

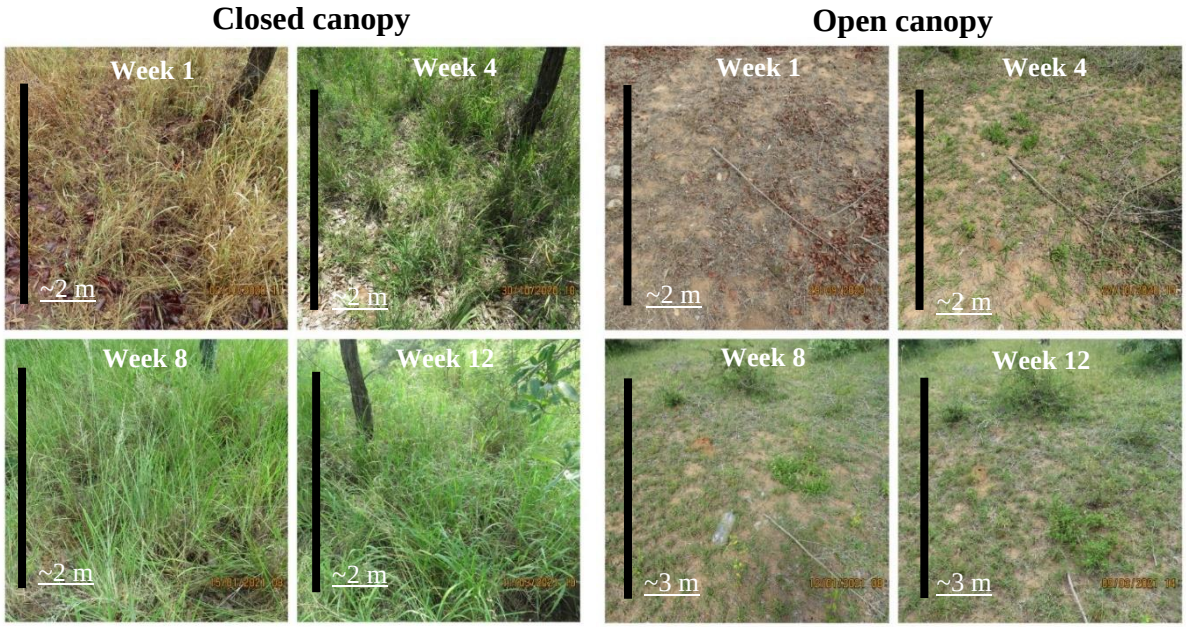

Figure 2.1: Progression of herbaceous biomass growth in Closed canopy (Left quadrant) and Open canopy (Right quadrant) at weeks 1 (September), 4 (October), 8 (December), and 12 (February).

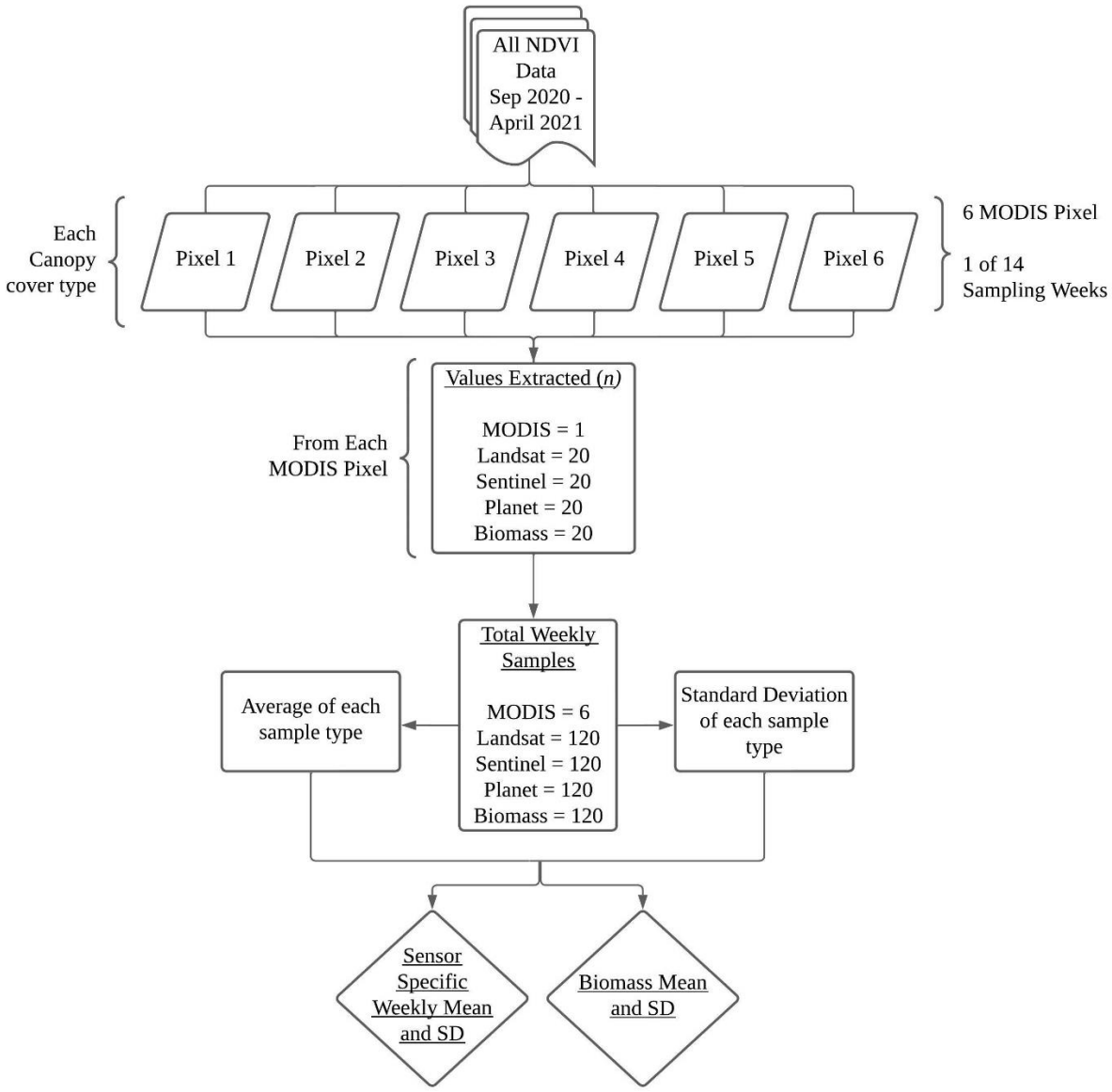

Figure 2.2: Diagram illustrating how NDVI, and biomass measurements were collected to provide weekly mean and SD values, using one of the 14 weeks as illustrative with each week corresponding to the dates at which MODIS data are captured.

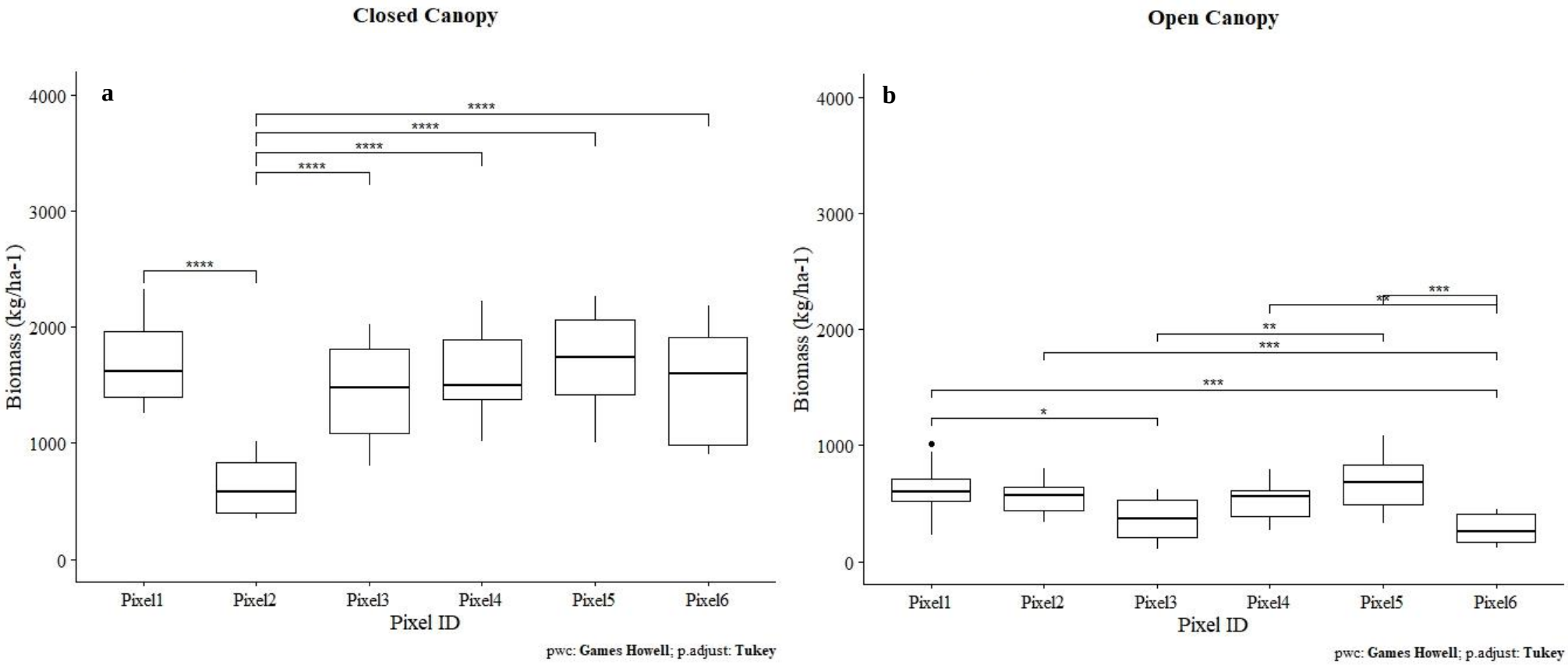

Figure 2.3: Average biomass range of each sampled pixel in Closed canopy (a), and Open canopy (b) from September 2020-April 2021. Note bars above boxplots indicate significant differences between pixels using the Games-Howell test ($p<0.05$) in Closed canopy, and the Tukey HSD test ($p<0.05$) in Open canopy

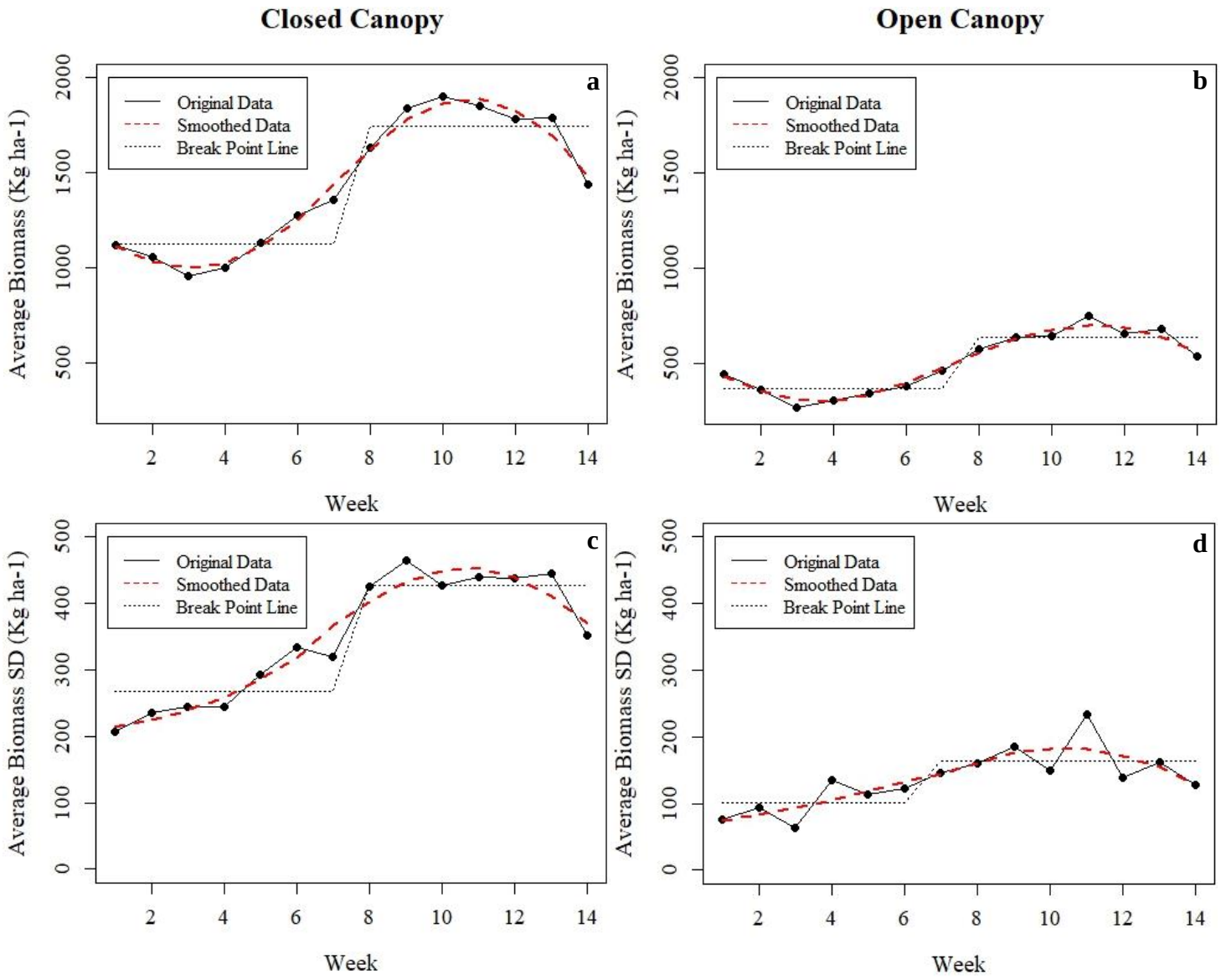

Figure 2.4: Mean weekly biomass measurements in Closed (a) and Open canopy (b), and mean biomass SD in Closed (c) and Open canopy (d). Black solid line shows original data, red line shows smoothed data (locally weighted smoothing), and the grey dashed line shows the probable change point in the time series.

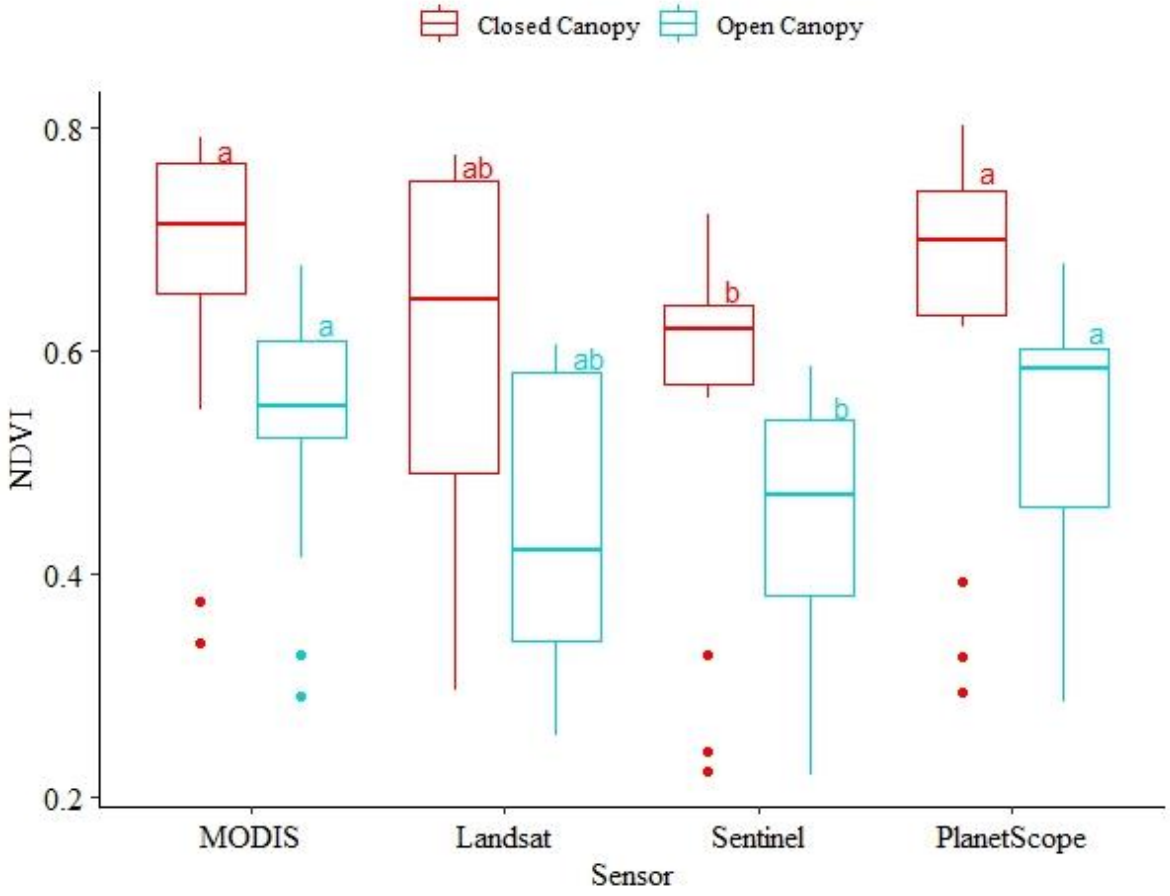

Figure 2.5: The NDVI range of sensors throughout the data collection period in both Closed (red) and Open (blue) canopy cover types. Note significant differences are denoted by letters (a - b) using the Dunn's test ($p<0.05$). Only Sentinel was significantly different from all other sensors.

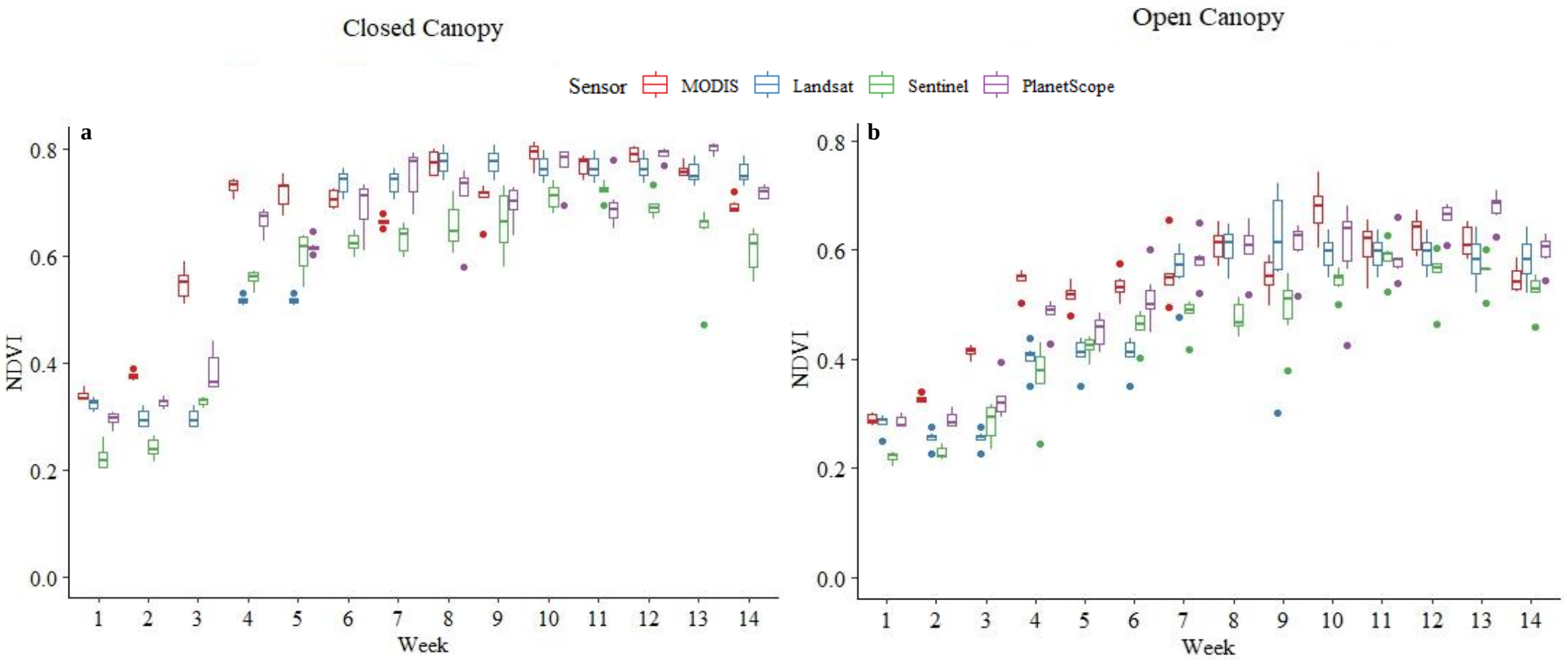

Figure 2.6: The weekly NDVI range for MODIS (red), Landsat (blue), Sentinel (green) and PlanetScope (purple) in Closed (a) and Open (b) canopy vegetation. Solid dots indicate outliers.

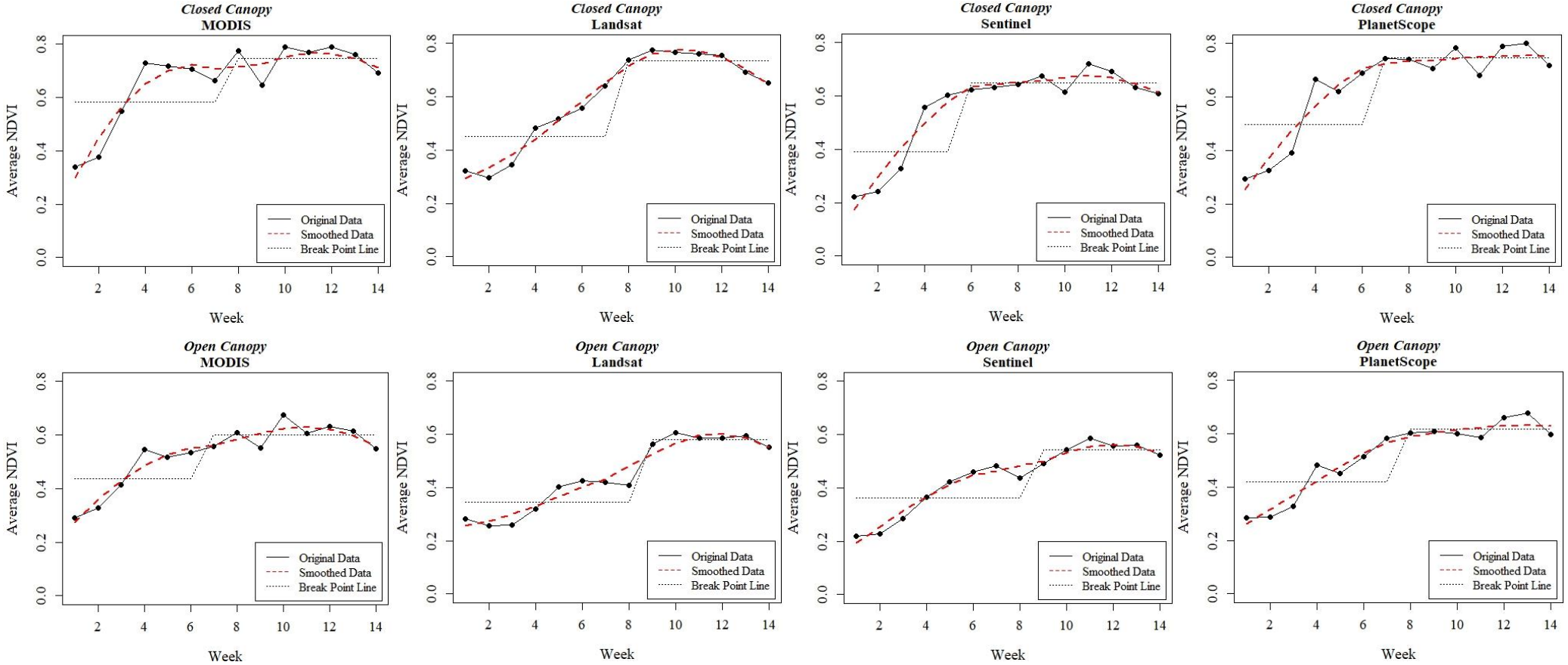

Figure 2.7: The average weekly NDVI of each sensor in Closed (top row) and Open canopy (bottom row) sites. The solid black line shows the original data points, the dashed red line shows the smoothed data (locally weighted smoothing), and the grey dashed line shows the probable change point in the time series.

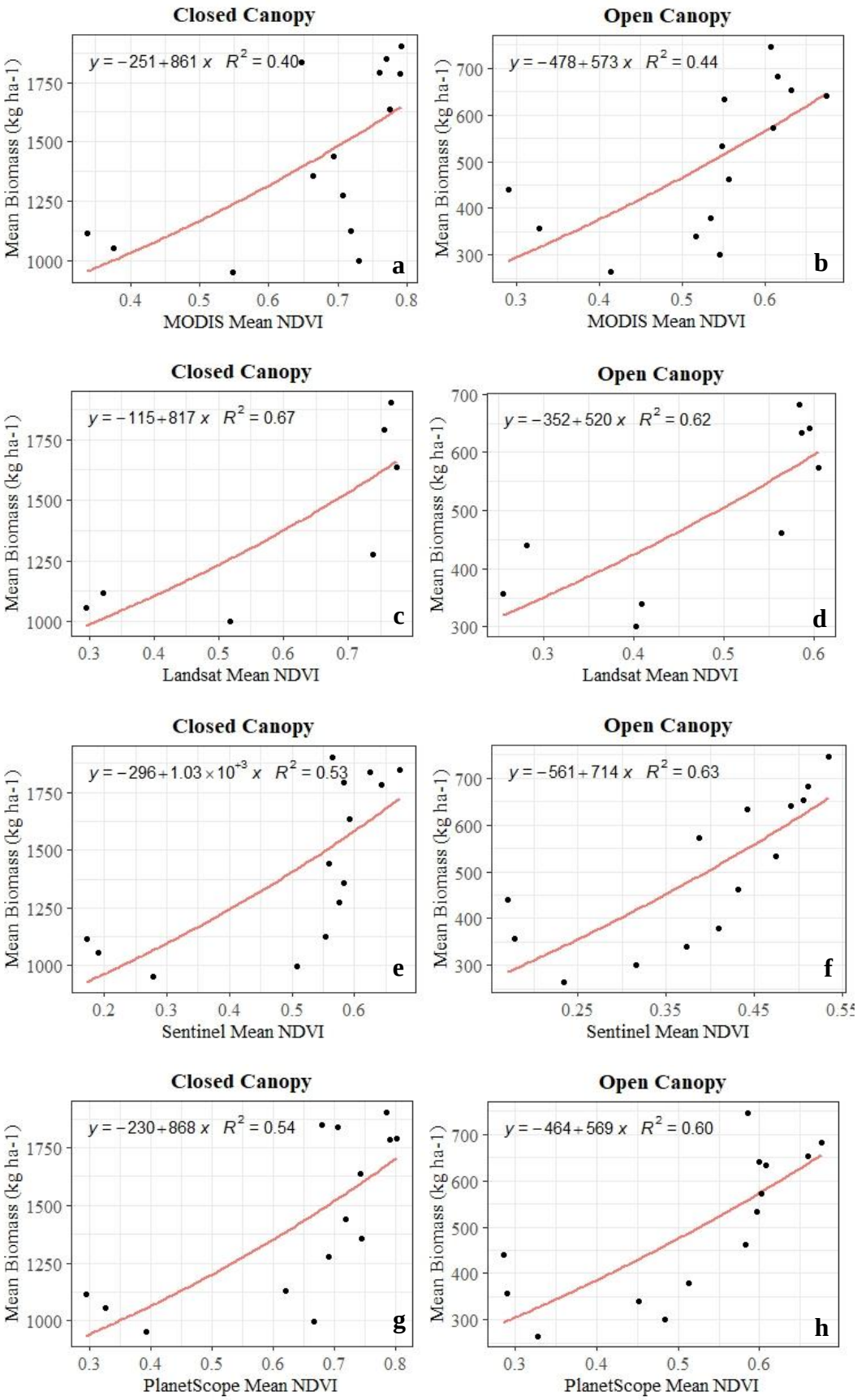

Figure 2.8: Relationship between herbaceous biomass and mean NDVI derived from MODIS (a, b), Landsat, (c, d) Sentinel, (e, f) and PlanetScope (g, h). Note only 7 and 9 Landsat NDVI values were available for Closed and Open canopy respectively

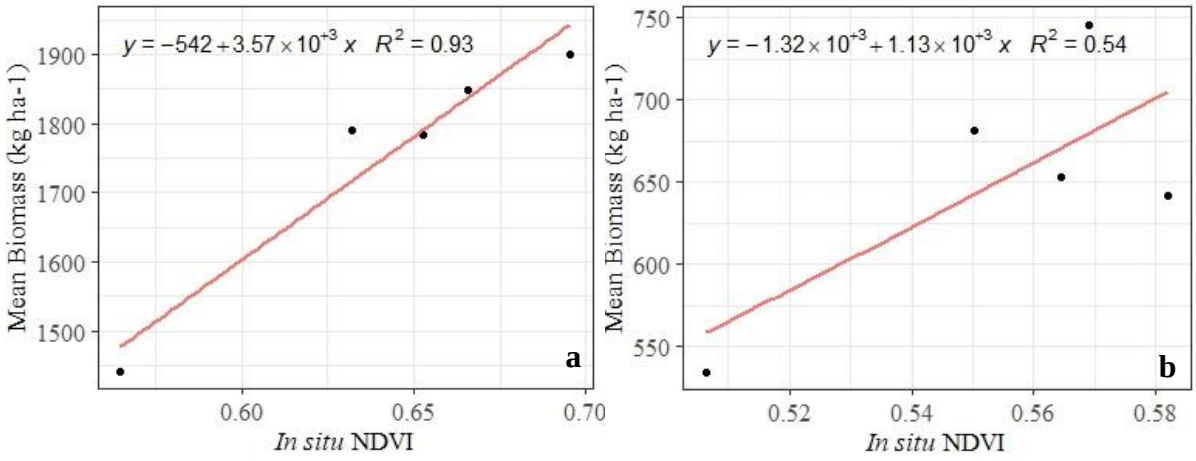

Figure 2.9: The relationship between *in situ* NDVI and mean biomass (Closed canopy-a, Open canopy-b), from February-April 2021.

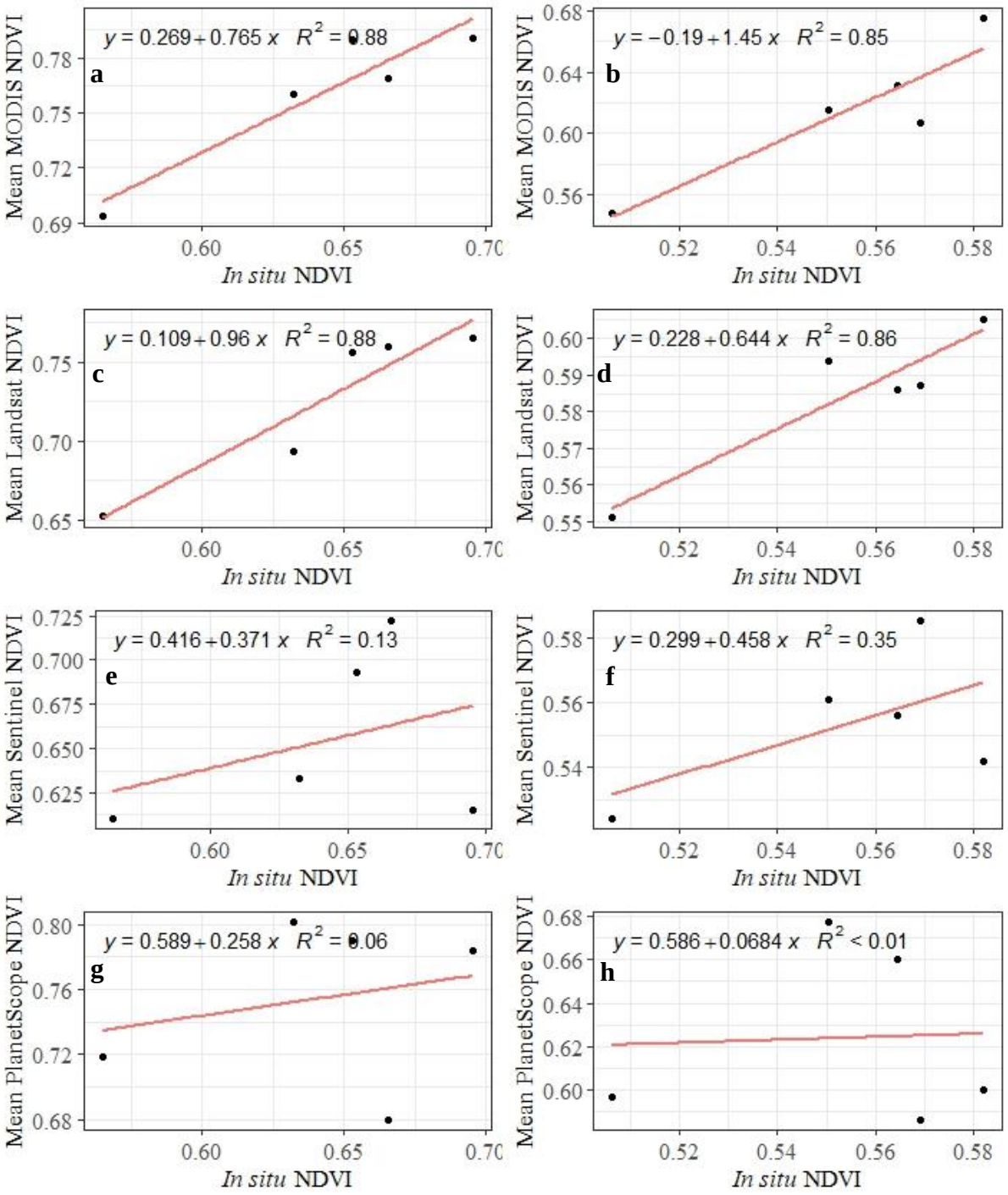

Figure 2.10: Relationship between *in situ* NDVI and satellite sensor NDVI in Closed and Open canopy for MODIS (a, b) Landsat (c, d), Sentinel (e, f), and PlanetScope (g, h).

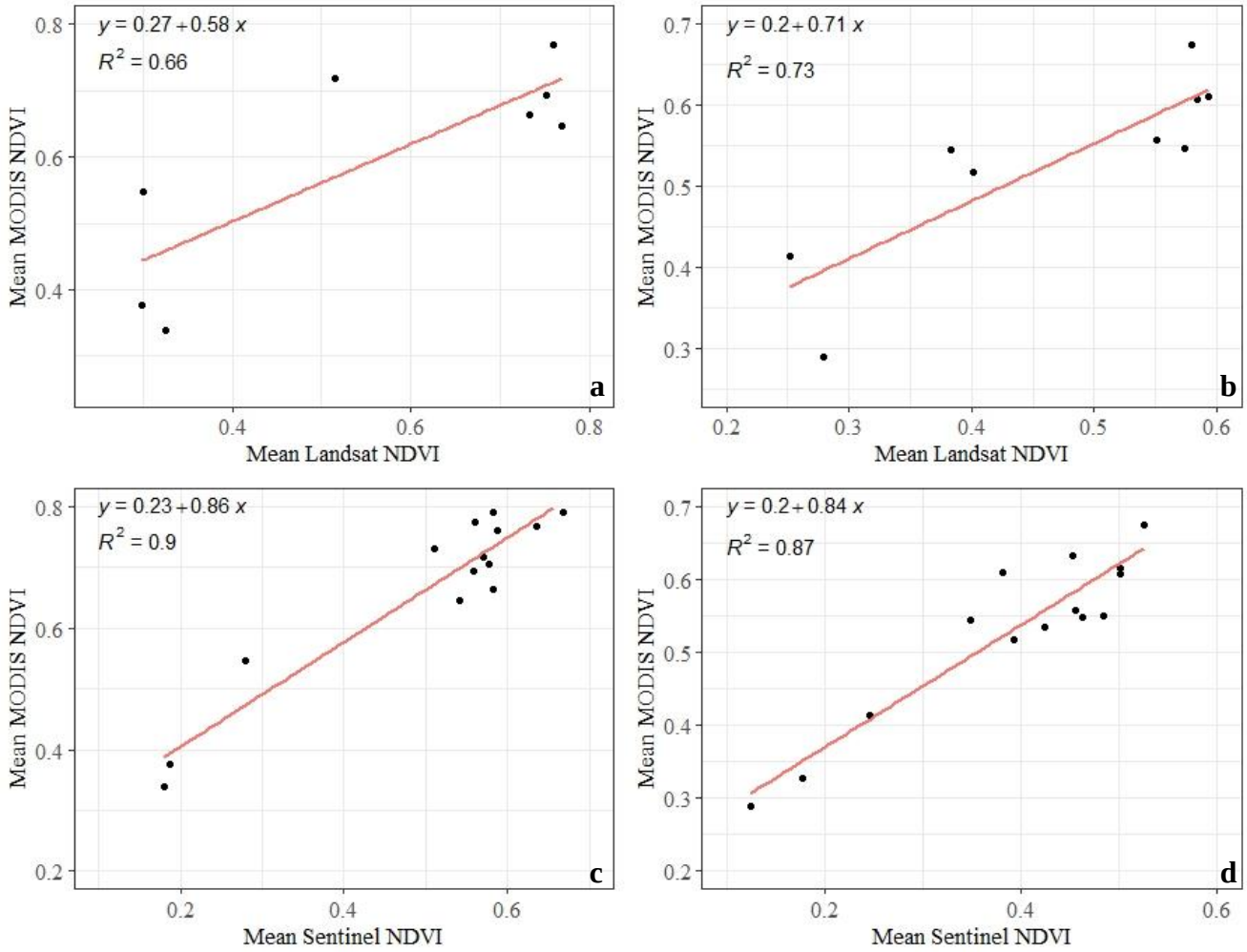

Figure 2.11: Relationship between MODIS NDVI and aggregated Landsat (a, b) and aggregated Sentinel NDVI (c, d) from September 2020-April 2021.

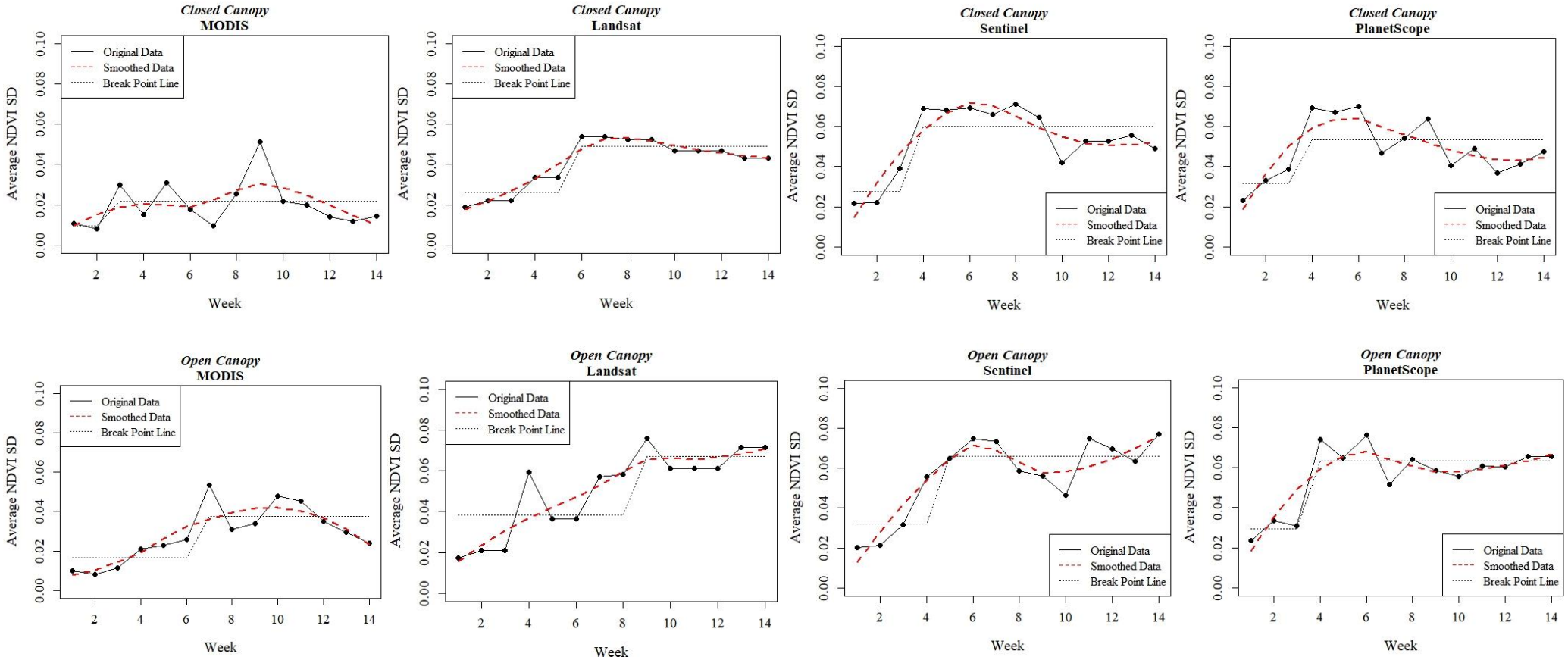

Figure 2.12: Mean weekly NDVI SD of MODIS, Landsat, Sentinel and Planet sensors in Closed canopy (Top Row) and Open canopy (Bottom Row). The solid black line shows original data with the red dashed line showing smoothed data (Locally weighted smoothing) and the grey dashed line showing the probable change points in the time series.

CHAPTER THREE: Influence of spatial scale on phenological metrics derived from remotely sensed NDVI time series in contrasting savanna landscapes, South Africa

3.1. Abstract

Vegetation phenology plays an essential role in our understanding of land surface processes, which are likely to be influenced by climate change at various spatio-temporal scales, affirming the need for a multi-scale monitoring approach. The non-linearity of vegetation phenology in African savannas makes it difficult to monitor long-term phenology trends. Climate change is expected to further modify savanna phenology in ways that are not yet understood. Due to its heterogeneous nature, savannas result in a system with phenologies that differ across space and time. Earth observation satellites have been used to monitor phenology at various spatial and temporal scales, predominantly in the temperate northern hemisphere. Several studies have evaluated phenology in southern hemisphere savannas using products with coarse spatial resolutions. However, these coarse products are ineffective at capturing accurate phenology estimates due the mixed composition of vegetation types associated with savanna environments. In this study, I used NDVI from four different satellite sensors to investigate how NDVI derived phenological metrics compare across spatial scales and how precipitation and temperature influence metrics at these different spatial scales in Closed and Open canopy cover over a seven year period (2016 - 2021). On average phenological metrics occurred later at coarser scale and earlier at finer scale. Phenological metrics varied significantly across years, with some metrics, with metric variation ranging between 9 to 30 days. The timing of rainfall was both positively and negatively correlated with different phenological metrics with the strength of these correlations differing between spatial scales. These show that spatial scale has a significant influence on the estimation of phenological metrics finding that support the notion that finer resolution products perform better at estimating phenology and should therefore be preferred over coarser resolution products to monitor savanna phenology.

Keywords: Canopy cover, Heterogeneity, NDVI, Phenology, Spatial scale, TIMESAT

3.2. Introduction

Savanna ecosystems are generally defined as an area with a combination of an uneven tree layer at variable densities, and a consistent grass layer (Scholes and Archer, 1997; Huntley and Walker, 2012). Approximately 18% of the Earth's terrestrial surface is occupied by savanna ecosystems (Grace *et al*., 2006), with about 50% of savanna ecosystems covering the African continent (Osborne *et al*., 2018). In southern Africa, savanna ecosystems support an increasing human population through socio-economic services such as fuel wood collection, traditional medicine, wild fruits, and cattle grazing (Shackleton, 2005; Twine, 2005). Savanna ecosystems also host the largest diversity of ungulates (Sankaran *et al*., 2005) and provide regulating ecosystem services such as carbon storage (Grace *et al*., 2006). These socio-economic and ecological functions of savanna ecosystems therefore support human livelihoods and biodiversity of plants and animals (Lehmann *et al.*, 2011). However, land degradation and the effects of climate change have changed species compositions and reduced vegetation productivity in these landscapes (Scheiter *et al*., 2012). These anthropogenic influences on savanna ecosystems call for monitoring techniques that can assist with conservation and management actions.

Plant phenology is the study of cyclic plant stages such as budburst, leaf emergence, and senescence (Lieth, 1974). The timing and drivers of phenological stages are seen as proxy indicators of climate change, climate variability and vegetation growth (Running and Hunt, 1993). Thus, monitoring vegetation phenology is an valuable component of land surface change research (Ma *et al*., 2013). Phenological cycles in southern African savannas are unpredictable as vegetation phenology is strongly linked to the onset of the first substantial precipitation events (Whitecross *et al*., 2017), which are highly variable across spatial and temporal scales (Lehmann *et al*., 2011). Coupled with the unpredictable phenological cycles, is the intrinsically heterogeneous nature of savanna ecosystems. The tree-grass ratios in savannas are influenced by several other factors such as fire, herbivory, soil moisture, nutrient availability, and topography (Scholes and Walker, 1993; Lehmann *et al*., 2014). Furthermore, many tree species flush new leaves before the onset of the first substantial precipitation events (Higgins *et al*., 2011; Whitecross *et al*., 2017), allowing them to develop when there is reduced competition from grasses (Scholes and Walker, 1993), thus further complicating the prediction of savanna phenology. These heterogeneous characteristics of savannas make it difficult to monitor savanna phenology.

Ground based phenological studies are useful as they record accurate timings of phenological stages and can differentiate these stages between different species (Piao *et al*., 2019). However, ground-based techniques are labour intensive and expensive, making them impractical for regional and continental scale phenological studies. The advancement of remote sensing technologies has provided an effective method of monitoring long-term phenology on a global scale (Davis *et al*., 2017; Gallinat *et al.*, 2021). Unlike ground-based observations, satellite sensors observe all ground features within the field of view of the satellite sensor (Matongera *et al*., 2021). The spatial resolution (instantaneous field of view), temporal resolution (frequency of data acquisition) and spectral resolution (wavelength range that a sensor can capture) differ between satellite sensors. Some of the most commonly used sources of satellite data for phenology research are the Advanced Very High Resolution Radiometer (AVHRR) (Fontana *et al*., 2008), Moderate Resolution Imaging Spectroradiometer (MODIS) (Gong *et al*., 2015), Landsat (Tomaszewska *et al*., 2020), and Sentinel-2 (Vrieling *et al*., 2018).

Vegetation phenology studies use specific wavelengths to derive Vegetation Indices (VIs), which are measures of vegetation state and condition (Vrieling *et al*., 2018). One of the most frequently used VIs is the Normalised Difference Vegetation Index (NDVI) which measures the photosynthetic activity of vegetation by quantifying the amount of reflected Near Infrared (NIR) light, and absorption of Red light (Tucker, 1979). The NDVI has been used for phenology characterisation in numerous studies, however, given that spatial and temporal resolutions differ between satellites sensors, the choice of satellite products needs to be considered. The spatial resolution of the data source used requires careful consideration in phenological studies, particularly in heterogeneous environments where the phenological stages differ between species (White *et al.*, 2009). Similarly, the temporal resolution of data sources can influence the accuracy of the estimation of phenological stages (Piao *et al*., 2019). For instance, AVHRR provides daily imagery at a spatial resolution of 1 km, which allows for incremental changes to be identified, but the low spatial resolution generalises vegetation development and does not capture species-specific development (Shen *et al*., 2015). Alternatively, Landsat has a spatial resolution of 30 m, making it better suited in capturing species-specific changes, however, its 16-day temporal resolution is not adequate enough to capture accurate changes in vegetation development (Robinson *et al*., 2017). More recently, high spatial resolution Sentinel-2 (10 m) and PlanetScope (3 m), with temporal resolutions of 5 days and 1 day respectively, make these sensors ideal for monitoring local

vegetation processes (Matongera *et al*., 2021), however, their recent deployments do not allow for analysis of long-term phenological trends.

Phenology studies classify vegetation stages, known as phenological metrics, into distinct events which include Start of Season (SOS), Peak of Season (POS), and End of Season (EOS). These phenological metrics are derived from VI time series data (Zeng *et al*., 2020). The methodologies used to identify phenological metrics from a VI time series are either threshold-based (e.g., 50% of the VI time series amplitude), or change detection based (e.g., where the largest increase/decrease occurs) (Zeng *et al*., 2020). The method used to extract phenological metrics can result in big differences (up to 100 days), thus phenological comparisons should only be drawn where similar methods are used (Beurs and Henebry, 2010).

Phenological metrics derived from course spatial resolution sensors are comprised of a variety of different plant species, thus capturing a mixed spectrum of vegetation activity (Zhang *et al*., 2017), which limits the representativeness of species-level phenology (Delbart *et al*., 2005). This is particularly relevant in heterogenous event-driven ecosystems such as savannas (Parrini and Erasmus, 2009). Many phenological studies are based on a single spatial and/or temporal scale, thus the findings are limited to those scales (Wiens, 1989; Levin 1992). Several studies have characterised South African savanna phenology using coarse spatial scale products such as AVHRR (e.g., Wessels *et al*., 2011) and MODIS (e.g., Archibald and Scholes, 2007; Whitecross *et al*., 2017). Considering the heterogeneous structure and event-driven nature of savanna ecosystems, the use of these coarse products makes it challenging to accurately monitor phenological behaviours, which differ between spatial scales. To the best of my knowledge, no studies have to this day used a combination of coarse and fine spatial resolution products to characterise savanna landscapes in South Africa. Utilising a multi-scale approach to derive phenological metrics can provide better insights into the spatially explicit phenology relationships in savanna landscapes.

This study, therefore, assesses how coarse spatial resolution (hereon referred to as ‘coarse scale’) and fine spatial resolution (hereon referred to as ‘fine scale’) NDVI products influence phenological metrics in Closed and Open canopy vegetation in a semi-arid savanna. In the Closed canopy site, I predicted that phenological metrics would vary across spatial scales due to the heterogenous tree-grass ratios and presence of early green-up tree species. In the Open canopy site, I expected that phenological metrics would be similar across spatial

scales due to its homogenous composition of mainly grasses and herbaceous vegetation. I further predicted that NDVI variability between sampled pixels would be larger at finer scales compared to coarser scales and to a greater extent in the Closed canopy site compared to the Open canopy site.

3.3. Methods

3.3.1. Data Collection

Time series preparation

I used TIMESAT version 3.3 (Eklund and Jonsson, 2017) to extract seasonal phenological metrics from fitted NDVI time series data. TIMESAT uses time series data from satellite derived vegetation indices, which allows for seasonal analysis of vegetation phenology (Eklund and Jonsson, 2017). Phenological metrics derived from TIMESAT included Start of Season (SOS), Peak of Season (POS), Length of Season (LOS) and End of Season (EOS) (Figure 3.1). The use of TIMESAT requires time series data to have a consistent number of vegetation index values (or images) per year throughout the full analysis period for accurate comparisons within sensors across years. All MODIS data were used as its time series dataset consists of 16-day Maximum Value Composites (MVC), which reduces the impact of cloud cover and subsequent data gaps in the NDVI time series. For phenology extraction, data gaps are undesirable as they reduce the accuracy in capturing the onset/offset of phenological metrics, making the selection of quality data crucial. Since the MODIS product is the least affected by cloud cover, this allowed for 23 MODIS images per year throughout the analysis period between 2015 and 2021 (n=161). In comparison, Landsat and Sentinel are more prone to data gaps: of all the satellites used, Landsat has the longest revisit period (one scene every 16 days) which makes it highly susceptible to cloud cover and subsequent data gaps, especially during the summer months. TIMESAT only estimates phenological metrics from the second complete time series (second year) and onwards. Duplication of the first years' time series is described in the TIMESAT manual (Eklundh and Jönsson, 2017) to artificially complete missing data, allowing for phenological metrics to be extracted for that year. Since Sentinel data are available from November 2015, I duplicated data from 2016 to create a complete 2015 time series, thereby forcing the TIMESAT program

to output the 2015/2016 seasons phenological metrics. To remedy the issue of data gaps due to cloud cover in both Landsat and Sentinel datasets, I used the year with the lowest number of available 'clean data' (cloud free) as the standard number for all years within that sensor's time series (MODIS *n*=23/year, Landsat *n*=12/year, Sentinel *n*=20/year). The total number of NDVI raster images for MODIS, Landsat, and Sentinel across the full temporal extent of the analysis were 161, 84 and 140 respectively. Although the total number of images differed between the satellites, the aim was to ensure a consistent number of images per year for each satellite, allowing comparisons of phenological metrics between years, within sensors.

To ensure that annual time series data were evenly distributed within sensors, I used linear interpolation as a method to fill in 'gaps' between data (Pan *et al*., 2017) using the *things* package in R (Baumgartner and Wilson, 2021). For example, if the Landsat raster for February was absent due to high cloud cover (high precipitation occurs between January and February in the study area), the Landsat raster of January and March would be used to create a linearly interpolated Landsat raster for February. Given the temporal extent restriction of the PlanetScope data (only data from September 2020-June 2021 was acquired), I used data from 2021 to complete the missing data from the corresponding months in 2020, thereafter I used linear interpolation to create raster scenes for July and August. After filling in data gaps, the average temporal distribution of images (i.e., the number of days that occur between each image) for MODIS, Landsat, Sentinel and PlanetScope were, 15.8 days, 30.41 days, 18.25 days, and 15.8 days, respectively.

Extracting phenology metrics

Before extracting phenological metrics, I smoothed the raw NDVI time series data using a moving average filter (Savitzky-Golay), due to its superior ability in minimising noise and maintaining the original time series trajectory (Pan *et al*., 2017). Smoothing of the data reduces the influence of outliers and discrepancies at different time intervals, allowing for more accurate phenological metric outputs (Eklund and Jonsson, 2017). The SOS and EOS values were based on the seasonal amplitude of the time series, which was set at 50% for both SOS and EOS (Figure 3.1). I used the Seasonal Trend decomposition by LOESS (STL) method which further smooths the time series using a locally weighted regression smoother (Cleveland *et al*., 1990). Once I defined and processed all parameters, I extracted phenological metrics and fitted NDVI time series values based on row and column identity,

ensuring that extracted data corresponded with sampled pixels. For both phenological metrics and fitted NDVI time series data, I calculated the mean and standard seviation (SD) of sampled pixels (Figure 3.2), with the average of these mean values being used as overall values for Closed and Open canopy sites. Finally, I acquired monthly precipitation and temperature data from the WRF weather station (Davis Vantage Pro 2) between 2015 to June 2021 in order to determine if precipitation and temperature trends correlated with the trends of the phenological metrics (Table A4 and A5, APPENDIX A). As a point of clarification, the austral summer occur across separate years (December to March), therefore 2015/2016 refers to the 2016 season, 2016/2017 refers to the 2017 season, and so on until 2020/2021.

3.3.2. Data Analysis

NDVI time series trends and comparisons between sensors

I used the minimum, maximum, mean, and standard deviation of the NDVI values from the fitted time series for each sensor for the duration of the study period (apart from PlanetScope, with only one season available) to calculate differences between Closed and Open canopy sites and between sensors. Due to the differing number of samples per sensor for these comparisons, I used MODIS values that closely matched the acquisition date of Landsat, Sentinel and PlanetScope. To determine if there were long-term changes in the NDVI time series of all sensors in both canopy cover types, I used the seasonally adjusted Mann-Kendall test. I used Sen's slope estimator to determine if the overall time series trend was increasing or decreasing. I used the Pettitt test method to determine if there were any abrupt change points in the NDVI time series. Change points indicate when there is a significant change in the measurer of central tendency of the time series (Bórnez *et al*., 2021). The comparisons of the NDVI time series of all sensors and their associated Sen Slope and change points may show how observations and different spatial scales influence the estimated rate of annual change in NDVI and probable change points. To test for differences in NDVI time series between sensors in the same canopy cover type, I used an unpaired students t-test.

Cross-correlation of time series NDVI

To establish whether there was a time delay between sensor time series, I performed a cross-correlation (*tseries* package in R, Trapletti and Hornik, 2020) to compare different time series datasets and identify how they matched up at different time intervals or lag intervals (Bourke, 1996). This is essential when comparing phenological metrics from different time series datasets as it ensures that phenological metrics are comparable since the number of days between images differs between all sensors used. Before performing cross-correlations, I standardised the NDVI time series of each sensor in both Closed and Open canopy, allowing for a mean of zero and a SD of one, which ensured that coefficients were on the same scale (Burnham and Anderson, 1998). Thereafter, I used the Dicky-Fuller test to determine if data were stationary, and normality was tested using the Shapiro-Wilks test. The lag interval identified in the cross-correlation was applied to the extracted phenological metrics to allow for improved accuracy in comparisons between sensors/scales. For example, if the correlation between MODIS and Landsat was strongest at a lag interval of -1, then the number of days between each Landsat composite (30.4 days) was subtracted from the phenological metrics derived from the Landsat NDVI time series.

Phenological metric comparison between different sensors in Closed and Open canopy

For this part, I compared the phenological metrics from the 2020/2021 season when all sensors had phenological metrics present. This was followed by a comparison of the average phenological metric values between 2015/2016 and 2020/2021 for MODIS, Landsat, and Sentinel sensors only. I used a repeated measures ANOVA to identify if there were significant differences in phenological metrics between sensors. Thereafter I did a pairwise comparison test to establish which sensor/s recorded significantly different phenological metrics. I used an independent samples t-test to verify if there was a significant difference in phenological metrics between Closed and Open canopy cover. Following the technique used by Fisher and Mustard (2007), I used linear regression models to test the relationship of phenological metrics between the sensors, using the phenological metrics from each growth season, excluding PlanetScope (n=6), for both Closed and Open canopy covers. Finally, I produced phenology maps depicting the mean value for each phenology metric over the study period to visually display the difference between Closed and Open canopy, and to show the mix-pixel effect at finer scales (Code in Appendix B).

Precipitation and temperature influence on phenology

Using the precipitation and temperature data collected from the WRF weather station, I calculated the total precipitation for each year. I created 5 climatic variables for each season, which included Early precipitation (Total October and November precipitation), Mid precipitation (Total January and February precipitation), Late precipitation (Total March and April precipitation), Total annual precipitation, and Average annual temperature. To interpret how precipitation and temperature influence phenological metrics, I evaluated the correlation between the Day of Year (DOY) for each phenological metric, and climatic variables, using a Pearson correlation test. Lastly, I used a repeated measures ANOVA to determine if there is a significant difference in precipitation and average temperature between years.

3.4. Results

NDVI time series comparison

Mean MODIS and Landsat NDVI values were not significantly different in both Closed ($t_{(166)} = 0.91$, $p = 0.360$) and Open canopy ($t_{(166)} = 0.82$, $p = 0.820$) (Figure 3.3). Sentinel NDVI was significantly lower than both MODIS and Landsat in both Closed (MODIS: $t_{(275)} = 5.40$, $p = 0.001$; Landsat: $t_{(165)} = -5.27$, $p = 0.001$) and Open canopy (MODIS: $t_{(275)} = 4.50$, $p = 0.001$; Landsat: $t_{(165)} = -5.97$, $p = 0.001$). The NDVI signal from all sensors in Open canopy showed a lower amplitude compared to the NDVI signal in Closed canopy (Figure 3.4). Mean SD for all sensors was significantly higher in Closed canopy ($t_{(4)} = 6.93$, $p = 0.002$) compared to the NDVI of sensors in Open canopy. For both sites, Landsat NDVI had the highest maximum and Sentinel NDVI the lowest maximum values (Table 3A, APPENDIX A).

The comparison of Mann-Kendall and Seasonal Sen's Slope results between the NDVI time series (2015/2016-2020/2021) of all sensors (except PlanetScope) in both canopy cover types showed no monotonic trends (Table 3.1) for all sensor time series in both canopy cover types. The Seasonal Sen's Slope value indicates the annual average change in NDVI for each sensor. All sensors in both canopy covers showed an increase in average annual NDVI over time, with the average annual NDVI increase in Open canopy being significantly higher than the annual NDVI increase in Closed canopy ($t_{(3)} = 3.38$, $p = 0.040$). MODIS had the greatest annual NDVI change difference between Closed and Open canopy covers with a

difference of 0.006. Landsat had the lowest difference in annual NDVI change between canopy covers, with a difference of 0.001 between Closed and Open canopy.

The time series of MODIS had significant change points in both canopy cover types (Closed canopy: k = 113, p = 0.020; Open canopy: k = 113, p = 0.001) with change points being detected on 17 November 2019 (k values represent the NDVI composite number) in both canopy types (Figure 3.4). There were no significant change points detected for Landsat ($p>0.05$) in both Closed and Open canopy. Lastly, Sentinel had significant change points detected in both canopy cover types (Closed canopy: k = 80, p = 0.040; Open canopy: k =80, p = 0.002) with change points occurring on 05 December 2018 in both canopy cover types.

Cross-correlation of time series NDVI

There was a lag of -1 composite between MODIS and Landsat, and MODIS and Sentinel in both sites (Table 3.2, Figure 1A, APPENDIX). Therefore, the number of days that one MODIS composite represents (15.80 days) was subtracted from the phenological metric values for Landsat and Sentinel. The correlation between Landsat and Sentinel, and MODIS and PlanetScope NDVI time series was strongest at a lag of zero, thus no correction was applied to the phenological metrics of these sensors.

Phenological metric comparison

In Closed canopy there was a significant difference in LOS between sensors ($F_{(2, 15)} = 4.50$, p = 0.020), where Sentinel was significantly lower than MODIS (p = 0.030, Figure 3.5). In Open canopy, both POS and LOS were significantly different between sensors (POS: $F_{(2, 15)} = 4.20$, p = 0.03; LOS: $F_{(2, 15)} = 4.20$, p = 0.030) with Sentinel being significantly lower than MODIS for both metrics (Figure 3.5). There were no significant differences in phenological metrics between Closed and Open canopy across all sensors ($t_{(142)} = -0.089$, p = 0.920, Figure 3.5). Generally, there was a larger gap between the 25 and 75 percentiles in Open canopy compared to Closed canopy. Interestingly, nearly all outliers occurred in the 2015/2016 and 2020/2021 seasons (Figure 3.5).

Average phenological metrics between 2015/2016-2020/2021 season

The average DOY that the phenological metrics occurred across all seasons between 2015/2016 and 2020/2021 (Table 3.3) were considerably different when compared to the DOY that the metrics occurred in the 2020/2021 season only (Table 3.4) (See Table 4A and 5A for metrics of each year, APPENDIX A). LOS, POS, and EOS were all longer/occurred later at MODIS scale compared to the other sensors scales in both Closed and Open canopy cover. The SOS occurred earlier in Closed canopy than on Open canopy for Landsat and Sentinel, while there was no difference in SOS between Closed and Open canopy for MODIS. Looking at all available sensors during these 6 years, the DOY at which each metric occurred decreased on a coarse to fine spatial scale gradient (i.e. from MODIS to PlanetScope) for all metrics, except for SOS where only Landsat SOS in Open canopy had a higher DOY than MODIS (Table 3.3). The average SD of each phenological metric in Closed and Open canopy showed large variations in the metric DOY between years (Table 3.5). These variations ranged from 9.5 to 29.0 days across all sensors. There were no obvious patterns in the SD for all metrics except for POS, which had a lower SD in Open canopy for all sensors compared to Closed canopy.

Phenological metrics for the 2020/2021 season

For all sensors, SOS, POS, and EOS occurred earlier in Closed canopy than Open canopy, with LOS being longer in the Closed canopy site compared to the Open canopy site (Table 3.4). POS occurred on average 9.3 days later in Open canopy compared to Closed canopy, with MODIS having the highest difference (24.2 days). For SOS, LOS, and EOS, the difference (SD) in DOY between Closed and Open canopy only varied between 2.2-2.6 days. There was no consistency in terms of phenological metrics occurring earlier or later as a function of scale. POS and EOS were captured at a later DOY at coarse scale (MODIS and Landsat) compared to finer scales (Sentinel and PlanetScope).

Phenological maps at sensor specific scale

At coarser scales, the SOS of nearly all sampled pixels occurred between 4 December (DOY-338) and 11 December (DOY-345), with all the finer scale pixels SOS occurring between 26 November (DOY-330) and 11 December (DOY-337) (Figure 3.6). POS derived

from MODIS imagery ranged between 5 March (DOY-64) and 15 March (DOY-74) in most sampled pixels, while Landsat derived POS was mostly between 22 February (DOY-53) and 04 March (DOY-63), and Sentinel derived POS showing a wide combination of dates (Figure 3.7). Canopy cover influence on LOS was not consistent across scales. MODIS for example had a LOS between 166-176 days in Open canopy, and 177-187 days in Closed canopy, but the difference was not as obvious with the other sensors (Figure 3.8). The EOS at Landsat scale ranged between 11 June (DOY-527) and 18 June (DOY-534) in most sampled pixels, while EOS at MODIS and Sentinel scale was between 3 June (DOY-519) and 10 June (DOY-526) for the majority of the pixels (Figure 3.9). Note that EOS DOY precedes into the following year.

Linear regressions of phenology metrics from different sensors

In Closed canopy, none of the Landsat and Sentinel phenology metrics showed significant relationships (Figure 3.10). Relationships between MODIS and Landsat were stronger for LOS and EOS, whereas the relationships of SOS and POS was stronger between MODIS and Sentinel, all of which were statistically significant. In both canopy cover types, LOS had the largest and POS had the lowest R^2 difference between sensors. In Open canopy, MODIS and Landsat metrics had the strongest relationships (Figure 3.11). This contrasts with Closed canopy where MODIS and Sentinel derived POS and SOS were the most closely related.

Influence of precipitation and temperature on phenological metrics

The average annual rainfall was 470.0 mm, with below average rainfall occurring in the 2015/2016 season (141.5 mm) and the 2017/2018 season (314.0 mm) (Figure 3.12). The average annual temperature was 21.0°C with December having the highest average monthly temperature of 24.5°C (Figure 3.12). The summer period had the highest rainfall with an average total of 434.0 mm between October and April (Figure 3.12). Monthly precipitation during winter from June through to September was low, with an average of only 3.8 mm. January and February received the highest total amount of rainfall with an average of 95.3 mm and 94.8, respectively. Monthly precipitation varied greatly in October, January, and February ranging between 33.3±48.5 mm, 95.3±53.0 mm, and 94.8±46.6 mm respectively.

There was a significant difference in average monthly precipitation between years ($H_{(5)} = 23.21$, $p = 0.003$). Precipitation in the 2015/2016 season was significantly lower than all other years, and 2016/2017 was significantly higher than the 2017/2018 season (Figure 2A, APPENDIX A). There was also a significant difference in average monthly temperatures between years ($H_{(11)} = 61.41$, $p = 0.001$), with the average monthly temperature of the 2017/2018 season being significantly lower than the monthly average of the 2018/2019 season (Figure 3A and 4A, APPENDIX A).

Mid precipitation (total January and February) correlated positively with LOS at MODIS ($r = 0.94$) and Landsat scale ($r = 0.76$), (Table 3.6). Mid precipitation was also positively correlated with EOS in both canopy cover types at MODIS and Landsat scales, while there was no correlation at Sentinel scale in Closed canopy (Table 3.6). Late precipitation (Total March and April) was positively correlated with EOS at all scales in Open canopy and only at MODIS scale in Closed canopy. Late precipitation was also positively correlated with LOS at Sentinel scale ($r = 0.81$) in Open canopy only (Table 3.6). Early precipitation (Total October and November) had a negative correlation with SOS at all scales in both canopy types (negative correlation means that the onset of SOS is observed earlier), and a positive correlation with LOS at MODIS ($r = 0.92$) and Landsat ($r = 0.90$) scale in Closed canopy, and only MODIS ($r = 0.86$) in Open canopy (Table 3.6). Interestingly, Early precipitation only correlated negatively with POS at Sentinel scale in both canopy types. Total seasonal precipitation correlated negatively with SOS at MODIS and Landsat scales in both canopy types, with LOS positively correlated at all scales in both canopy types. Lastly, there were no significant correlations between average seasonal temperature and phenological metrics.

3.5. Discussion

The aim of this study was to determine how the spatial resolution of different satellite products influenced the scaling relationship of phenological metrics in Closed and Open canopy sites of a semi-arid savanna landscape. The results showed that Sentinel derived NDVI was significantly lower than that derived from MODIS and Landsat. As predicted, the average NDVI and the average NDVI variability of each sensors' time series was higher in Closed canopy than in Open canopy. The average SD between pixels of each sensor was similar in both canopy cover types; however, variability increased at finer scales.

Phenological metrics at Sentinel scale were significantly different to those at MODIS and Landsat scales: the LOS was shorter in Closed and Open canopy and POS occurred earlier in both canopy types. In both canopy cover types, SOS, POS, and EOS occurred later, and LOS was longer at coarser scales (MODIS) compared to the finer scales of the other sensors. Phenology between the 2015/2016-2020/2021 seasons varied with metric variability ranging from 9.5 days to 29.0 days. There appeared to be no pattern regarding variability at different scales, however, POS and EOS had the highest variability at Sentinel scale, while SOS and LOS had the highest variability at Landsat and MODIS scale respectively. The relationship of phenological metrics between sensors showed that LOS had the largest and POS had the smallest difference in R^2 between sensors. The relationship of phenological metrics between Landsat and Sentinel was weak and insignificant for all metrics. There was a strong correlation between precipitation and the onset/offset of phenological metrics. Interestingly, the strength of these correlations varied at different scales, with the timing of precipitation (Early, Mid, and Late) influencing the onset/offset of metrics at different scales.

The average NDVI time series of Sentinel was noticeable lower than that of MODIS and Landsat. This may be attributed to the inclusion of bare-ground and individual tree-grass patches that fine scale observation capture, whereas ground cover features were aggregated at coarser spatial resolutions. This is known as the modifiable areal unit problem (MAUP) which essentially relates to how spatial analysis results change when the scale of observations changes (Jelinski and Wu, 1996). This phenomenon occurs even in homogenous environments (Levin, 1992), which further emphasises the importance of spatial scale considerations in heterogeneous environments. In terms of average NDVI variability between sampled pixels, variability increased at finer scales, which again, is likely due to the patchy nature of savannas that coarser scale observations do not capture. Although the spectral resolution of each sensor differs slightly (Table 3.1), which may affect the calculated NDVI of each sensor (Huete *et al*., 1997), previous studies have established that there is still a strong relationship between the NDVI of different sensors (Steven *et al*., 2003). The NDVI time series of all sensors in both canopy cover types increased across years, which may be due to the low base level of the 2015/2016 season as a result of the drought that occurred in that season (Swemmer *et al*., 2020). However, the average annual NDVI increase was higher in Open canopy for all the sensors, PlanetScope excluded. This difference could be due to trees being more resilient to drought conditions compared to grasses (Swemmer, 2020), thus higher grass recovery rates would result in a bigger annual NDVI increase in Open canopy.

Additionally, extensive cattle grazing and its subsequent promotion of bush encroachment (O'Connor *et al*., 2014), and rapid coppice regrowth due to wood harvesting (Mograbi *et al*., 2015) in the Open canopy site are also likely causes of higher annual NDVI increases compared to the Closed canopy site. Significant change points were detected in the MODIS and Sentinel NDVI time series which occurred in November 2019 and December 2018 respectively. These change points could indicate the recovery of the Closed and Open canopy systems from the effects of the 2015/2016 drought or they could simply indicate periods where the systems had remained stable and had not been adversely affected by variable rainfall. However, for this research, these change points provide an indication as to when these Closed and Open canopy systems remained relatively stable, and how phenological metrics behaved within this period.

The average phenological metrics between the 2015/2016 and 2020/2021 seasons showed significant differences in LOS, POS, and EOS between sensors. Interestingly, there was no substantial difference in MODIS SOS in both canopy cover types. The average SOS was the same in both canopy cover types (341 DOY-7th December) which is surprising as it was expected that early greening of trees in the Closed canopy site would result in an earlier SOS. At finer Landsat and Sentinel scale, SOS occurred earlier (Landsat - 5 days, Sentinel-2 days) in Closed canopy, showing that even with a small sample size, finer scales observations are better suited to capturing early greening. However, early greening varies across years due to natural rainfall variability in southern Africa (Lehmann *et al*., 2011), temperature (Campo-Bescós *et al*., 2013) and day length (Higgins *et al*., 2011) among many other environmental cues. This variation suggests that focusing on the average SOS in savanna landscapes can be misleading. For example, SOS in the 2020/2021 season occurred 30± days earlier and in the 2015/2016 season 20± days later than the average due to the early rainfall and drought events occurring in those seasons respectively. Furthermore, the temporal gap between observations can result in different SOS inferences, with one study suggesting SOS can differ by 30 days between temporal resolutions (Xie and Wilson, 2020). SOS in this study had the highest variability (22 days) in both canopy cover types compared to other metrics, making it tough to establish any trend, patterns, or differences between sites. Instead, a study in a similar landscape found that the dependence of grasses on rainfall contributed to a large variation in grass SOS, compared to small SOS variation for trees which can store water and nutrients (Archibald and Scholes, 2007).

The influence of scale was more pronounced on LOS, POS, and EOS in both canopy cover types. The average LOS decreased from coarse to fine scale in both canopy cover types with an average difference of 34 days between MODIS and Sentinel. Canopy cover did not influence the average LOS for all sensors with the largest difference being only one day at Sentinel scale. Interestingly, LOS of the 2020/2021 season showed the same pattern of a decrease in LOS from coarse to fine scale, however, at very fine PlanetScope scale LOS increased (20 days longer than Sentinel) in both canopy cover types. This increase at PlanetScope scale also occurred for POS and EOS, demonstrating a non-linear relationship between phenological metrics and spatial scale. The average POS occurred earlier in Closed canopy for all sensors. The average difference in POS between canopy cover types increased from fine (1 day-Sentinel) to coarse (8 days - MODIS scale). This delay in POS between canopy types was likely due to the timing of mid-season precipitation, and the constant and extensive grazing pressure exerted on the Open canopy site. Interestingly this rainfall variability and possibly the grazing pressure, were more pronounced at coarser scales, whereas there was almost no difference at finer scales. This could be due to ecological time lags associated with increased spatial scale observations (Wiens, 1989). Lastly, like LOS and POS, the average EOS occurred later at coarse scale and earlier at finer scales with no considerable difference between canopy cover types. As is the case with LOS and POS at PlanetScope scale, EOS also increased at this very fine scale. Owing to only one season's worth of PlanetScope NDVI being used, it cannot be certain if this later occurrence of POS, LOS and EOS is a function of scale as more samples are needed to confirm if this is a consistent trend.

The visual representations of phenological metrics clearly show how phenology varies between spatial scales. The SOS at MODIS scale occurred between 4 (DOY-338) and 11 (DOY-345) December for all sampled pixels in both canopy cover types, however, at finer scales SOS occurred between 18 (DOY-322) November and 11 (DOY - 345) December, demonstrating how coarser scales cannot capture the finer scale variation in the onset of SOS. Interestingly, the LOS and EOS phenology maps at Landsat and Sentinel scale clearly show the presence of a riparian zone which significantly increased the LOS of vegetation in these areas due to increased water availability. However, this was not captured by coarse scale MODIS, which further demonstrates how coarse scale observations do not accurately capture landscape characteristics that can influence phenological metrics.

In addition, I tested the relationship between the annual metrics of the different sensors, which informs on whether metrics remain stable through all scale comparisons. I predicted that the relationship between phenological metrics at different scales would be more strongly related between coarser scales (MODIS and Landsat) as they aggregate a mixture of species-specific phenology within their coarser pixels. I also expected a stronger relationship in the Open canopy site due to its homogenous nature. Indeed, all MODIS and Landsat phenological metrics had strong relationships (except EOS in Open canopy), with the strongest relationship being found in Open canopy for all the metrics (except LOS). SOS had a similarly strong relationship in both canopy cover types. Fisher and Mustard (2007) also found a strong SOS relationship ($R^2 = 0.60$) between MODIS (500 m) and Landsat (30 m) from deciduous vegetation. My results indicate a weak relationship between coarse and fine scale derived phenological metrics, and that vegetation composition can further influence these relationships.

Environmental cues such as precipitation and temperature may also influence not only annual phenological metric variability but also the relationship of metrics between sensors as vegetation responds differently to environmental cues at different scales (Tang *et al*., 2016). The correlations between phenological metrics and climatic variables (precipitation and temperature) suggest that the timing of rainfall influenced the onset of metrics differently, at different scales (Table 3.6). It is well known that savanna phenology in southern Africa is primarily driven by water availability (Scholes and Archer, 1997). However, the impact of water availability on phenology at different scales is less understood. Higher amounts of Early rainfall resulted in an earlier onset of SOS in both canopy cover types, and longer LOS particularly at MODIS scale. Interestingly, Late rainfall extended EOS significantly in Open canopy at all scales, however in Closed canopy the strength of this correlation weakened at finer scales. This could be due to the reliance on water availability by grasses in Open canopy, whereas the greater density of trees in Closed canopy would reduce evapotranspiration (Ludwig *et al*., 2001), thus extending the water availability period. Surprisingly, Mid rainfall did not have a significant impact on POS, instead Early rainfall reduced the onset of POS significantly only at Sentinel scale in Open canopy but at both MODIS and Sentinel in Closed canopy, suggesting that Early rainfall enabled grasses to peak earlier at fine scales. Temperature had no influence on phenological metrics in this study, although a study in the savanna biome southwest of the study area, found that temperature increases contributed to the onsets of SOS (Barrett and Brown, 2021). The use of annual

average temperature likely resulted in an absence of correlations between temperature and phenological metrics, as it does not represent the inter-seasonal changes in temperature which are a stronger determinant of savanna phenology (Campo-Bescós *et al*., 2013).

To conclude, my study sought to assess the trends of NDVI time series captured at different spatial scales, how phenological metrics are influenced by these spatially different time series, and how precipitation and temperature impact phenological metrics at different scales. I found that the average time series NDVI decreased from coarse to fine scale, and NDVI variability increased at finer scales. Spatial scale had a significant influence on LOS, POS, and EOS with the onset/length of these metrics decreasing at finer scales. Only POS was different between canopy cover types as its onset occurred later in Open canopy. Early, Mid and Late rainfall influenced various phenological metrics with the strength of this influence differing between scales and canopy cover type. Results thus suggest that fine resolution sensors should be used in future savanna phenology studies as they are better suited to capturing fine scale variability associated with savanna systems.

3.6. References

Archibald, S. and Scholes, R.J., 2007. Leaf green-up in a semi-arid African savanna-separating tree and grass responses to environmental cues. *Journal of Vegetation Science*, 18(4), 583-594.

Barrett, A. and Brown, L., 2021. Effects of rainfall, temperature, and photoperiod on the phenology of ephemeral resources for selected bushveld woody plant species in southern Africa. *PloS One*, 16(5), e0251421.

Baumgartner, J.B., and Wilson P.D., 2021. *things*: Mostly spatial things. R package version 0.0.3.9000

Beurs, K.M.D. and Henebry, G.M., 2010. Spatio-temporal statistical methods for modelling land surface phenology. *Phenological Research*, 177-208.

Bórnez, K., Verger, A., Descals, A. and Peñuelas, J., 2021. Monitoring the Responses of Deciduous Forest Phenology to 2000–2018 Climatic Anomalies in the Northern Hemisphere. *Remote Sensing*, 13(14), 2806.

Bourke, P., 1996. Cross correlation. *Cross Correlation", Auto Correlation—2D Pattern Identification*.

Burnham, K.P. and Anderson, D.R., 1998. Practical use of the information-theoretic approach. In *Model selection and inference*, 75-117. Springer, New York, NY.

Campo-Bescós, M.A., Muñoz-Carpena, R., Kaplan, D.A., Southworth, J., Zhu, L. and Waylen, P.R., 2013. Beyond precipitation: Physiographic gradients dictate the relative importance of environmental drivers on savanna vegetation. *PloS One*, 8(8), e72348.

Cleveland, R.B., Cleveland, W.S., McRae, J.E. and Terpenning, I., 1990. STL: A seasonal-trend decomposition. *Journal of Official Statistics*, 6(1), 3-73.

Davis, C.L., Hoffman, M.T. and Roberts, W., 2017. Long-term trends in vegetation phenology and productivity over Namaqualand using the GIMMS AVHRR NDVI3g data from 1982 to 2011. *South African Journal of Botany*, 111, 76-85.

Delbart, N., Kergoat, L., Le Toan, T., Lhermitte, J. and Picard, G., 2005. Determination of phenological dates in boreal regions using normalized difference water index. *Remote Sensing of Environment*, 97(1), 26-38.

Eklundha, L. and Jönsson, P., 2017. TIMESAT 3.3 with seasonal trend decomposition and parallel processing Software Manual. *Lund, Sweden: Lund University*.

Fisher, J.I. and Mustard, J.F., 2007. Cross-scalar satellite phenology from ground, Landsat, and MODIS data. *Remote Sensing of Environment*, 109(3), 261-273.

Fontana, F., Rixen, C., Jonas, T., Aberegg, G. and Wunderle, S., 2008. Alpine grassland phenology as seen in AVHRR, VEGETATION, and MODIS NDVI time series-a comparison with in situ measurements. *Sensors*, 8(4), 2833-2853.

Gallinat, A.S., Ellwood, E.R., Heberling, J.M., Miller-Rushing, A.J., Pearse, W.D. and Primack, R.B., 2021. Macrophenology: insights into the broad-scale patterns, drivers, and consequences of phenology. *American Journal of Botany*, 108(11), 2112-2126.

Gong, Z., Kawamura, K., Ishikawa, N., Goto, M., Wulan, T., Alateng, D., Yin, T. and Ito, Y., 2015. MODIS normalized difference vegetation index (NDVI) and vegetation phenology dynamics in the Inner Mongolia grassland. *Solid Earth*, 6(4), 1185-1194.

Google Developers. 2021. *Earth Engine Data Catalog | Google Developers*. [online] Available at: <https://developers.google.com/earth-engine/datasets> [Accessed 4 July 2021].

Grace, J., José, J.S., Meir, P., Miranda, H.S. and Montes, R.A., 2006. Productivity and carbon fluxes of tropical savannas. *Journal of Biogeography*, 33(3), 387-400.

Higgins, S.I., Delgado-Cartay, M.D., February, E.C. and Combrink, H.J., 2011. Is there a temporal niche separation in the leaf phenology of savanna trees and grasses? *Journal of Biogeography*, 38(11), 2165-2175.

Huete, A.R., Liu, H.Q., Batchily, K.V. and Van Leeuwen, W.J.D.A., 1997. A comparison of vegetation indices over a global set of TM images for EOS-MODIS. *Remote Sensing of Environment*, 59(3), 440-451.

Huntley, B.J. and Walker, B.H. eds., 2012. *Ecology of tropical savannas* (Vol. 42). Springer Science & Business Media.

Jelinski, D.E. and Wu, J., 1996. The modifiable areal unit problem and implications for landscape ecology. *Landscape Ecology*, 11(3), 129-140.

Lehmann, C.E., Anderson, T.M., Sankaran, M., Higgins, S.I., Archibald, S., Hoffmann, W.A., Hanan, N.P., Williams, R.J., Fensham, R.J., Felfili, J. and Hutley, L.B., 2014. Savanna vegetation-fire-climate relationships differ among continents. *Science*, 343(6170), 548-552.

Lehmann, C.E., Archibald, S.A., Hoffmann, W.A. and Bond, W.J., 2011. Deciphering the distribution of the savanna biome. *New Phytologist*, 191(1), 197-209.

Levin, S.A., 1992. The problem of pattern and scale in ecology: the Robert H. MacArthur award lecture. *Ecology*, 73(6), 1943-1967.

Lieth, H., 1974. Purposes of a phenology book. In *Phenology and seasonality modelling*, 3-19. Springer, Berlin, Heidelberg.

Ludwig, F., de Kroon, H., Prins, H.H. and Berendse, F., 2001. Effects of nutrients and shade on tree-grass interactions in an East African savanna. *Journal of Vegetation Science*, 12(4), 579-588.

Ma, X., Huete, A., Yu, Q., Coupe, N.R., Davies, K., Broich, M., Ratana, P., Beringer, J., Hutley, L.B., Cleverly, J. and Boulain, N., 2013. Spatial patterns and temporal dynamics in savanna vegetation phenology across the North Australian Tropical Transect. *Remote Sensing of Environment*, 139, 97-115.

Matongera, T.N., Mutanga, O., Sibanda, M. and Odindi, J., 2021. Estimating and Monitoring Land Surface Phenology in Rangelands: A Review of Progress and Challenges. *Remote Sensing*, 13(11), 2060.

Mograbi, P.J., Erasmus, B.F., Witkowski, E.T.F., Asner, G.P., Wessels, K.J., Mathieu, R., Knapp, D.E., Martin, R.E. and Main, R., 2015. Biomass increases go under cover: woody vegetation dynamics in South African rangelands. *PLoS One*, 10(5), 0127093.

O'Connor, T.G., Puttick, J.R. and Hoffman, M.T., 2014. Bush encroachment in southern Africa: changes and causes. *African Journal of Range & Forage Science*, 31(2), 67-88.

Osborne, C.P., Charles-Dominique, T., Stevens, N., Bond, W.J., Midgley, G. and Lehmann, C.E., 2018. Human impacts in African savannas are mediated by plant functional traits. *New Phytologist*, 220(1), 10-24.

Pan, Z., Hu, Y. and Cao, B., 2017. Construction of smooth daily remote sensing time series data: a higher spatiotemporal resolution perspective. *Open Geospatial Data, Software and Standards*, 2(1), 1-11.

Parrini, F. and Erasmus, B.F.N., 2009. Spatial and temporal heterogeneity of phenology patterns in Kruger National Park, South Africa: different drivers for different areas. *sine loco*

Piao, S., Liu, Q., Chen, A., Janssens, I.A., Fu, Y., Dai, J., Liu, L., Lian, X.U., Shen, M. and Zhu, X., 2019. Plant phenology and global climate change: Current progresses and challenges. *Global Change Biology*, 25(6), 1922-1940.

Robinson, N.P., Allred, B.W., Jones, M.O., Moreno, A., Kimball, J.S., Naugle, D.E., Erickson, T.A. and Richardson, A.D., 2017. A dynamic Landsat derived normalized difference vegetation index (NDVI) product for the conterminous United States. *Remote Sensing*, 9(8), 863.

Running, S.W. and Hunt Jr, E.R., 1993. Generalization of a forest ecosystem process model for other biomes, BIOME-BCG, and an application for global-scale models. *Physiological Ecology*, 141-158

Sankaran, M., Hanan, N.P., Scholes, R.J., Ratnam, J., Augustine, D.J., Cade, B.S., Gignoux, J., Higgins, S.I., Le Roux, X., Ludwig, F. and Ardo, J., 2005. Determinants of woody cover in African savannas. *Nature*, 438(7069), 846-849.

Scheiter, S., Higgins, S.I., Osborne, C.P., Bradshaw, C., Lunt, D., Ripley, B.S., Taylor, L.L. and Beerling, D.J., 2012. Fire and fire-adapted vegetation promoted C4 expansion in the late Miocene. *New Phytologist*, 195(3), 653-666.

Scholes, R.J. and Archer, S.R., 1997. Tree-grass interactions in savannas. *Annual Review of Ecology and Systematics*, 28(1), 517-544.

Scholes, R.J., and Walker, B.H., 1993. *An African savanna: synthesis of the Nylsvley study*. Cambridge University Press.

Shackleton, S.E., 2005. *The significance of the local trade in natural resource products for livelihoods and poverty alleviation in South Africa*. PhD Thesis, Rhodes University, South Africa.

Shen, M., Piao, S., Dorji, T., Liu, Q., Cong, N., Chen, X., An, S., Wang, S., Wang, T. and Zhang, G., 2015. Plant phenological responses to climate change on the Tibetan Plateau: research status and challenges. *National Science Review*, 2(4), 454-467.

Steven, M.D., Malthus, T.J., Baret, F., Xu, H. and Chopping, M.J., 2003. Intercalibration of vegetation indices from different sensor systems. *Remote Sensing of Environment*, 88(4), 412-422.

Swemmer, A.M., 2020. Locally high, but regionally low: the impact of the 2014–2016 drought on the trees of semi-arid savannas, South Africa. *African Journal of Range & Forage Science*, 37(1), 31-42.

Tang, J., Körner, C., Muraoka, H., Piao, S., Shen, M., Thackeray, S.J. and Yang, X., 2016. Emerging opportunities and challenges in phenology: a review. *Ecosphere*, 7(8), e01436.

Tomaszewska, M.A., Nguyen, L.H. and Henebry, G.M., 2020. Land surface phenology in the highland pastures of montane Central Asia: Interactions with snow cover seasonality and terrain characteristics. *Remote Sensing of Environment*, 240, 111675.

Trapletti A, Hornik K 2020. *tseries: Time Series Analysis and Computational Finance*. R package version 0.10-48., https://CRAN.R-project.org/package=tseries.

Tucker, C.J., 1979. Red and photographic infrared linear combinations for monitoring vegetation. *Remote Sensing of Environment*, 8(2), 127-150.

Twine, W.C., 2005. Socio-economic transitions influence vegetation change in the communal rangelands of the South African Lowveld. *African Journal of Range and Forage Science*, 22(2), 93-99.

Vrieling, A., Meroni, M., Darvishzadeh, R., Skidmore, A.K., Wang, T., Zurita-Milla, R., Oosterbeek, K., O'Connor, B. and Paganini, M., 2018. Vegetation phenology from Sentinel-2 and field cameras for a Dutch barrier island. *Remote Sensing of Environment*, 215, 517-529.

Wessels, K., Steenkamp, K., Von Maltitz, G. and Archibald, S., 2011. Remotely sensed vegetation phenology for describing and predicting the biomes of South Africa. *Applied Vegetation Science*, 14(1), 49-66.

White, M.A., de Beurs, K.M., Didan, K., Inouye, D.W., Richardson, A.D., Jensen, O.P., O'keefe, J., Zhang, G., Nemani, R.R., van Leeuwen, W.J. and Brown, J.F., 2009. Intercomparison, interpretation, and assessment of spring phenology in North America estimated from remote sensing for 1982–2006. *Global Change Biology*, 15(10), 2335-2359.

Whitecross, M.A., Witkowski, E.T. and Archibald, S., 2017. Assessing the frequency and drivers of early-greening in broad-leaved woodlands along a latitudinal gradient in southern Africa. *Austral Ecology*, 42(3), 341-353.

Wiens, J.A., 1989. Spatial scaling in ecology. *Functional Ecology*, 3(4), 385-397.

Xie, Y. and Wilson, A.M., 2020. Change point estimation of deciduous forest land surface phenology. *Remote Sensing of Environment*, 240, 111698

Zeng, L., Wardlow, B.D., Xiang, D., Hu, S. and Li, D., 2020. A review of vegetation phenological metrics extraction using time-series, multispectral satellite data. *Remote Sensing of Environment*, 237, 111511.

Zhang, X., Wang, J., Gao, F., Liu, Y., Schaaf, C., Friedl, M., Yu, Y., Jayavelu, S., Gray, J., Liu, L. and Yan, D., 2017. Exploration of scaling effects on coarse resolution land surface phenology. *Remote Sensing of Environment*, 190, 318-330.

3.7. Tables and Figures

Table 3.1: Summary of Mann-Kendall and Seasonal Sen's Slope results for all sensors in both canopy cover types.

Sensor	Mann-Kendall statistic	Kendall's Tau	Variance (S)	*p* value	Interpretation	Seasonal Sens's Slope
MODIS Closed Canopy	137	0.28	1019.6	0.001	Reject H_0	0.0063
MODIS Open Canopy	193	0.40	1019.6	0.001	Reject H_0	0.0120
Landsat Closed canopy	78	0.31	532.0	0.001	Reject H_0	0.0093
Landsat Open Canopy	90	0.35	532.0	0.001	Reject H_0	0.0104
Sentinel Closed Canopy	118	0.28	886.6	0.001	Reject H_0	0.0078
Sentinel Open Canopy	170	0.40	886.6	0.001	Reject H_0	0.0110

Table 3.2: Results of cross-correlation between sensors in both Closed and Open canopy, where bolded values indicate the strongest correlation.

Closed Canopy								
Cross-Correlation between Sensors (*y-x*)	R^2 at lag intervals between t -3 and 3							Days between Composites
	-3	-2	-1	0	1	2	3	
MODIS - Landsat	0.29	0.69	**0.91**	0.88	0.61	0.22	-0.19	MODIS-15.8
MODIS - Sentinel	0.63	0.84	**0.95**	0.93	0.79	0.58	0.34	Landsat-30.4
MODIS - PlanetScope	0.60	0.79	0.93	**0.98**	0.89	0.72	0.52	
Landsat - Sentinel	0.01	0.40	0.75	**0.92**	0.86	0.55	0.12	Sentinel-18.2
Sentinel - PlanetScope	0.52	0.74	0.81	**0.95**	0.83	0.49	0.28	
Open Canopy								PlanetScope-15.8
MODIS - Landsat	0.28	0.68	**0.91**	0.89	0.65	0.28	-0.11	
MODIS - Sentinel	0.60	0.80	**0.93**	0.91	0.82	0.63	0.4	
MODIS - PlanetScope	0.61	0.81	0.94	**0.99**	0.92	0.76	0.56	
Landsat-Sentinel	-0.10	0.39	0.73	**0.92**	0.86	0.58	0.17	
Sentinel - PlanetScope	0.05	0.41	0.77	**0.91**	0.80	0.33	0.19	

Table 3.3: The average DOY each of the phenological metrics occurs within Closed and Open canopy vegetation between the **2015-2021** season, for all sensors. The difference in DOY between canopy cover types is also shown.

Sensor	SOS			LOS			POS			EOS		
	Closed	Open	*diff*	Closed	Open	*diff*	Closed	Open	*diff*	Closed	Open	*diff*
MODIS	341.8	341.8	0.0	183.1	183.8	-0.7	432.8	441.4	-8.6	525.0	526.8	-1.8
Landsat	341.1	346.1	-5.0	154.1	153.7	0.4	425.2	428.6	-3.4	517.2	519.7	-2.5
Sentinel	340.2	342.1	-1.9	149.7	148.4	1.3	414.9	416.1	-1.2	508.2	508.8	-0.6

Table 3.4: DOY each of the phenological metrics occurs within Closed and Open canopy vegetation for the **2020-2021** season, for all sensors. The difference in DOY between canopy cover types is also shown. The SD of all sensors for each metric shows the variation between sensors.

Sensor	SOS			LOS			POS			EOS		
	Closed	Open	*diff*	Closed	Open	*diff*	Closed	Open	*diff*	Closed	Open	*diff*
MODIS	301.0	307.8	6.8	217.2	216.4	-0.8	401.3	425.5	24.2	518.5	524.0	5.5
Landsat	307.9	314.9	7.0	183.7	178.0	-5.7	407.5	410.2	2.7	522.1	523.3	1.2
Sentinel	304.8	315.4	10.6	152.3	148.3	-4.0	375.4	383.8	8.4	475.4	481.9	6.5
Planet	296.8	301.1	4.3	171.5	169.9	-1.6	402.3	417.7	15.4	498.4	501.0	2.6
SD	4.8	6.8	2.6	27.3	28.4	2.2	14.4	18.1	9.3	21.5	20.2	2.5

Table 3.5: The average standard deviation in phenological metrics between the 2015/2016-2020/2021 seasons in Closed and Open canopy sites, shown as the number of days.

Sensor	SOS		LOS		POS		EOS	
	Closed	Open	Closed	Open	Closed	Open	Closed	Open
MODIS	22.2	18.7	26.0	29.2	16.5	14.3	12.0	17.3
Landsat	28.9	28.8	19.4	17.6	14.7	13.3	9.5	12.8
Sentinel	20.0	15.5	15.6	19.9	22.6	17.1	18.5	20.9

Table 3.6: Correlation between total precipitation in Jan - Feb, March-April, October-November, total seasonal, and phenological metrics between sensors in Closed and Open canopy cover. Bold font indicates a statistically significant relationship ($p < 0.05$).

Total January and February Precipitation

Sensor	SOS	LOS	POS	EOS
Closed Canopy				
MODIS	**-0.73**	**0.94**	-0.52	0.69
Landsat	**-0.76**	**0.76**	-0.66	**0.82**
Sentinel	-0.48	0.58	-0.72	-0.02
Open Canopy				
MODIS	**-0.79**	**0.95**	-0.37	**0.79**
Landsat	-0.70	0.69	-0.69	**0.80**
Sentinel	-0.66	**0.84**	-0.67	0.30

Total March and April Precipitation

Sensor	SOS	LOS	POS	EOS
Closed Canopy				
MODIS	-0.10	0.47	0.07	**0.85**
Landsat	-0.55	0.24	-0.49	**0.63**
Sentinel	0.28	0.32	-0.08	0.57
Open Canopy				
MODIS	-0.46	0.60	-0.15	**0.90**
Landsat	-0.53	0.36	-0.38	**0.90**
Sentinel	0.02	**0.81**	0.06	**0.79**

Total October and November Precipitation

Sensor	SOS	LOS	POS	EOS
Closed Canopy				
MODIS	**-0.91**	**0.92**	**-0.78**	0.32
Landsat	-0.71	**0.90**	-0.63	0.70
Sentinel	**-0.83**	0.55	**-0.88**	0.44
Open Canopy				
MODIS	**-0.82**	**0.86**	-0.56	0.39
Landsat	-0.67	0.75	-0.75	0.50
Sentinel	**-0.92**	0.53	**-0.93**	-0.18

Total Seasonal Precipitation

Sensor	SOS	LOS	POS	EOS
Closed Canopy				
MODIS	**-0.77**	**0.95**	-0.58	0.64
Landsat	**-0.81**	**0.78**	-0.73	**0.82**
Sentinel	-0.49	0.51	-0.74	-0.10
Open Canopy				
MODIS	**-0.85**	**0.96**	-0.45	0.76
Landsat	**-0.75**	0.73	-0.75	**0.82**
Sentinel	-0.68	**0.80**	-0.69	0.25

Average Seasonal Temperature

Sensor	SOS	LOS	POS	EOS
Closed Canopy				
MODIS	-0.01	0.10	0.09	0.32
Landsat	0.09	0.06	0.13	0.47
Sentinel	0.14	-0.06	0.13	0.09
Open Canopy				
MODIS	-0.09	0.17	0.02	0.24
Landsat	0.09	-0.22	0.03	0.14
Sentinel	-0.06	0.22	0.02	0.16

Statistically significant correlations (p-value < 0.05) denoted by bold font

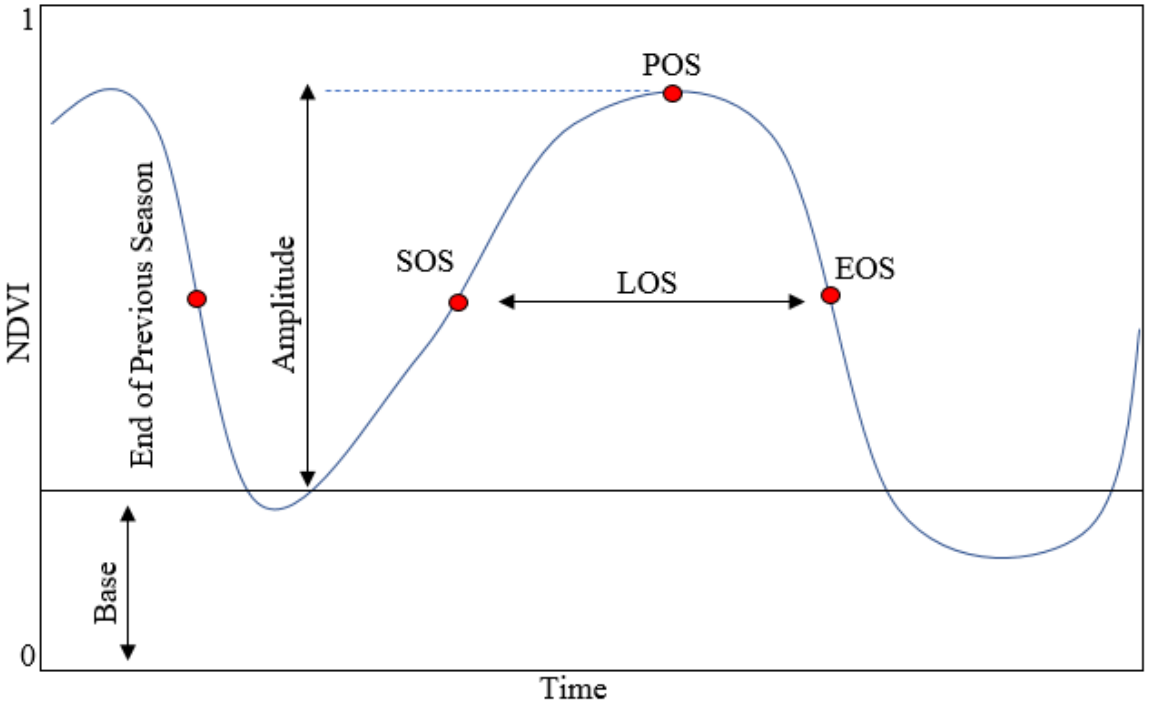

Figure 3.1: Conceptual principle of phenological metric extraction from time series data. The blue line represents a hypothetical NDVI time series, where the Start of Season (SOS) and End of Season (EOS) are determined based on a defined percentage of the seasonal amplitude. The Length of Season (LOS) is the time between SOS and EOS while the base level indicates the average minimum value of the time series.

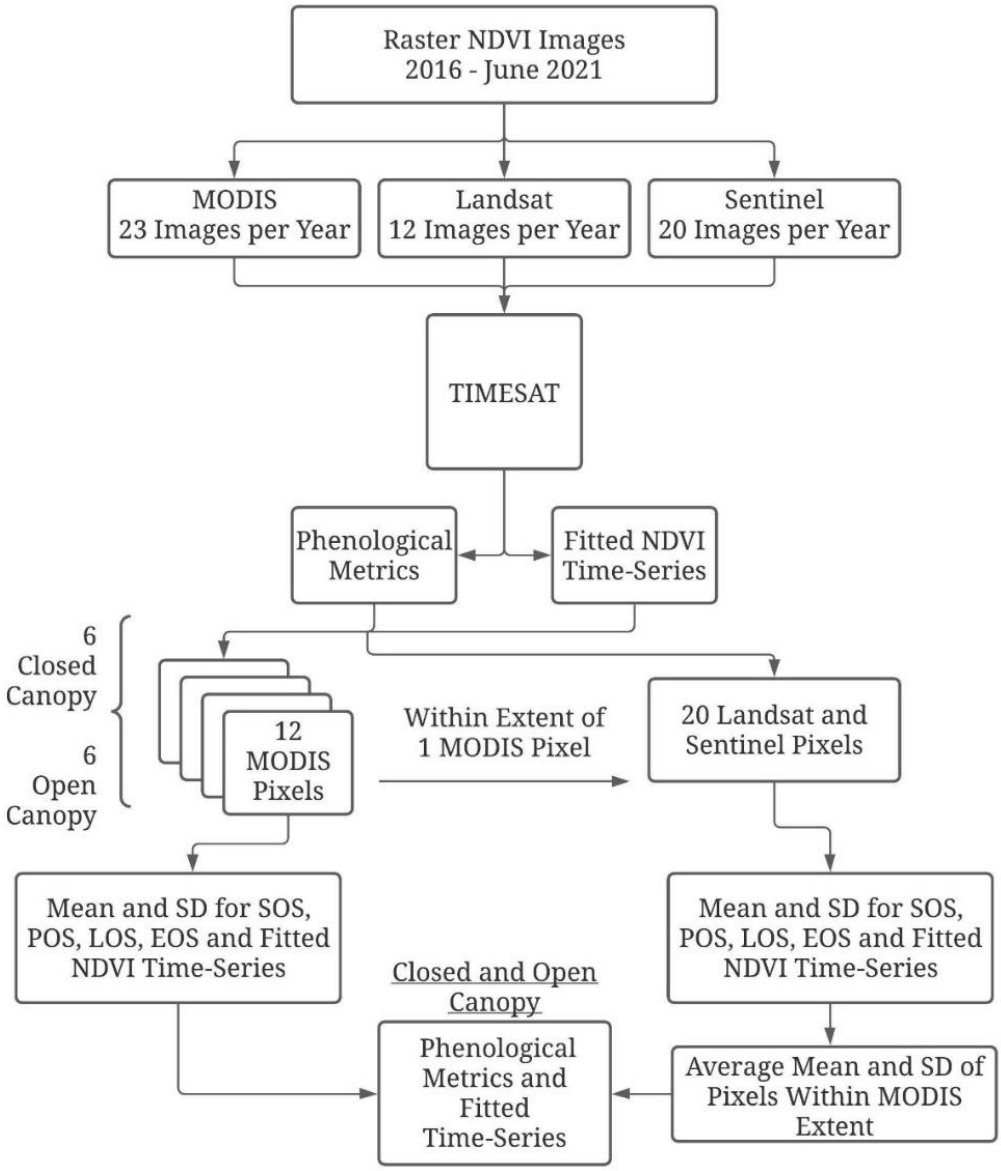

Figure 3.2: Data collection process showing how phenological and fitted NDVI time series data were processed to determine values for Closed and Open canopy sites.

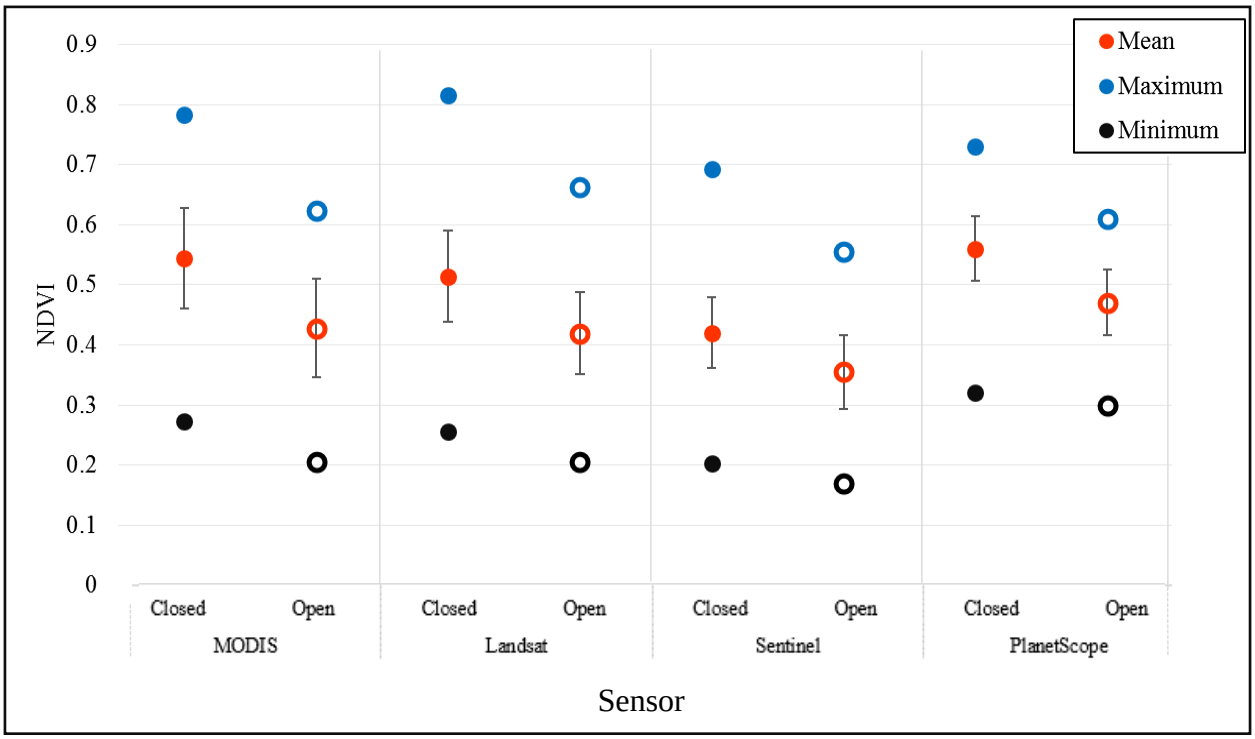

Figure 3.3: Comparison of sensor NDVI maximum (blue), minimum (black), mean (red) and standard deviation between the 2015/2016-2020/2021 season. Solid dots represent Closed canopy and hollow dots represent Open canopy. Note PlanetScope values are for the 2020/2021 season only.

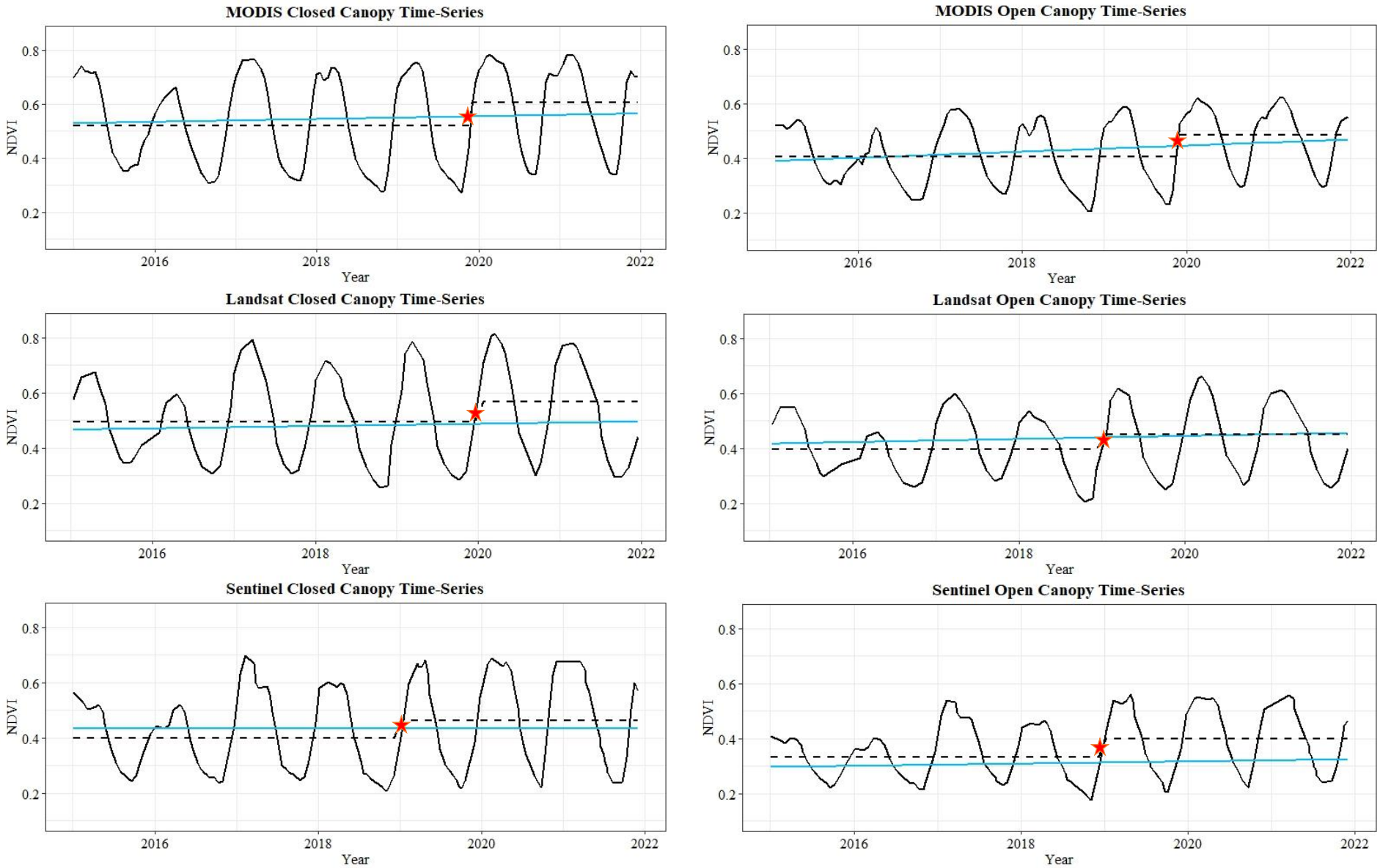

Figure 3.4: NDVI time series (Solid black line) from 2015 - 2021 of MODIS, Landsat, and Sentinel in Closed canopy (Left column) and Open canopy (Right column), with change points (red star) and Sen's slope (solid blue line).

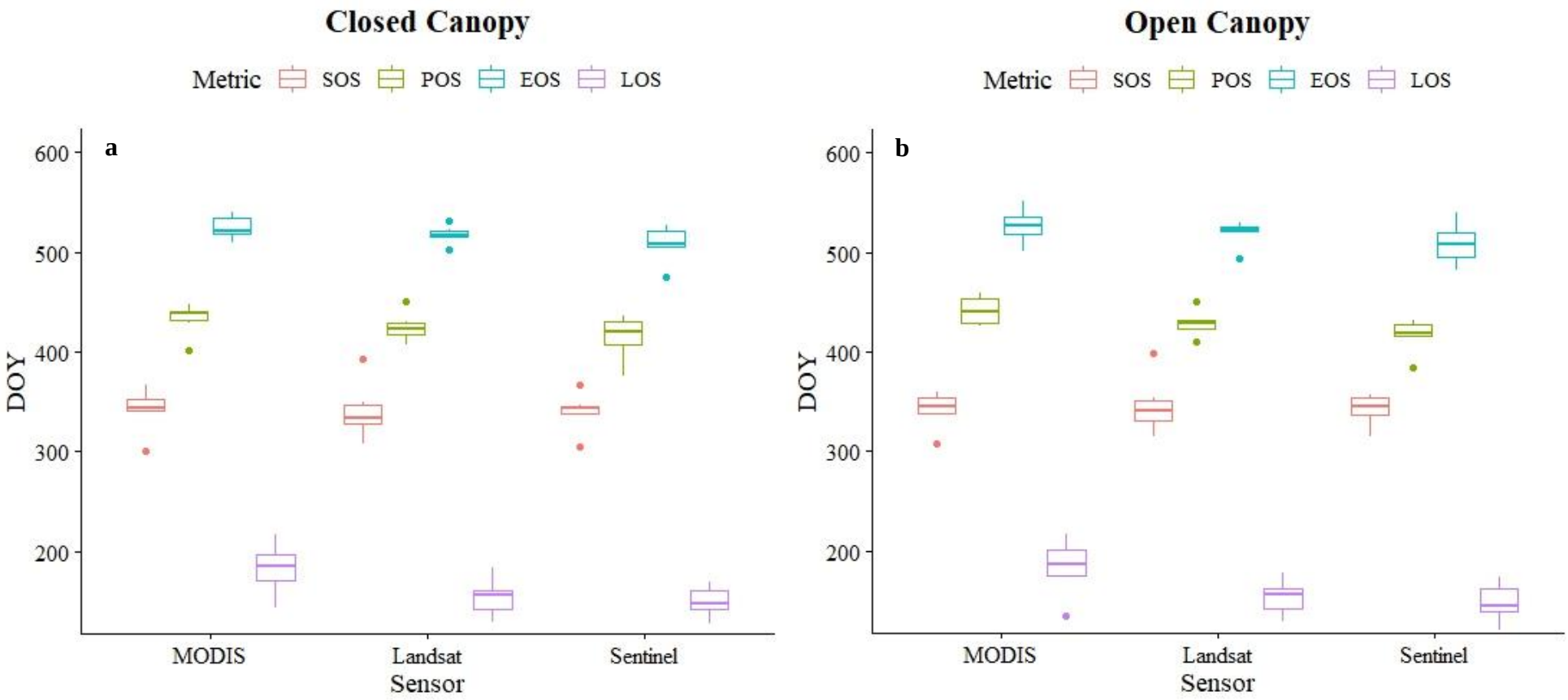

Figure 3.5: Boxplot of phenological metrics of all sensors between 2015/2016-2020/2021 seasons in Closed canopy (a) and Open canopy (b). Note that LOS is not a date but rather the number of days within a season.

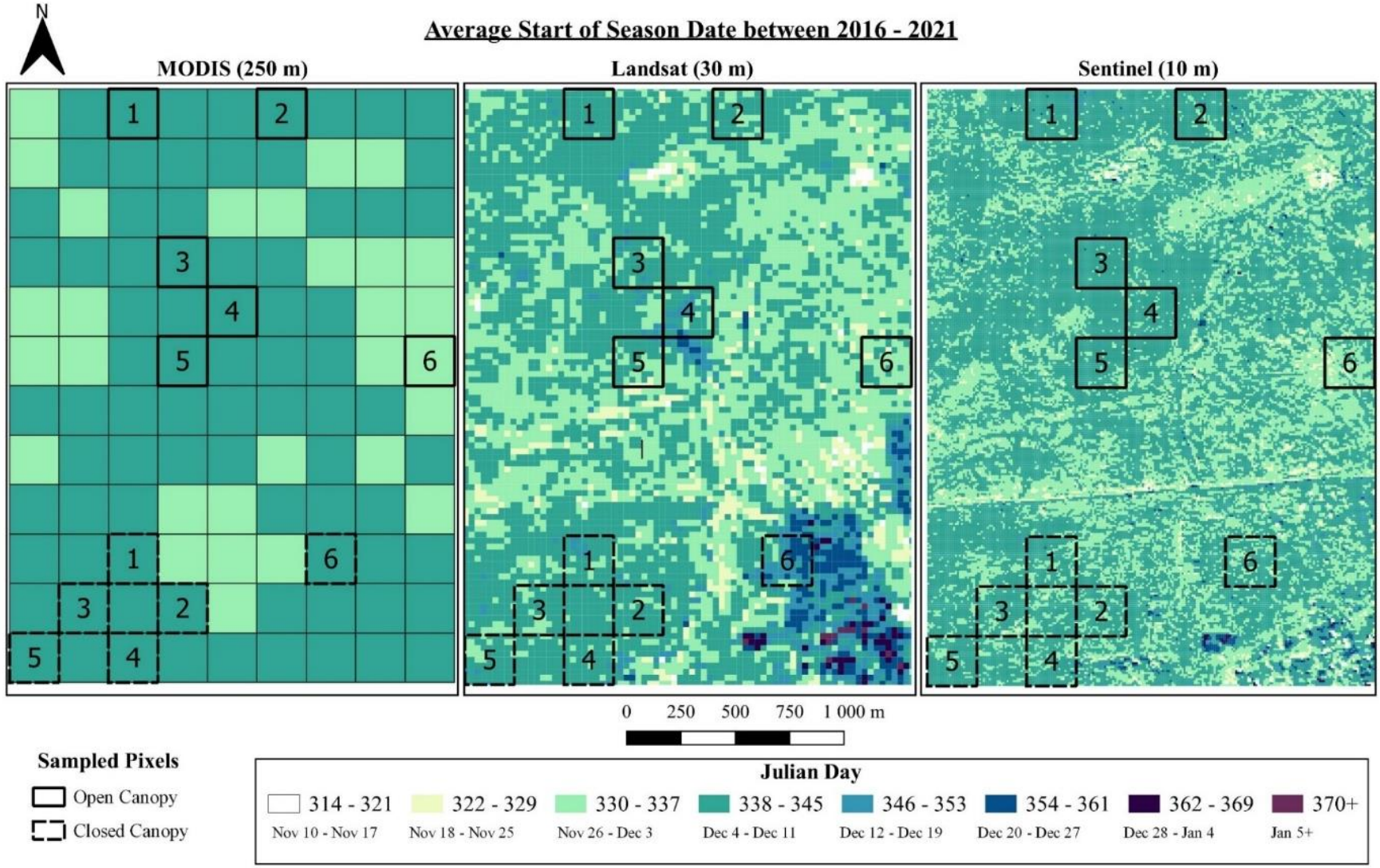

Figure 3.6: The average Start of Season (SOS) between 2016-2021 in Closed canopy (solid squares) and Open canopy (dashed squares) at MODIS (250 m), Landsat (30 m), and Sentinel (10 m) scales.

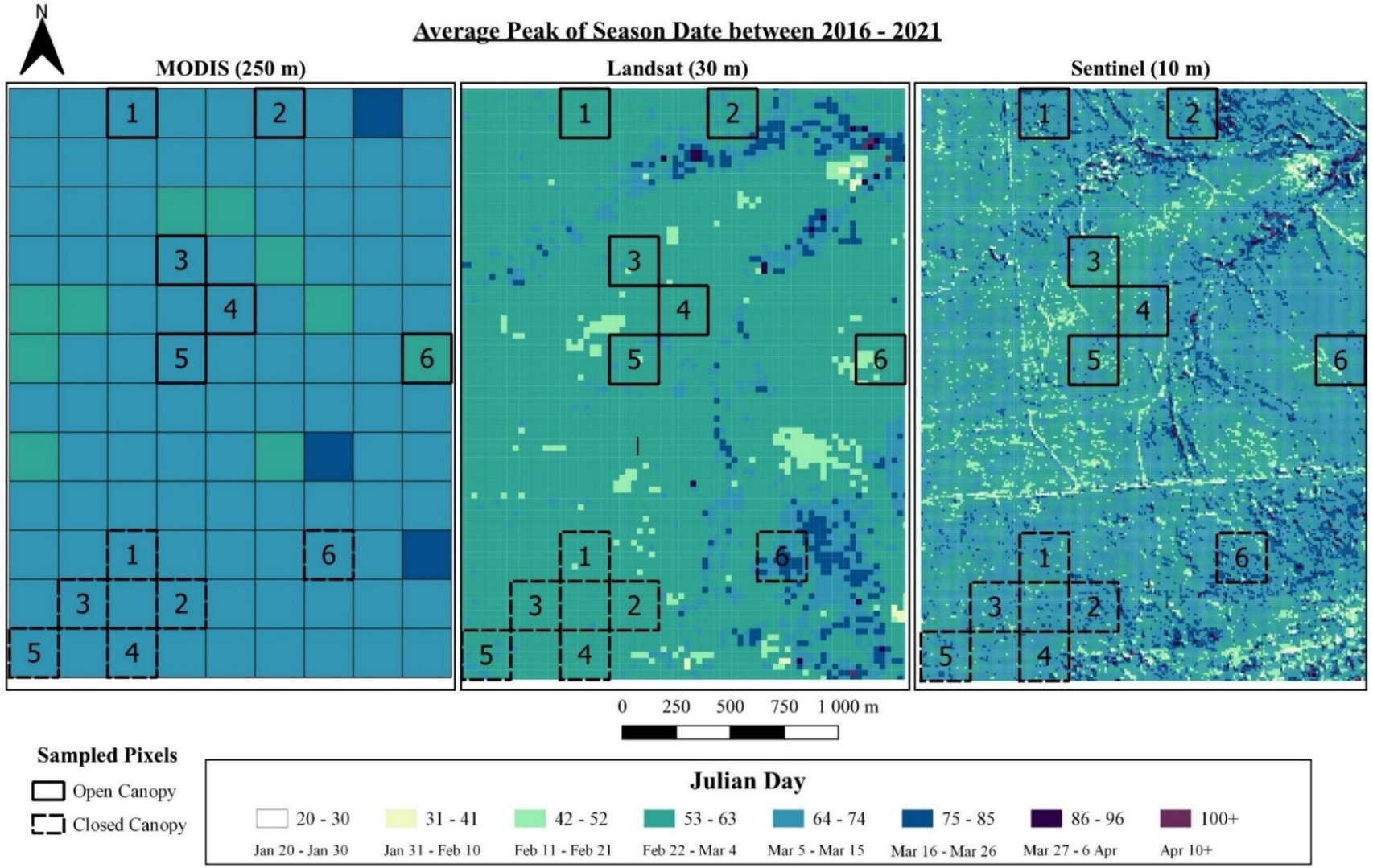

Figure 3.7: The average Peak of Season (POS) between 2016-2021 in Closed canopy (solid squares) and Open canopy (dashed squares) at MODIS (250 m), Landsat (30 m), and Sentinel (10 m) scales.

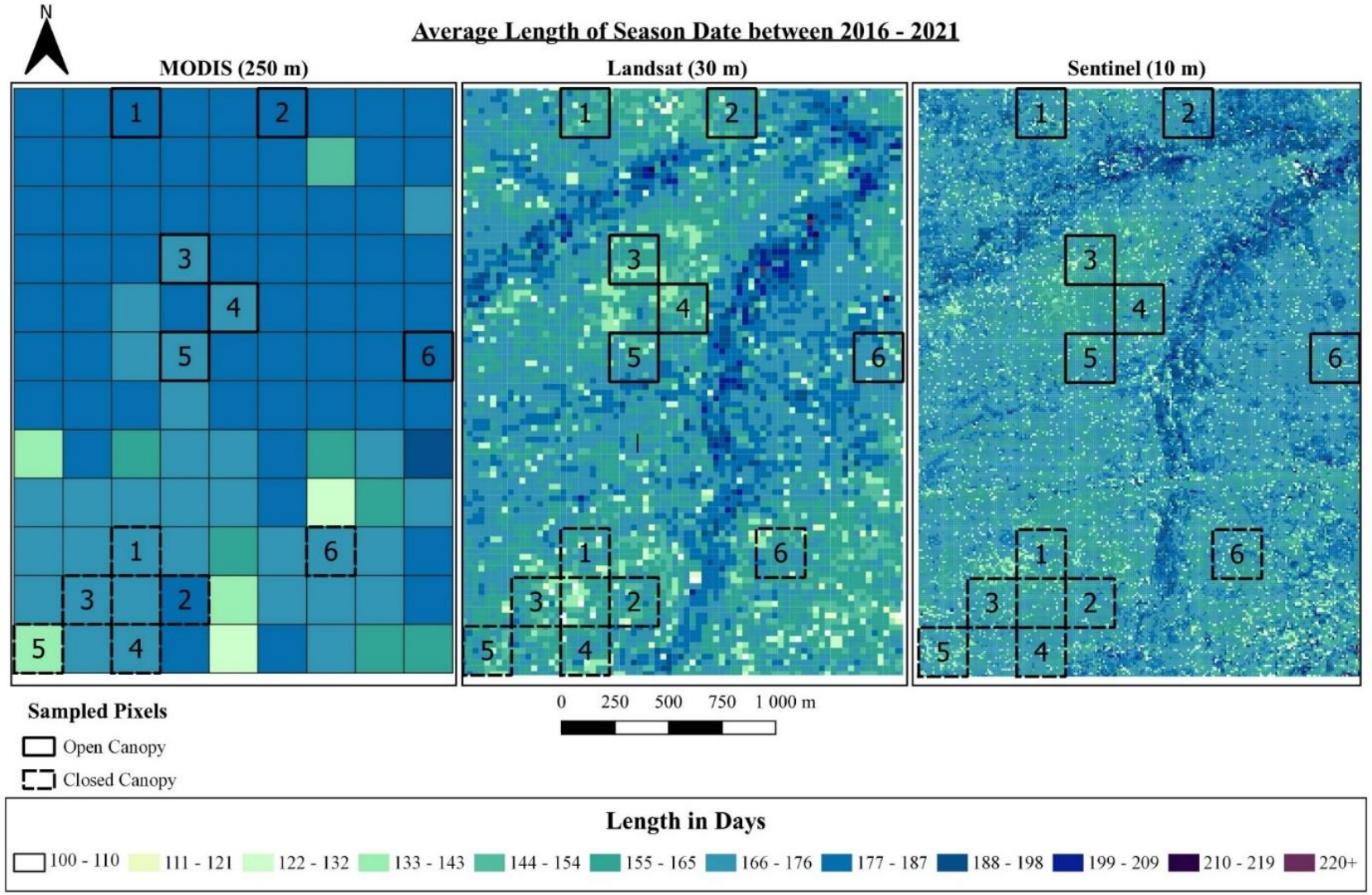

Figure 3.8: The average Length of Season (LOS) between 2016-2021 in Closed canopy (solid squares) and Open canopy (dashed squares) at MODIS (250 m), Landsat (30 m), and Sentinel (10 m) scales.

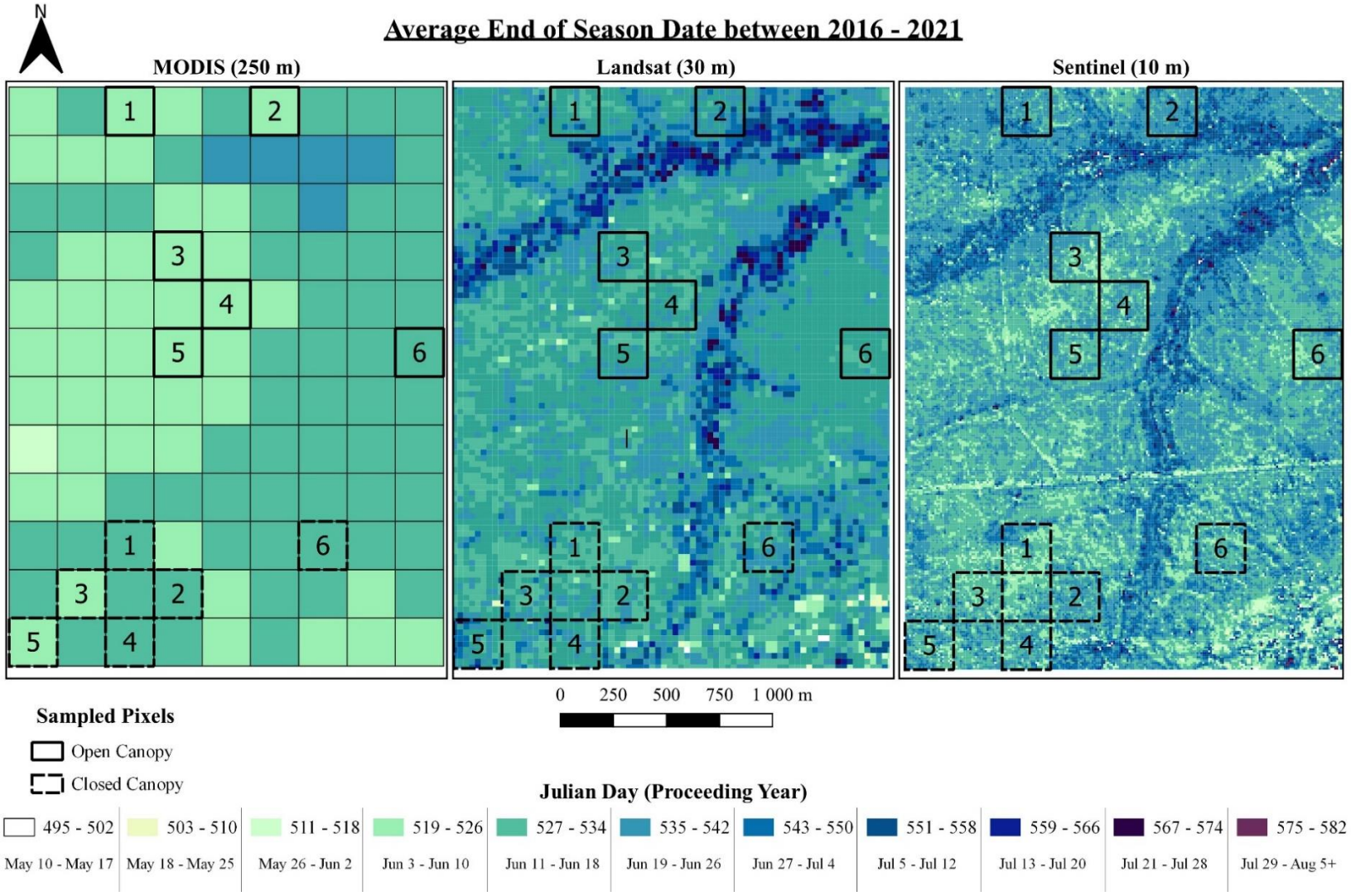

Figure 3.9: The average End of Season (EOS) between 2016-2021 in Closed canopy (solid squares) and Open canopy (dashed squares) at MODIS (250 m), Landsat (30 m), and Sentinel (10 m) scales.

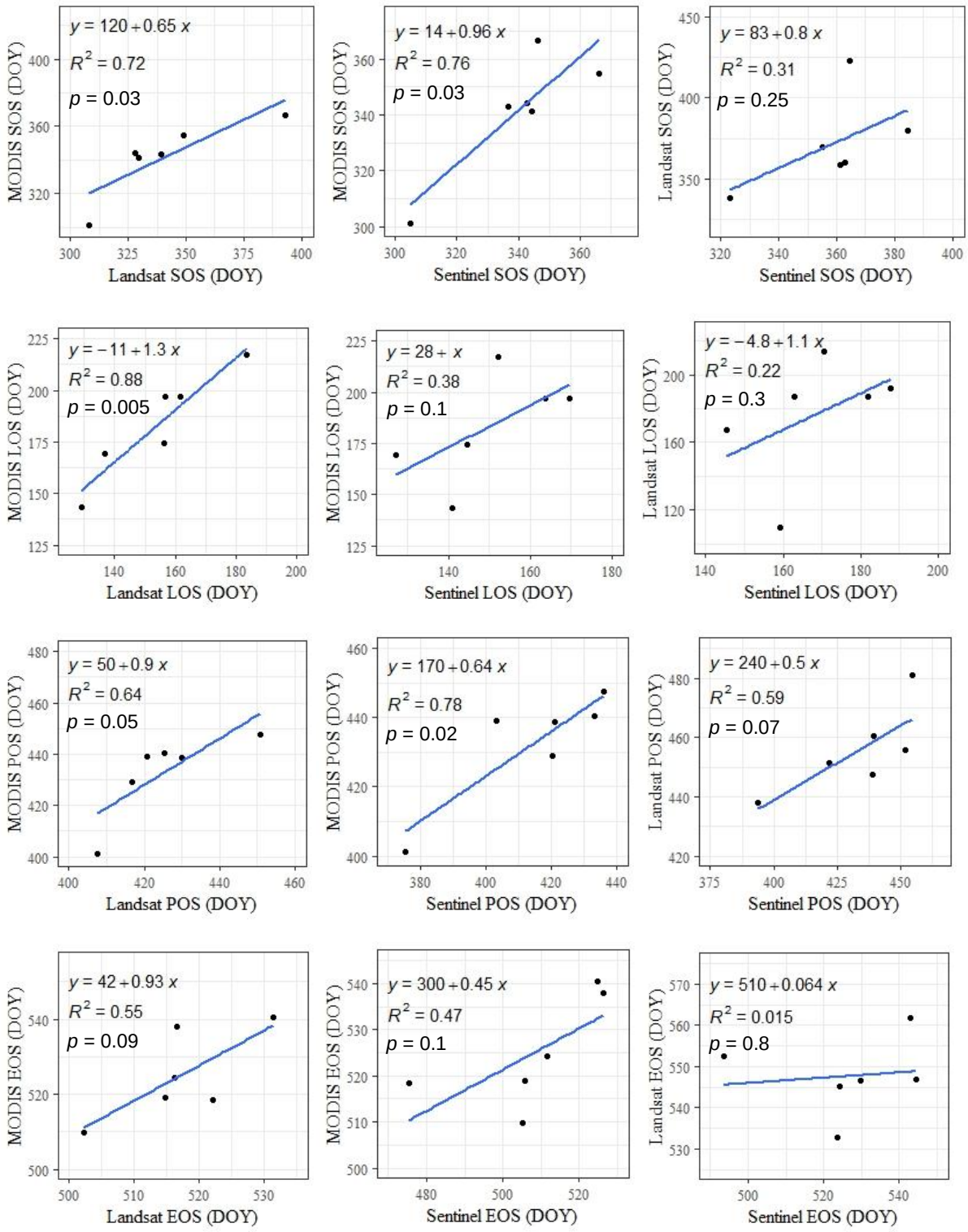

Figure 3.10: Linear regression models of phenological metrics between sensors in Closed canopy vegetation, where rows 1-4 show the regressions of SOS, LOS, POS, and EOS respectively with the regression equation and correlation value shown within each model.

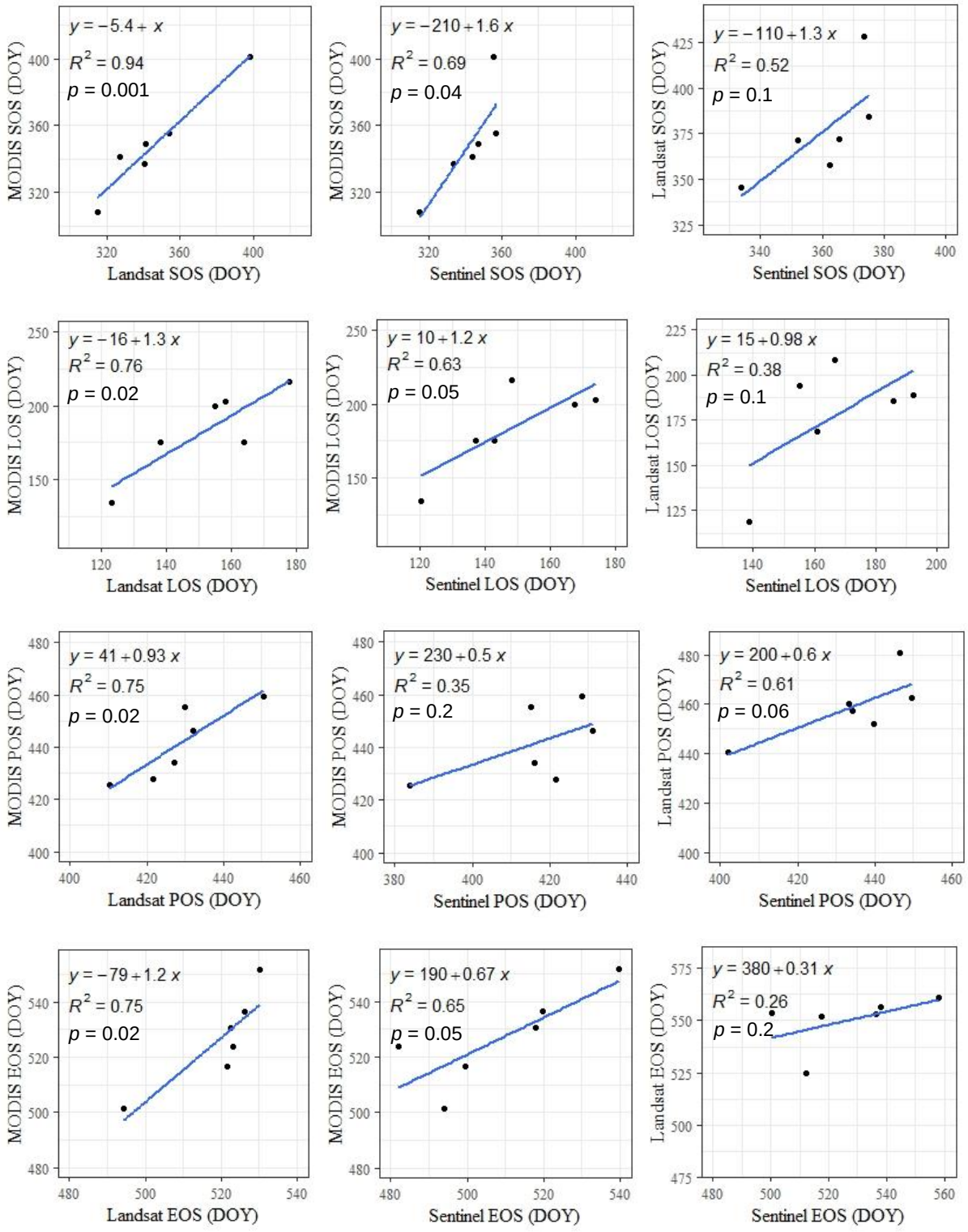

Figure 3.11: Linear regression models of phenological metrics between sensors in Open canopy vegetation, where rows 1-4 show the regressions of SOS, LOS, POS, and EOS respectively with the regression equation and correlation value shown within each model.

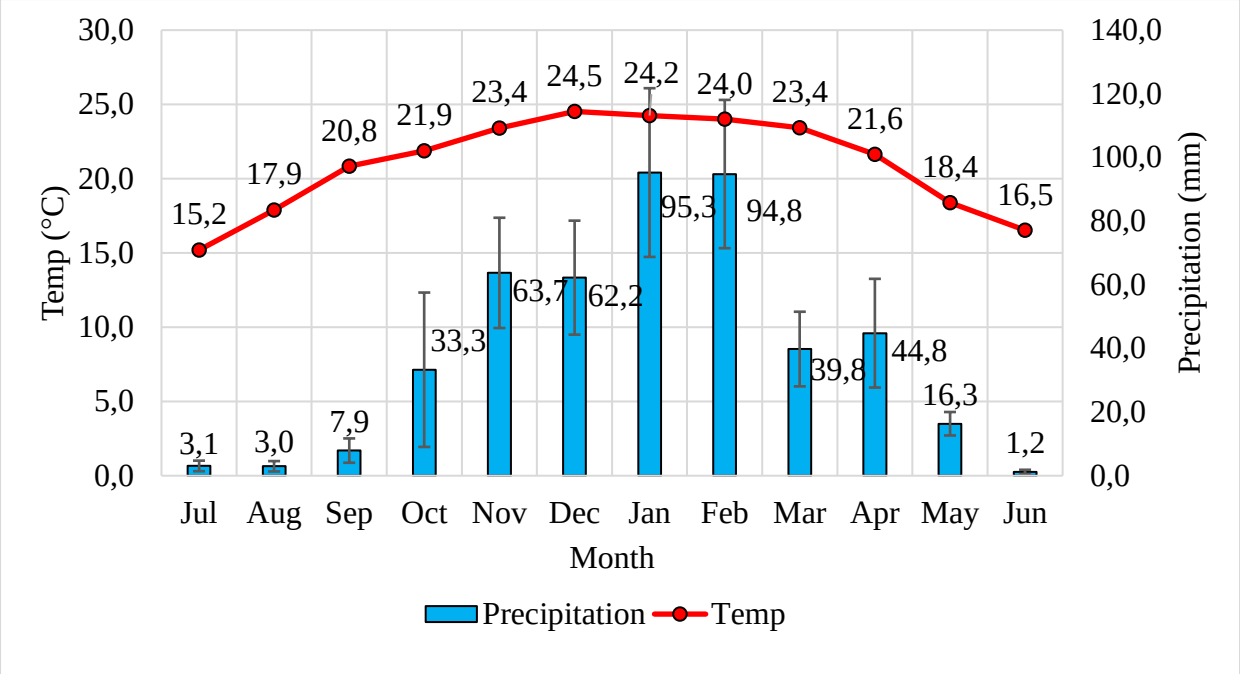

Figure 3.12: Average monthly precipitation and temperature of the study area between 2015 and 2021, derived from the WRF weather station. The red line shows the average monthly temperature, and the blue bars show the average monthly precipitation and SD.

CHAPTER FOUR: Synthesis

It is well established that the spatial and temporal scale of observations in ecological ecosystems directly influences both patterns and variance of an observed variable (Wiens, 1989; Levin, 1992; Jelinski and Wu, 1996; Wu, 2004), such as phenology (Zhang *et al*., 2015; Cole and Sheldon, 2017). This is particularly evident in heterogeneous savanna systems, where vegetation is characterised as being highly variable at both spatial and temporal scales (du Toit, 2003) in both tree (Staver, 2018), and herbaceous vegetation layers (Augustine, 2003).

In savanna ecosystems, this phenomenon emerges for several reasons. Firstly, changing the spatio-temporal scale of observation will change the average and the variance of the observation due to statistical aggregation. Secondly, environmental drivers which shape savanna structure and productivity such as precipitation, vary across space and time (Good and Caylor, 2011), particularly in African savannas (Lehmann *et al*., 2011). And thirdly, the response of individual species to such environmental drivers differs between species (Inouye *et al*., 2019). Furthermore, climate change is expected to intensify precipitation events (O'Gorman and Schneider, 2009) which, along with the influence of anthropogenic activities (Osborne *et al*., 2018) is expected to further influence phenological processes in savanna ecosystems (Ma *et al*., 2013) at different spatio-temporal scales (Park *et al*., 2021). All these factors make it challenging to identify long-term phenological trends and differentiate natural variability from anthropogenically-induced variability.

The use of remotely sensed satellite products has been considered the most effective method in monitoring large scale vegetation phenology (Zhang *et al.*, 2006). However, the spatial and temporal resolutions of these remotely sensed products differ between sensors, thus phenological metrics derived from different sensors are not interchangeable in these heterogeneous environments. This highlights the importance of multi-scale phenological comparisons which can provide better insights into the spatially explicit phenological relationships in savanna landscapes. Acknowledging the above considerations, in this study, I investigated how spatial scale influenced sensor derived NDVI estimates of biomass (Objective 1-Chapter 2) and phenological metrics (Objective 2-Chapter 3) in contrasting vegetation covers. This study followed the assumption that the biomass samples and satellite derived NDVI products used in this study are representative of the landscape. The main

conclusions found in this study demonstrated that the strength of the relationship between NDVI and herbaceous biomass is influenced by the spatial scale of observations, with Sentinel at 10 m spatial resolution having the strongest relationship, while MODIS at 250 m spatial resolution had the weakest relationship. Phenological metrics differed significantly between spatial scales and between canopy cover types. Phenological metrics were highly variable across all sensors with metrics varying by 9 to 30 days across seasons. There were strong correlations between the timing of rainfall and phenological metrics with the strength of correlations differing between spatial scales and canopy cover. Here I discuss the significance of these findings and suggest both ecological and monitoring considerations and implications based on the results found in this study.

4.1. Monitoring Implications

Biomass estimates

In chapter 2, I found that finer scaled products Sentinel (10 m) and PlanetScope (3 m) were better predictors of herbaceous biomass compared to MODIS (250 m) and Landsat (30 m). This could be attributed to both the spatial and temporal properties of these different products. For example, the finer spatial scales of Sentinel and PlanetScope represent the measures of herbaceous biomass more accurately, whereas coarser scale NDVI measures aggregate a variety of different herbaceous biomass densities, which do not accurately reflect what was measured on the ground. However, in the establishment of relationships between NDVI and biomass, finer spatial scale does not necessarily mean stronger linear relationships. For example, Cunliffe *et* al. (2020) found a weak relationship ($R^2 = 0.23$) between NDVI and dry biomass at a very fine spatial scale of 0.2 m in a shrub tundra landscape. Additionally, the presence of non-photosynthetic plant tissues (woody branches) and bare ground patches, which are prominent features in savanna landscapes, can alter the reflectance readings of the NDVI instruments (Cunliffe *et* al., 2020). This supports the need to use non-linear models when constructing relationships between NDVI and field measurements (Santin-Janin *et* al., 2009), as NDVI also tends to saturate at very fine scales i.e., high amounts of green biomass (Hobbs, 1995). However, further studies are needed to accurately determine at what fine spatial scale threshold/s, NDVI saturation occurs in savanna landscapes.

Another important consideration in NDVI-herbaceous biomass relationships, is the influence of canopy cover. In this study, it was clear from ground-based measurements, that the average herbaceous biomass was higher in Closed canopy, yet MODIS derived NDVI estimates of biomass did not differ between canopy covers. Wessels *et al*. (2006) similarly found that the relationship between the coarse-scale AVHRR (1 km) NDVI and herbaceous biomass did not differ between Closed and Open canopy. This reinforces the need to consider spatial scale when monitoring herbaceous biomass estimates when using NDVI as a proxy of biomass. Additionally, the temporal resolution of NDVI products should also be considered, as this study found that 16-day revisit period of Landsat resulted in comparatively fewer Landsat NDVI samples (n = 9) which limited the accuracy of comparisons with all other sensors. This was due to the high amounts of cloud cover that occurred in this study area, particularly during the rainy season. This suggests that biomass monitoring assessments conducted during the rainy season should consider using an NDVI product with a frequent acquisition rate. My results suggest that the use of NDVI as a proxy for herbaceous biomass in savanna landscapes needs careful consideration of the spatial scales of products, as the accuracy of biomass estimates derived from NDVI may be significantly reduced.

Phenology estimates

In chapter 3, I found that the onset and length of phenological metrics occur earlier at fine and later at coarser spatial scales, respectively. This supports the notion that conclusions drawn from phenological studies are limited to the spatial scale they were derived from, i.e., restricts their transferability to other contexts (Chase *et al*., 2018; Park *et al*., 2021). In this study, I used herbaceous biomass measurements to validate the strength of the NDVI-Biomass relationships at different spatial scales. However, this *in situ* method is time-consuming and cannot provide samples for large areas. Zhang *et al*. (2017) similarly suggest that in heterogeneous environments, coarse spatial resolution products can result in skewed phenological metrics and do not relate well with *in situ* observations (Fu *et al*., 2014). Yet, in South Africa, there are currently very few alternative methods that can be used to validate satellite derived phenological metrics. The development of a phenocam network i.e., vegetation time-lapses captured using digital cameras over long periods (Brown *et al*., 2016) and a further extension of the carbon flux tower (measure greenhouse gas emissions) network in South Africa would allow for site-level analysis of phenology and could be used to

develop more accurate phenology models derived from satellite sensors (Vrieling *et al*., 2018).

This study also found that all phenological metrics were highly variable across all sensors, with phenological metrics varying by 9 to 30 days across scales. Surprisingly, no consistent pattern was observed in terms of phenological metric variability differing across scales throughout the study period. African savanna phenology is strongly related to the wet/dry seasonal cycles (Higgins *et al*., 2011), which is highly variable across spatial and temporal scales (Lehmann *et al*., 2011), leading to unpredictable and irregular phenological events in African savannas (Whitecross *et al*., 2017). This high variability makes it difficult to identify any long-term phenological patterns, particularly with fine spatial scale products, which have limited data availability. To address this issue, several studies have used sensor fusion techniques which involves the joining (fusing) of images from multiple sensors which have different spatial and temporal properties (Filgueiras *et al*., 2020).

Liao *et al*. (2017) for example, developed a NDVI data fusion model which was effective in generating high spatial and temporal resolution NDVI images in heterogeneous environments. This would be beneficial in analysing long-term phenological metrics at fine spatial scales, in heterogenous savannas. However, this model is not compatible across all environments as the calculation of coefficients between the images of 'fused' sensors differs based on site-specific weather conditions (Liao *et al*., 2017), thus future studies should adopt a sensor fusion model that can be applied in southern African savannas. Such a model, in conjunction with multi-scale phenological observations, could provide a powerful method for characterising phenology derived from satellite sensors with different spatial and temporal properties (Piao *et al*., 2019).

4.2. Ecological Implications

It was expected that NDVI variability would be lower in Open canopy due to its homogenous vegetation structure and composition relative to Closed canopy. Results from this study showed that NDVI variability increased from coarse to fine scale and was similar in both canopy cover types. This similar NDVI variability in both Closed and Open canopy suggest that the influence of land use practices in savanna ecosystems need to be considered, as these activities can alter landscape patterns either deliberately or inadvertently (Hobbs,

1997). For example, Higgins *et al*. (1999), suggest that land use processes such as grazing, reduce woody plant species richness, biomass, and vegetation regeneration capacity. This study found that herbaceous biomass was significantly lower in Open canopy (where extensive grazing occurs), but contrary to Higgins *et al*. (1999), biomass was increasing annually at a higher rate than the Closed canopy site based on the NDVI time series from 2015 to 2021. This could be due to fuel wood collection by local communities, which has previously been linked to vertical canopy biomass increases due to rapid coppice regrowth (Mograbi *et al*., 2015), and the encroachment of unpalatable woody biomass (Wiegand *et al*., 2006). This implies that extractive land use practices have a paradoxical impact on savanna landscapes, by both increasing and decreasing vegetation biomass.

Interestingly, this study found that on average POS occurred earlier in Closed canopy compared to Open canopy for all sensors. However, this difference decreased from coarse to fine scale (MODIS-8 Days, Landsat-3 Days, Sentinel-1 Day). This not only implies a difference in seasonal peaks of trees versus grasses but also shows how spatial scale influenced the level of difference between the two sites. This effect is likely due to spatio-temporal scale variation, as increases in spatial scale can cause time lags in the ecological processes (Wiens, 1989). For all other phenological metrics, there was no clear difference in the onset or length of metrics between Closed and Open canopy. However, there were year-to-year differences in all phenological metrics across all scales between Closed and Open canopy.

4.3. Recommendations for Future Studies

This study provided a unique insight into the influence of spatial scale on NDVI derived biomass and phenological metric estimates in a South African savanna landscape. However, many studies have highlighted the complexity and incompatibility when comparing phenological metrics across spatial scales (Tian *et al*., 2020; Zhang *et al*., 2017). This has advocated the need for multi-scale approaches to improve our understanding of phenological processes (Zeng *et al*., 2020), as these processes are influenced by several environmental cues (precipitation, photoperiod, and temperature), which interact differently at different spatio-temporal scales (Wiens, 1989), especially in heterogeneous savanna systems. However, remotely sensed based phenology estimates need to be validated, which is challenging,

particularly in South Africa where the most commonly used means of validation are *in situ* biomass estimates (Wessels *et al*., 2006; Higginbottom and Symeonakis, 2019; Berger *et al*., 2020). To accompany this validation method, the development of a phenocam network with accompanying carbon flux towers in South Africa would provide a valuable means of validating satellite derived phenology. This will allow for better insights into species-specific phenology as the high resolution images gathered by a phenocam network could facilitate differentiation between species. Furthermore, data fusion models developed for southern African savannas could allow for long-term phenological trends at fine spatial scales to be observed, which are currently limited to ~10 years.

It is also important to acknowledge the limitations that emerged from this study, which may assist in designing improved methodologies for future studies. For example, due to the spatially nested sampling design of this study, samples were subject to pseudoreplication. Additionally, I was not able to measure the NDVI from the top-of-canopy vegetation as the handheld NDVI reader was not long enough to reach these areas. This compromised the comparison between satellite derived and *in situ* derived NDVI measures of top-of-canopy vegetation. It is also important to consider that only one season of PlanetScope data were used in this study, which would limit the findings of this study. Furthermore, biomass samples were not collected at the same time of day throughout the study. If feasible, future studies should consider using unmanned aerial vehicles (drones) with multispectral capabilities. Additionally, results from this study may not apply to neighbouring areas due to the relatively small sample size, which does not represent the tree-grass ratio complexity expressed at larger spatial scales in savanna environments. Thus, increasing the sample size will provide results more representative of savanna heterogeneity. Given the above considerations, a combination of approaches such as multi-scale phenology analysis with data fusion models, phenocam imagery and carbon flux tower data, could provide a comprehensive spatially explicit understanding of savanna phenology which may assist in distinguishing between natural and human induced phenology variability.

4.4. References

Augustine, D.J., 2003. Spatial heterogeneity in the herbaceous layer of a semi-arid savanna ecosystem. *Plant Ecology*, 167(2), 319-332.

Berger, C., Lux, H., Urban, M., Schmullius, C., Baade, J., Thiel, C., Wigley-Coetsee, C. and Smit, I., 2020, September. Annual Grass Biomass Mapping with Landsat-8 and Sentinel-2 Data Over Kruger National Park, South Africa. In *IGARSS 2020-2020 IEEE International Geoscience and Remote Sensing Symposium*, 4323-4326

Brown, T.B., Hultine, K.R., Steltzer, H., Denny, E.G., Denslow, M.W., Granados, J., Henderson, S., Moore, D., Nagai, S., SanClements, M. and Sánchez-Azofeifa, A., 2016. Using phenocams to monitor our changing Earth: toward a global phenocam network. *Frontiers in Ecology and the Environment*, 14(2), 84-93.

Chase, J.M., McGill, B.J., McGlinn, D.J., May, F., Blowes, S.A., Xiao, X., Knight, T.M., Purschke, O. and Gotelli, N.J., 2018. Embracing scale-dependence to achieve a deeper understanding of biodiversity and its change across communities. *Ecology Letters*, 21(11), 1737-1751.

Cole, E.F. and Sheldon, B.C., 2017. The shifting phenological landscape: Within-and between-species variation in leaf emergence in a mixed-deciduous woodland. *Ecology and Evolution*, 7(4), 1135-1147.

Cunliffe, A.M., Assmann, J.J., Daskalova, G.N., Kerby, J.T. and Myers-Smith, I.H., 2020. Aboveground biomass corresponds strongly with drone-derived canopy height but weakly with greenness (NDVI) in a shrub tundra landscape. *Environmental Research Letters*, 15(12), 125004.

du Toit, J.T., 2003. Large herbivores and savanna heterogeneity. *The Kruger experience: Ecology and management of savanna heterogeneity*, 292-309.

Filgueiras, R., Mantovani, E.C., Fernandes-Filho, E.I., Cunha, F.F.D., Althoff, D. and Dias, S.H.B., 2020. Fusion of MODIS and Landsat-like images for daily high spatial resolution NDVI. *Remote Sensing*, 12(8), 1297.

Fu, Y.H., Piao, S., Op de Beeck, M., Cong, N., Zhao, H., Zhang, Y., Menzel, A. and Janssens, I.A., 2014. Recent spring phenology shifts in western C entral E urope based on multiscale observations. *Global Ecology and Biogeography*, 23(11), 1255-1263.

Good, S.P. and Caylor, K.K., 2011. Climatological determinants of woody cover in Africa. *Proceedings of the National Academy of Sciences*, 108(12), 4902-4907.

Higginbottom, T. and Symeonakis, I., 2019. Downscaling GIMMS3g NDVI-based biomass predictions using empirical orthogonal teleconnections. *Unpublished*

Higgins, S.I., Delgado-Cartay, M.D., February, E.C. and Combrink, H.J., 2011. Is there a temporal niche separation in the leaf phenology of savanna trees and grasses? *Journal of Biogeography*, 38(11), 2165-2175.

Higgins, S.I., Shackleton, C.M. and Robinson, E.R., 1999. Changes in woody community structure and composition under contrasting landuse systems in a semi-arid savanna, South Africa. *Journal of Biogeography*, 26(3), 619-627.

Hobbs, R., 1997. Future landscapes and the future of landscape ecology. *Landscape and Urban Planning*, 37(1-2), 1-9.

Hobbs, T.J., 1995. The use of NOAA-AVHRR NDVI data to assess herbage production in the arid rangelands of Central Australia. *International Journal of Remote Sensing*, 16(7), 1289-1302.

Inouye, B.D., Ehrlén, J. and Underwood, N., 2019. Phenology as a process rather than an event: from individual reaction norms to community metrics. *Ecological Monographs*, 89(2), e01352.

Jelinski, D.E. and Wu, J., 1996. The modifiable areal unit problem and implications for landscape ecology. *Landscape Ecology*, 11(3), 129-140.

Lehmann, C.E., Archibald, S.A., Hoffmann, W.A. and Bond, W.J., 2011. Deciphering the distribution of the savanna biome. *New Phytologist*, 191(1), 197-209.

Levin, S.A., 1992. The problem of pattern and scale in ecology: the Robert H. MacArthur award lecture. *Ecology*, 73(6), 1943-1967.

Liao, C., Wang, J., Pritchard, I., Liu, J. and Shang, J., 2017. A spatio-temporal data fusion model for generating NDVI time series in heterogeneous regions. *Remote Sensing*, 9(11), 1125.

Ma, X., Huete, A., Yu, Q., Coupe, N.R., Davies, K., Broich, M., Ratana, P., Beringer, J., Hutley, L.B., Cleverly, J. and Boulain, N., 2013. Spatial patterns and temporal dynamics in savanna vegetation phenology across the North Australian Tropical Transect. *Remote Sensing of Environment*, 139, 97-115.

Mograbi, P.J., Erasmus, B.F., Witkowski, E.T.F., Asner, G.P., Wessels, K.J., Mathieu, R., Knapp, D.E., Martin, R.E. and Main, R., 2015. Biomass increases go under cover: woody vegetation dynamics in South African rangelands. *PLoS One*, 10(5), e0127093.

O'Gorman, P.A. and Schneider, T., 2009. The physical basis for increases in precipitation extremes in simulations of 21st-century climate change. *Proceedings of the National Academy of Sciences*, 106(35), 14773-14777.

Osborne, C.P., Charles-Dominique, T., Stevens, N., Bond, W.J., Midgley, G. and Lehmann, C.E., 2018. Human impacts in African savannas are mediated by plant functional traits. *New Phytologist*, 220(1), 10-24.

Park, D.S., Newman, E.A. and Breckheimer, I.K., 2021. Scale gaps in landscape phenology: challenges and opportunities. *Trends in Ecology & Evolution*, 36(8), 709-721.

Piao, S., Liu, Q., Chen, A., Janssens, I.A., Fu, Y., Dai, J., Liu, L., Lian, X.U., Shen, M. and Zhu, X., 2019. Plant phenology and global climate change: Current progresses and challenges. *Global Change Biology*, 25(6), 1922-1940.

Santin-Janin, H., Garel, M., Chapuis, J.L. and Pontier, D., 2009. Assessing the performance of NDVI as a proxy for plant biomass using non-linear models: a case study on the Kerguelen archipelago. *Polar Biology*, 32(6), 861-871.

Staver, A.C., 2018. Prediction and scale in savanna ecosystems. *New Phytologist*, 219(1), 52-57.

Tian, J., Zhu, X., Wu, J., Shen, M. and Chen, J., 2020. Coarse-resolution satellite images overestimate urbanization effects on vegetation spring phenology. *Remote Sensing*, 12(1), 117.

Vrieling, A., Meroni, M., Darvishzadeh, R., Skidmore, A.K., Wang, T., Zurita-Milla, R., Oosterbeek, K., O'Connor, B. and Paganini, M., 2018. Vegetation phenology from Sentinel-2 and field cameras for a Dutch barrier island. *Remote Sensing of Environment*, 215, 517-529.

Wessels, K.J., Prince, S.D., Zambatis, N., MacFadyen, S., Frost, P.E. and Van Zyl, D., 2006. Relationship between herbaceous biomass and 1-km2 Advanced Very High Resolution Radiometer (AVHRR) NDVI in Kruger National Park, South Africa. *International Journal of Remote Sensing*, 27(5), 951-973.

Whitecross, M.A., Witkowski, E.T. and Archibald, S., 2017. Assessing the frequency and drivers of early-greening in broad-leaved woodlands along a latitudinal gradient in southern Africa. *Austral Ecology*, 42(3), 341-353.

Wiegand, K., Saltz, D. and Ward, D., 2006. A patch-dynamics approach to savanna dynamics and woody plant encroachment–insights from an arid savanna. *Perspectives in Plant Ecology, Evolution and Systematics*, 7(4), 229-242.

Wiens, J.A., 1989. Spatial scaling in ecology. *Functional Ecology*, 3(4), 385-397.

Wu, J., 2004. Effects of changing scale on landscape pattern analysis: scaling relations. *Landscape Ecology*, 19(2), 125-138.

Zeng, L., Wardlow, B.D., Xiang, D., Hu, S. and Li, D., 2020. A review of vegetation phenological metrics extraction using time-series, multispectral satellite data. *Remote Sensing of Environment*, 237, 111511.

Zhang, H., Yuan, W., Liu, S., Dong, W. and Fu, Y., 2015. Sensitivity of flowering phenology to changing temperature in China. *Journal of Geophysical Research: Biogeosciences*, 120(8), 1658-1665.

Zhang, X., Friedl, M.A. and Schaaf, C.B., 2006. Global vegetation phenology from Moderate Resolution Imaging Spectroradiometer (MODIS): Evaluation of global patterns and comparison with in situ measurements. *Journal of Geophysical Research: Biogeosciences*, 111(G4).

Zhang, X., Wang, J., Gao, F., Liu, Y., Schaaf, C., Friedl, M., Yu, Y., Jayavelu, S., Gray, J., Liu, L. and Yan, D., 2017. Exploration of scaling effects on coarse resolution land surface phenology. *Remote Sensing of Environment*, 190, 318-330.

APPENDIX A

Table 1A: Details of satellites and associated data used for this study. Note the narrow bandwidth ranges of Red and NIR of Sentinel, with NIR not overlapping any of the other sensors' NIR ranges

Satellite	**Terra**	**Landsat 8**	**Sentinel-2C**	**PlanetScope**
Sensor	MODIS	Operational Land Imager	Multispectral Imager	PS2.SD, PSB.SD
Product	MOD13Q1	Surface Reflectance	TOA Reflectance (Atmospherically Corrected)	Surface Reflectance
Spatial resolution (m)	250	30	10	3
Temporal resolution	16 day MVC	16 days	5 days	Daily
Wavelength (µm)	Red (band 1) 620 - 670 NIR (band 2) 841 - 876	Red (band 4) 636 - 673 NIR (band 5) 851 - 879	Red (band 4) 664.4 - 665 NIR (band 8) 833 - 835.1	Red (band 3) 590 - 670 NIR (band 4) 780 - 860
Bandwidth (µm)	Red-50 NIR - 35	Red-37 NIR-28	Red - 0.6 NIR - 2.1	Red - 80 NIR - 80
Tile Reference	H20v11	Path 169, 168, Row 77	T36JTT	NA
Provider	NASA LP DAAC	USGS	Copernicus	PlanetLabs

Table 2A: Weekly comparisons of sensor NDVI in Closed and Open canopy. Note that sensors sharing the same letter are **Not** significantly different

Closed canopy					
Week	Kruskal Wallis test	Pairwise Rank Sum Tests			
		MODIS	Landsat	Sentinel	PlanetScope
1	<0.001	a	a	b	c
2	<0.001	a	b	c	b
3	<0.001	a	b	b	c
4	<0.001	a	b	c	d
5	<0.001	a	b	c	c
6	<0.005	a	a	b	ab
7	<0.001	a	b	a	b
8	<0.001	a	a	b	ab
9	<0.005	a	b	a	a
10	<0.005	a	a	b	ab
11	<0.005	a	a	b	ab
12	<0.005	a	a	b	a
13	<0.001	a	a	b	c
14	<0.001	a	b	c	a
Open canopy					
Week	Kruskal Wallis test	Pairwise Rank Sum Tests			
		MODIS	Landsat	Sentinel	PlanetScope
1	<0.005	a	a	b	a
2	<0.001	a	b	b	c
3	<0.001	a	b	ab	c
4	<0.001	a	b	b	c
5	<0.005	a	b	b	b
6	<0.001	a	b	bc	ac
7	<0.05	ab	ab	a	b
8	<0.005	a	a	b	a
9	<0.05	a	ab	b	ab
10	>0.05	NA	NA	NA	NA
11	>0.05	NA	NA	NA	NA
12	<0.005	ab	ab	a	b
13	<0.005	ab	a	a	b
14	<0.05	a	ab	a	b

Table 3A: Results of the t-test comparisons between mean, minimum, maximum, and SD of NDVI between MODIS, Landsat, and Sentinel in Closed and Open canopy sites. Note the NDVI of PlanetScope only captures one season (2020-2021), making it not directly comparable, but the values show the range of its time series.

Closed Canopy						
Sensor	Mean	Minimum	Maximum	Time series SD	Average SD Between Pixels	*P value*
MODIS (*n*=161)	0.544	0.272	0.783	0.166	0.016	
Landsat (*n*=84)	0.514	0.255	0.815	0.163	0.039	>0.050
Sentinel (*n*=140)	0.420	0.203	0.693	0.152	0.046	<0.001*
PlanetScope (*n*=23)	0.560	0.320	0.730	0.136	0.031	>0.050
Open Canopy						
MODIS (*n*=161)	0.428	0.206	0.623	0.117	0.018	
Landsat (*n*=84)	0.419	0.206	0.662	0.122	0.040	>0.050
Sentinel (*n*=140)	0.355	0.170	0.556	0.107	0.042	<0.001*
PlanetScope (*n*=23)	0.470	0.300	0.610	0.109	0.022	>0.050

Table 4A: Seasonal phenological metrics in Closed canopy, showing DOY for SOS, LOS, POS, and EOS for each sensor with the mean and SD of sensor specific phenological metrics displayed at the bottom of the table.

Closed Canopy	MODIS Phenological Metrics				Landsat Phenological Metrics				Sentinel Phenological Metrics			
Season	SOS	LOS	POS	EOS	SOS	LOS	POS	EOS	SOS	LOS	POS	EOS
1	366.7	143.2	447.7	509.8	393.0	129.0	450.7	502.3	346.2	140.9	436.0	505.3
2	341.1	196.9	439.2	538.0	329.4	156.7	420.8	516.6	344.4	163.7	403.3	526.4
3	344.4	174.6	429.0	519.0	327.9	156.5	416.9	514.8	342.9	144.7	420.4	505.9
4	354.8	169.6	440.6	524.3	349.0	136.8	425.4	516.3	366.3	127.2	433.3	511.7
5	343.1	197.0	438.7	540.6	339.3	161.6	430.0	531.4	336.8	169.7	421.1	524.8
6	301.0	217.2	401.3	518.5	307.9	183.7	407.5	522.1	304.8	152.3	375.4	475.4
Average	341.8	183.1	432.8	525.0	341.1	154.1	425.2	517.2	340.2	149.7	414.9	508.2
SD	22.2	26.0	16.5	12.0	28.9	19.4	14.7	9.5	20.0	15.6	22.6	18.5

Table 5A: Seasonal phenological metrics in Open canopy, showing DOY for SOS, LOS, POS, and EOS for each sensor with the mean and SD of sensor specific phenological metrics displayed at the bottom of the table.

Open Canopy	MODIS Phenological Metrics				Landsat Phenological Metrics				Sentinel Phenological Metrics			
Season	SOS	LOS	POS	EOS	SOS	LOS	POS	EOS	SOS	LOS	POS	EOS
1	360.4	134.3	459.3	501.2	398.3	129.0	450.5	494.4	355.3	120.4	428.5	494
2	348.9	202.7	455.2	551.7	341.6	158.3	429.9	530.3	347.3	174.1	415.2	539.7
3	341.2	175.4	427.9	516.6	327.3	163.9	421.8	521.6	344.1	137.0	421.5	499.4
4	355.5	175.0	446.3	530.6	353.9	138.3	432.2	522.6	357	142.8	431.3	518.0
5	337.1	199.3	434.0	536.4	340.7	155.0	427.1	526.2	333.8	167.7	416.2	519.8
6	307.8	216.4	425.5	524.0	314.9	178.0	410.2	523.3	315.4	148.3	383.8	481.9
Average	341.8	183.8	441.4	526.8	346.1	153.7	428.6	519.7	342.1	148.4	416.1	508.8
SD	18.7	29.2	14.3	17.3	28.8	17.6	13.3	12.8	15.5	19.9	17.1	20.9

Table 6A: Summary of correlations of phenological metrics between sensors in Closed and Open canopy cover sites.

		Closed Canopy			Open Canopy		
Metric	Regression variable *y* - *x*	R^2	Adjusted R^2	p-value	R^2	Adjusted R^2	p-value
SOS	MODIS - Landsat	0.72	0.65	0.030*	0.94	0.92	0.001**
	MODIS - Sentinel	0.76	0.69	0.030*	0.69	0.61	0.040*
	Landsat - Sentinel	0.31	0.12	0.250	0.52	0.40	0.100
LOS	MODIS - Landsat	0.88	0.85	0.005**	0.76	0.70	0.020*
	MODIS - Sentinel	0.38	0.23	0.100	0.64	0.54	0.050*
	Landsat - Sentinel	0.22	0.02	0.300	0.28	0.23	0.100
POS	MODIS - Landsat	0.64	0.55	0.050*	0.75	0.69	0.020*
	MODIS - Sentinel	0.77	0.72	0.020*	0.35	0.20	0.200
	Landsat - Sentinel	0.59	0.50	0.070	0.60	0.51	0.060
EOS	MODIS - Landsat	0.55	0.43	0.090	0.75	0.68	0.020*
	MODIS - Sentinel	0.47	0.34	0.100	0.65	0.56	0.050*
	Landsat - Sentinel	0.01	-0.20	0.800	0.26	0.07	0.200

*Significant (<0.05) **Highly Significant (<0.01)

Table 7A: Average monthly precipitation in the study area from 2016-2021 with total annual precipitation and 6-year monthly averages and standard deviations.

Season	Jul	Aug	Sep	Oct	Nov	Dec	Jan	Feb	Mar	Apr	May	Jun	Total
2015/2016	0.0	1.7	2.0	8.0	26.0	23.0	26.0	24.0	22.0	0.2	8.4	0.2	141.5
2016/2017	9.2	0.0	20	31.6	71.4	42.8	122.0	136.0	81.4	40.7	28.6	3.2	586.5
2017/2018	4.7	8.5	2.0	12.0	37.0	30.4	61.3	48.3	51.2	38.2	20.4	0.0	314.0
2018/2019	0.4	1.8	2.6	7.6	51.8	103.0	65.2	118.0	18.0	91.2	11.6	0.0	471.2
2019/2020	0.0	0.6	6.2	10.0	124.0	70.0	129.0	126.0	31.0	77.4	12.0	1.9	587.7
2020/2021	3.6	5.2	14.6	131.0	72.6	104.0	169.0	117.0	35.2	21.0	17.0	1.9	690.7
Average	3.0	3.0	7.9	33.3	63.7	62.2	95.3	94.8	39.8	44.8	16.3	1.2	465.3
SD	3.6	3.3	7.6	48.5	34.6	35.8	53.0	46.6	23.5	34.2	7.4	1.3	204.1

Table 8A: Average monthly temperatures in the study area from 2016-2021 with average annual temperatures and 6-year monthly averages and standard deviations.

Season	Jul	Aug	Sep	Oct	Nov	Dec	Jan	Feb	Mar	Apr	May	Jun	Seasonal Ave
2015/2016	14.3	17.0	21.1	22.4	23.8	24.4	23.8	24.0	23.0	23.3	17.4	16.3	20.9
2016/2017	14.9	17.0	21.1	22.4	23.6	24.4	23.8	24.0	23.0	22.0	17.5	15.7	20.7
2017/2018	16.4	16.9	20.3	20.8	21.6	23.3	23.3	23.2	24.0	21.2	18.7	16.5	20.5
2018/2019	15.2	19.1	22.7	20.7	22.6	25.9	24.9	24.6	24.3	21.5	18.8	16.6	21.4
2019/2020	16.1	19.3	20.0	23.7	24.9	24.2	25.1	24.1	22.9	20.8	18.5	16.6	21.3
2020/2021	14.6	17.7	19.8	21.4	23.9	24.9	24.7	24.0	23.4	21.1	19.5	17.6	21.0
Average	15.2	17.8	20.8	21.9	23.4	24.5	24.3	24.0	23.4	21.6	18.4	16.5	21.0
SD	0.85	1.09	1.0	1.1	1.14	0.8	0.74	0.4	0.5	0.9	0.8	0.5	0.3

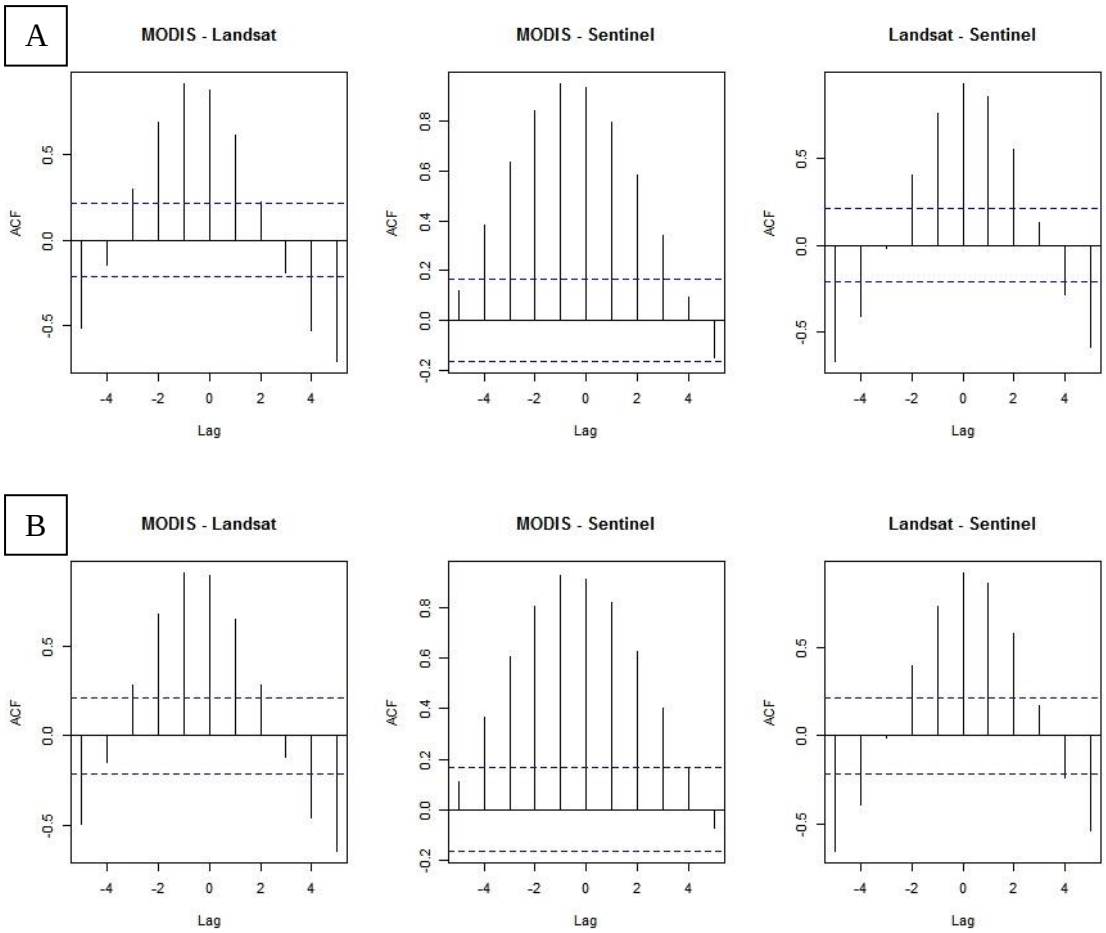

Figure 1A: The cross-correlation of NDVI time series between sensors at lag intervals of -5 and 5 in Closed (A) and Open (B) canopy.

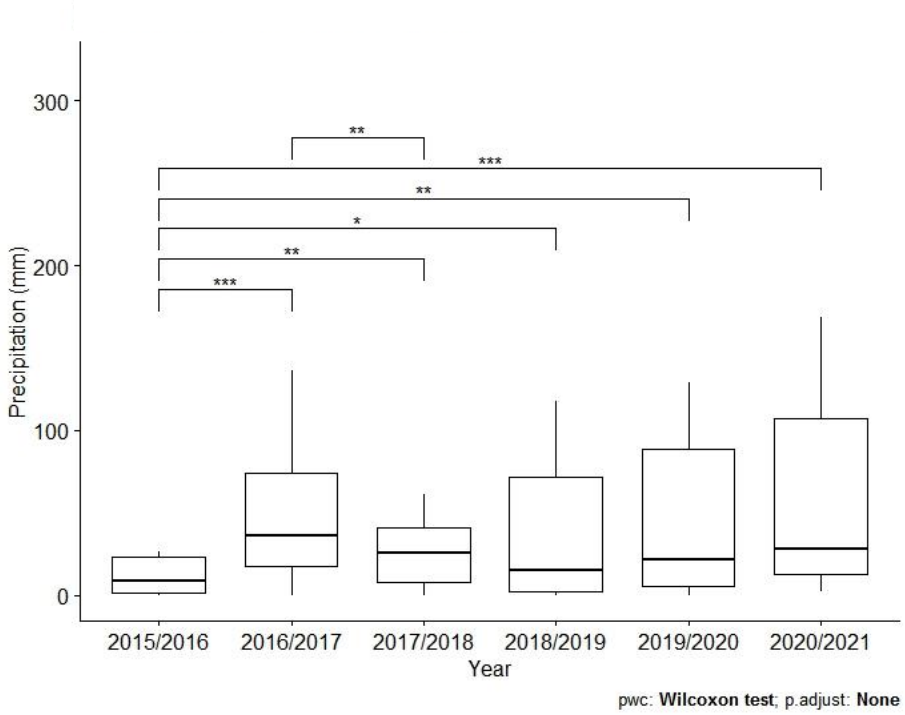

Figure 2A: Boxplot of the average monthly precipitation in the study area from 2015-2021 with significant difference indicated by above bars displaying (*) significant (**) very significant, and (***) very highly significant.

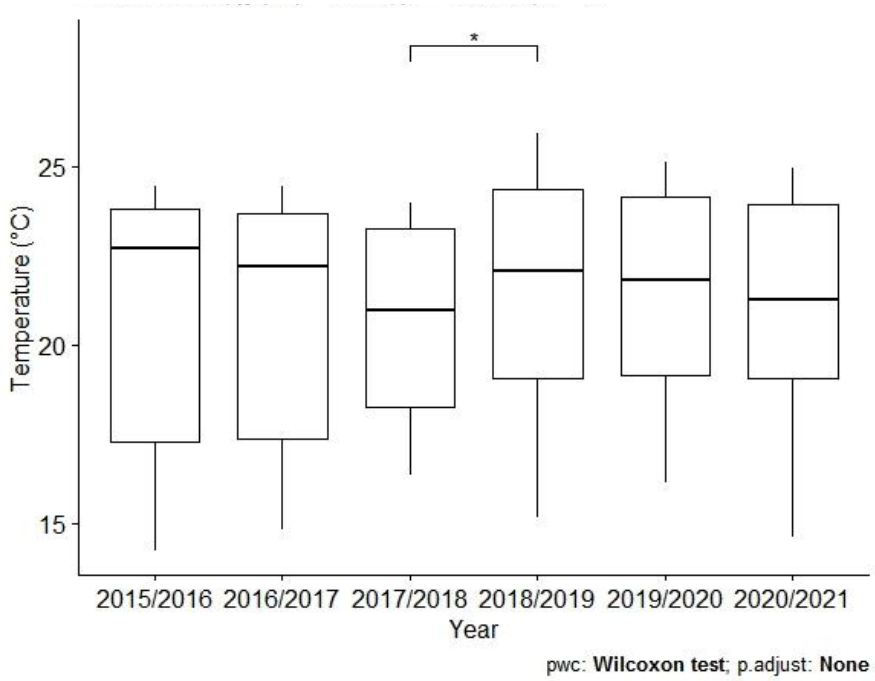

Figure 3A: Boxplot of average monthly temperatures in the study area from 2015-2021 with above bar indicating significant differences (*) between years.

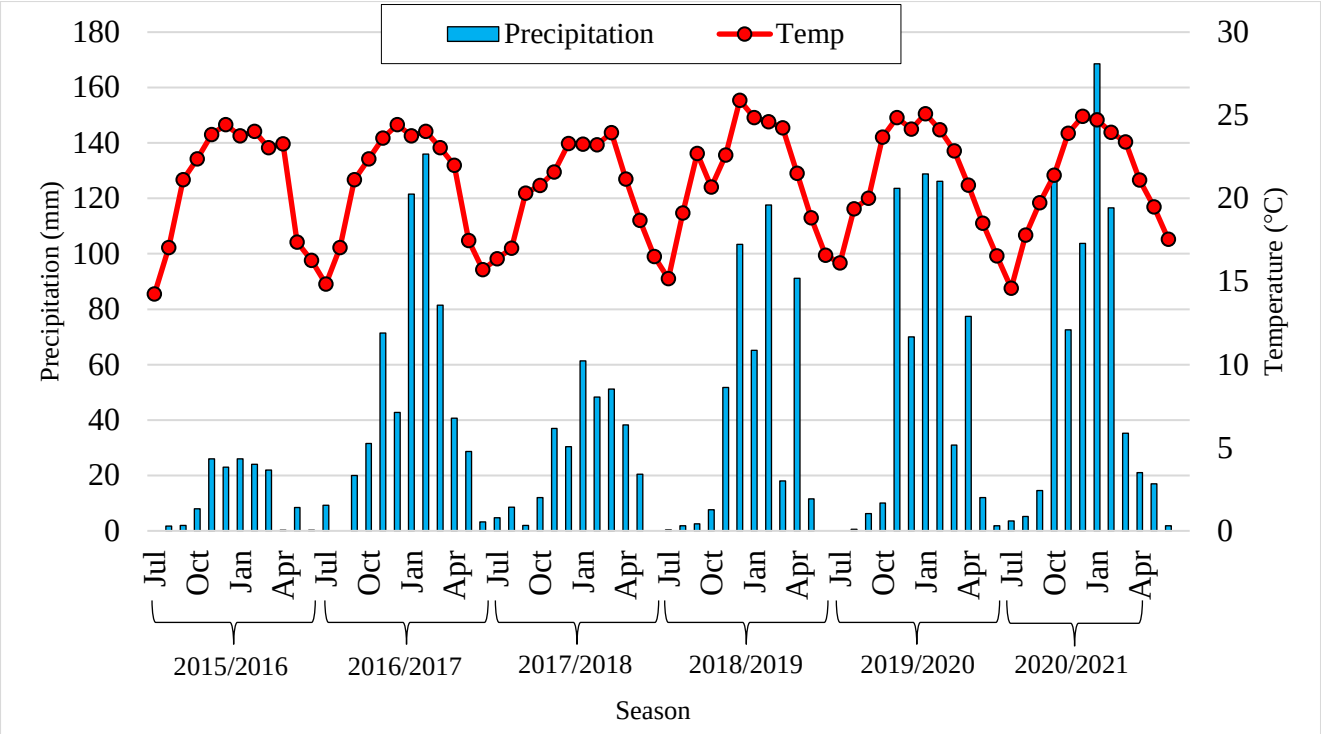

Figure 4A: The average monthly precipitation and temperature of all months from July 2015-June 2021.

APPENDIX B

Google Earth Engine Code

MODIS

```
#Set processing extent
var table_bounds = function(image){
return image.clip(studyarea);
};
#Select the collection of images by date and NDVI
var collection =ee.ImageCollection('MODIS/006/MOD13Q1' )
               .filterDate('2015-01-01', '2021-06-13')
                .select("NDVI")
                .filterBounds(studyarea);

#set image collection extent
var ndvicollection = collection.map(table_bounds);
#apply no value mask to collection
var totalObsCount = ndvicollection
        .select('NDVI')
        .count();
print(ndvicollection);

#apply cloud cover mask to collection
var collectionCloudMasked = ndvicollection.map(maskClouds);
var batch = require('users/fitoprincipe/geetools:batch');

#Download collection (Used to Download all Data sources)
batch.Download.ImageCollection.toDrive(ndvicollection, 'MOD13Q1-
NDVI',
               {scale: 250,
              crs: 'EPSG:4326',
              region: studyarea,
               fileFormat: 'GeoTIFF',
               type: 'float',
                maxPixels: 1e12
});
```

Landsat

```
#Load Landsat 8 imagery and filter it
var collection = ee.ImageCollection('LANDSAT/LC08/C01/T1_SR')
                .filter(ee.Filter.eq('WRS_PATH', 169))
                .filter(ee.Filter.eq('WRS_ROW', 77))
                .filterDate('2015-01-01', '2021-06-13')
                .set('SENSOR_ID', 'OLI')
                .sort("CLOUD_COVER", false);
var count = collection.size();
print("Collection", count);

#Clip to study extent
var collection = collection.map(function(image) { return
image.clip(WRB); });
  print("Collection filtered", collection);

#Function to cloud mask from the Fmask band of Landsat 8 SR data.
function maskL8sr(image) {
  var cloudShadowBitMask = ee.Number(2).pow(3).int();
  var cloudsBitMask = ee.Number(2).pow(5).int();
  var qa = image.select('pixel_qa');
  var mask = qa.bitwiseAnd(cloudShadowBitMask).eq(0)
      .and(qa.bitwiseAnd(cloudsBitMask).eq(0));
  return image.select('B[1-7]').multiply(0.0001)
  .addBands(image.select(['B10', 'B11']).multiply(0.1))
  .updateMask(mask);
}
#Compute the Normalized Difference Vegetation Index (NDVI)
var getNDVI = function(img){
  return
img.addBands(img.normalizedDifference(['B5','B4']).rename('NDVI'));
};
var ndvi = l8ndvi.select('NDVI');
```

Sentinel

```
#Load Sentinel imagery and filter it
var collection = ee.ImageCollection('COPERNICUS/S2')
                .filterDate('2021-04-12', '2021-06-10')
                .filterBounds(table)
                .sort("CLOUD_COVER", false);
var count = collection.size();
print("Collection", count);

# Clip to study area
var collection = collection.map(function(image) { return
image.clip(studyarea); });
print("Collection filtered", collection);

#Function to cloud mask from the S2 dataset
function maskS2clouds(image) {
  var qa = image.select('QA60');

#Bits 10 and 11 are clouds and cirrus, respectively.
  var cloudBitMask = 1 << 10;
  var cirrusBitMask = 1 << 11;

#Both flags should be set to zero, indicating clear conditions.
  var mask = qa.bitwiseAnd(cloudBitMask).eq(0)
      .and(qa.bitwiseAnd(cirrusBitMask).eq(0));
  return image.updateMask(mask).divide(10000);
}

#Apply SIAC and retrieve bottom of atmosphere (BOA) reflectance
var siac = require('users/marcyinfeng/utils:SIAC');
var sen2 = siac.get_sur(collection.first());

#Compute the Normalized Difference Vegetation Index (NDVI).
var getNDVI = function(img){
  return
img.addBands(img.normalizedDifference(['B8','B4']).rename('NDVI'));
};
```

Convert Raster to Binary Format

```
Outputfolder<-"C:/Users/Where to Store Binary Files"

allNDVITIF<- list.files("C:/Users/ Raster NDVI Files ",
                        full.names = TRUE,
                        pattern = ".tif$")

#Change file-format to binary for TIMESAT
for(i in 1:length(allNDVITIF)){
  tc <- raster(allNDVITIF[i])
  #NAs can cause trouble with TIMESAT. Replacing with -999
  tc[is.na(tc)] <- -999
#switch filename-convention for correct sorting
flname <-
paste0(substr(basename(allNDVITIF[i]),1,20),"_",substr(basename(allNDVITIF[
i]),1,3),"_NDVI-TS")
#Create Binary files
writeRaster(tc, filename=paste0(dataPath,'/timesatPREP/',flname),
format="IDRISI", overwrite=T)}
#List new, TIMESAT-compatible files
allNDVITS <- list.files(paste0(dataPath,"/timesatPREP/"), full.names=T,
pattern=".rst$",recursive=F)
#Create TIMESAT image-list
imglist <- c(length(allNDVITS),allNDVITS)
fileCr<-file( paste0(dataPath,'/forTIMESAT/TIMESATlist.txt'))
writeLines(imglist,fileCr)
close(fileCr)
```

Creating Phenology Maps

Adopted from-(http://rstudio-pubs
static.s3.amazonaws.com/452032_a5df2d3f782444fc830d43548a304ec5.html)

```
library(raster)
library(curl)
library(rgdal)
library(rts)
library(stringr)
dataPath<-("C:/Users/R/Rasters/Location of Raster Files)
TSpath <-"C:/Users/timesat33/compiled/Win64"
rasterData <- list.files(path=dataPath, pattern='.tif$', recursive=F,
ignore.case=T, full.names=T)
rasterFiles <- basename(rasterData)
hemisphere <- 0
exRST <- raster(rasterData[1])
if (as.numeric(ncol(exRST)) <= 28 || as.numeric(nrow(exRST)) <= 25)
DOYs <- unique(substr(basename(rasterData),10,11))
YEARs <- unique(substr(basename(rasterData),4,5))

##Function to read TIMESAT outputs using TIMESAT-tools
bintiff <- function (rast,base_image){
  timesatbinobj <- file(rast, "rb")
  raw_vector <- readBin(timesatbinobj, n=file.info(rast)$size, what="int",
signed=T, endian="little",size=2)
  close(timesatbinobj)
  data_matrix <- matrix(raw_vector,nrow(base_image),
ncol(base_image),byrow=T)
  tiff_raster <- raster(data_matrix, template=base_image)
  return(tiff_raster)
}

#Reading raw TIMESAT output (Variant B; Timesat-fortran tools)
path_tpaFile <-paste0(TSpath,"/MODIS_Settings_TS.tpa")
#Path to TIMESAT-seas2img-tool for converting
pTSpath <- gsub("compiled/Win64/","compiled/Win64", TSpath)
seasImg <- gsub("compiled/Win64","timesat_fortran/tools/TSF_seas2img",
pTSpath)
}
```

```
#TIMESAT will not calculate phenology for the very first season, hence the
following correction-variable

if (hemisphere == 1){
  corr <- 1
}else{
  corr <- 2
}
noSeasons
noSeasons  <- length(YEARs) - corr
setwd(paste0(dataPath,"/temp/"))
base_image = exRST
base_image
}
#Looping through season-indicators and writing output for each
for (d in 1:3){

  SeasonIndicator <- d

  #Peaktime is indicator #5
  if (d == 3){
    SeasonIndicator <- 5
  }

  if(SeasonIndicator == 1){
    descrinfo <- "SoS"
  }else if(SeasonIndicator == 2){
    descrinfo <- "EoS"
  }else if(SeasonIndicator == 5){
    descrinfo <- "PoS"
  }
  noSeasons
  #Loop through seasons, create output for each
  for (s in 1:noSeasons){
    startIX <- 1 + (23*(s))
    endIX <- 23 + (23*(s))
    print(paste0("Reading/converting ", descrinfo, " ",
s,"/",noSeasons,"..."))
#Calling seas2img via command-prompt
```

```
system(paste0("\"",seasImg,"\" \"",path_tpaFile,"\" ",SeasonIndicator, " ",
startIX," ",endIX, " 0 0 NSE",SeasonIndicator,"_",s," 2" ), wait=TRUE,
show.output.on.console = F)


#Convert binary to tiff
r <-bintiff(paste0(dataPath,"/temp/NSE",SeasonIndicator,"_",s,"_season1")
,base_image)%%23
writeRaster(r, filename =
paste0(dataPath,"/timesat/",as.numeric(YEARs[s])+1,"_",descrinfo),
format="GTiff", overwrite=T)
  }
#Parsing Tiffs of Start, Peak, End of Season
timesatRasterALL <- list.files(paste0(dataPath,"/timesat/"),
pattern=".tif$", recursive=F, full.names=T)
timesatRasterSOS <- stack(timesatRasterALL[grepl("_SoS",timesatRasterALL)])
timesatRasterPOS <- stack(timesatRasterALL[grepl("_PoS",timesatRasterALL)])
timesatRasterEOS <- stack(timesatRasterALL[grepl("_EoS",timesatRasterALL)])
timesatRasterALL
###Checking for integrity of seasonal metrics
#Filter out TIMESAT-NAs
timesatRasterSOS[timesatRasterSOS == 0] <- NA
timesatRasterPOS[timesatRasterPOS == 0] <- NA
timesatRasterEOS[timesatRasterEOS == 0] <- NA
}
#Calculation of mean Seasonal Metrics + output
meanSOS <- calc(timesatRasterSOS,fun=mean,na.rm=T)
meanPOS <- calc(timesatRasterPOS,fun=mean,na.rm=T)
meanEOS <- calc(timesatRasterEOS,fun=mean,na.rm=T)
#Write to Raster
writeRaster(meanSOS, filename=paste0(dataPath,'/timesat/SOS-MEAN'),
format="GTiff", overwrite = T )
writeRaster(meanPOS, filename=paste0(dataPath,'/timesat/POS-MEAN'),
format="GTiff", overwrite = T )
writeRaster(meanEOS, filename=paste0(dataPath,'/timesat/EOS-MEAN'),
format="GTiff", overwrite = T )

}
```

GPS Calculations

Circular Error of Probability (CEP) and standard deviations of X and Y coordinates were calculated using DNRGPS (Minnesota Department of Natural Resources, 2012). Average GPS error was x=<0.52m, y=0.50m with CEP 98=0.93m in WRF with GPS error being significantly lower in TCR with x=<0.17m, y=0.20m and CEP 98=0.40m. The difference in average GPS error can be attributed to the difference in vegetation density between the two sites.